Application of hydrochemical and tracer techniques to investigate the source of seepage water in deep gold mines: A case study at South Deep Gold Mine, Gauteng Province, South Africa

UNIVERSITY OF THE
WITWATERSRAND,
JOHANNESBURG

HYDROGEOLOGY RESEARCH REPORT (GEOL7052)

Submitted by

Mothipa Bridget Ramangoa

Student number: 464682

Supervisor: Prof. Tamiru Abiye

A research report submitted to the Faculty of Science, University of the Witwatersrand, Johannesburg, in partial fulfilment of the requirements for the degree of Master of Science in Hydrogeology, School of Geosciences

April 2021

DECLARATION

I, Mothipa Bridget Ramangoa (Student number: 464682), declare that this research report is my own, unaided work. It is being submitted for the Master of Science at the University of the Witwatersrand, Johannesburg. To my knowledge, this work has not been submitted before for any degree or examination at any other University. I further declare the following:

- I am aware that plagiarism (the use of someone else's work without their permission and/or without acknowledging the original source) is against the University Policy.
- I have followed the required conventions in referencing the thoughts, ideas, and visual materials of others.
- I understand that the University of the Witwatersrand may take disciplinary action against me if there is a belief that this is not my own unaided work, or that I have failed to acknowledge the source of the ideas or words in my writing.

(Signature of candidate)

3rd day of July 2021 at the University of the Witwatersrand, Johannesburg.

ABSTRACT

A hydrogeological study was conducted to investigate the possible sources of seepage at South Deep Gold Mine (SDGM), near Westonaria town, Gauteng Province. The aim of the study was to promote efficient mine water management through a better understanding of the source of seepage by utilising integrated hydrochemical and tracer techniques to assist the mine with strategic mine planning and design, and financial implications. Underground field observations, cross-sections, mine survey data, monitoring borehole data were used to provide a better understanding of the hydrogeological characteristics at SDGM.

Hydrochemical facies characterised seepage water into 4 groups: (i) Mg-SO_4 water type, suggesting SO_4^{2-} contamination from the mine and/ or a mix of different water types; (ii) NaCl water type, indicating regional groundwater source; (iii) Ca-SO_4 water type due to the existence of sulphides bearing rocks and; (iv) Ca-Mg-SO_4 water type signifying SO_4^{2-} contaminated water as a result to historical and/ or current mining activities .

The stable isotope analysis conceptually characterised the seepage water into three groups: (i) un-evaporated isotopic composition indicating condensation effect/water mass mixing, (ii) local rain composition suggesting recharge occurring through direct rainfall, and (iii) samples on the evaporation line suggesting secondary evaporation during and/ or before rainfall recharge. Seepage water contained detectable amounts of tritium indicating recharge/aquifer renewability. Tritium signature varied from 0.0 TU to 1.8 TU. Tritium content between 0.8-1.8 TU was interpreted as recharged in the past +20 to 35 years and the low tritium content (<0.8 TU) samples are categorised as sub modern, recharged before 1950s, indicating that the recharge mainly occurred approximately +35 to +70 years ago.

Based on the hydrogeological conceptualisation of the main source of seepage within the study, seepage is mainly associated with or observed near backfilled areas, places closer to active mining, along the abutment zones, the geological structures such as faults and mining-induced fractures, worsened/compounded by inadequate mine-water management. Seepage water was also observed on drilled boreholes which holed to active or old mining levels. Possibly groundwater may flow into the mine void through borehole voids that drilled up to the lava position or intersected structures with the potential of connecting the aquifer and the mine void.

This report recommends strict and long-term excess water and service water management underground to ensure the safety of the mine`s employees, minimizing corrosion on rock support, and damage of mine property. A better understanding of the source and cause of seepage at the mine will assist in safe mine planning and enhance management of service and excess water underground.

Keywords: Underground Gold Mining, Water seepage, Environmental isotopes, Tritium, Hydrochemistry

In memory of my father

Nkhese Theodor Ramango

1948 – 1994

ACKNOWLEDGEMENTS

I would like to send a big thanks to South Deep Gold Mine (Mr Benford Mokoatle) for granting the opportunity to use the mine's data and equipment in writing this report, with special gratitude to Mr. Simon Mporetji, Mr Tyson Mutobvu, Mr Rugen Pillaye , Mr Moloko Tjiane and Mr. Bambo Dubula for always availing themselves to helping me.

I would like to express my sincere gratitude to my academic supervisor, Professor Tamiru Abiye for guidance and for being patient with me throughout this project. I would like to acknowledge and thank Mr. Mike Butler from iThemba Labs for his dedication to assisting with isotope analysis which was instrumental for this research.

Many thanks to Mr. Simamkele Baqa, Mr. Jabulani Sello, Miss Despina Tshipala, and Mr. Lumko Ncapai for sharing their knowledge and expertise throughout my research studies. I would have not been able to cope with the stress and pressure that comes with research studies if it was not for the support received from my family and best friend Pauline Lengwati. I cannot find words to express how appreciative I am.

Lastly, I would also like to thank my colleagues for their motivation and for allowing me to undertake this work amidst a busy schedule**.**

TABLE OF CONTENTS

LIST OF FIGURES

LIST OF TABLES

LIST OF ABBREVIATIONS AND ACRONYMS

CRD	Cumulative Rainfall Departure
CRG	Central Rand Group
DWAF	Department of Water Affairs and Forestry (now DWA - Department of Water Affairs
DO	Dissolved Oxygen
EC	Electrical Conductivity
ESI	Environmental Stable Isotope
E.P.M	Equivalents Per Million
FOG	Fall Of Ground
GMWL	Global Meteoric Water Line
IAEA	International Atomic Energy Agency
m	metres
MAP	Mean Annual Precipitation
Meq l^{-1}	Milli equivalent per litre
LMWL	Local meteoric water line
LOM	Life Of Mine
SI	Saturation Indices
SMOW	Standard Mean Ocean Water
SD EMP	South Deep Environmental Management Programme
SDGM	South Deep Gold Mine
TDS	Total Dissolved Solids
WRG	West Rand Group

CHAPTER 1

INTRODUCTION

1.1 General Introduction

In South Africa, underground gold mining began in the 1900s and has since been the primary economic factor making Gauteng the prosperous province that it is today. Conversely, mining activities have the potential to alter the hydrological and topographical characteristics of its surrounding areas, consequently affecting the runoff generation, soil moisture, evapotranspiration, and hydrogeological characteristics in an area (DWAF, 2008). Furthermore, mining (particularly underground mining) may modify in-situ permeability and underground flow patterns through enhanced rock permeability and fracture networks (Aston and Singh, 1983; Bridgwood et al., 1983). Generally, modified hydrogeological characteristics such as in-situ permeability and fracture networks can cause and/ or lead to increased groundwater inflows into the mine void.

Inflows into underground mine workings pose a serious threat to the production and safety of the mine (Xi-bing et al., 2012; Wu et al., 2013; Zhang et al., 2018; Guan et al., 2019 after Hanhu and Yunquan 2011). Groundwater inflows into the underground mine workings have been observed in several mines and this has resulted in catastrophic consequences such as fall of ground incidents and loss of lives.

Groundwater inflows and/ or seepage water into underground mine workings have the potential to impact underground mine stability, mining operation, health, and safety of the mining personnel as well as the impact on the mine production (Singh, 1986). Generally, groundwater inflow and/ or seepage inflow(s) into mine workings can be mining-induced, natural, or a combination of both natural and mine-induced (Singh, 1986). Mine-induced water seepage can occur as a result of enhanced fracture networks or rock matrix caused by blasting activities, partially sealed (and/ or not sealed) exploration holes which can act as conduits/preferential flow pathways, while the natural phenomenon of water seepage results from water inflows due to the mine cutting aquifers or mining below the piezometric water table (Fernandez et al., 1988). A combination of both mine-induced and natural water seepage problems has been experienced in rare instances.

Several cases of mine water inrush and seepage events have been reported globally (Ma et al., 2018; Guan et al., 2019). However, relatively few studies, including those by Funke (1990), Mulenga et al. (1992), and Ashton et al. (2001), have been conducted in Africa. Some of these studies have shown that seepage water can/may be caused by the nearby tailings' dams, geological structures (faults, dykes, etc), mining-induced fractures, nearby major surface water bodies in and around the mining area, and poor mine water management (Mulenga, 1993; DWAF, 2008; Mengistu et al., 2015). Nonetheless, safe mining production has recently improved worldwide, largely due to modern science and technology with fewer reported incidents of water inrush.

Few studies have been done in South Africa on seepage in mines while a lot of studies focuses on the impact of mining on water resources in South Africa. Mengistu et al. (2015), used environmental stable isotope (ESI) and hydrochemical information to assess the source of excess water at a pumping shaft located near the town of Stilfontein, North West Province, South Africa. The outcome indicated that the water observed at the Shaft is mainly from seepage of a nearby mine tailings dam and from the dolomite aquifer in the area. DWAF, (2008) summarised/highlighted the influence of mining on water seepage/ingresses into the mining voids, the common sources of seepage and their impacts on mining working areas in the South African mining industry.

There is clearly a knowledge gap/ published work of seepage in mine working areas in South African. This study utilises hydrochemical and tracer techniques to investigate the source(s) of seepage at a deep gold mine in the Witwatersrand basin, Gauteng Province, South Africa, adding knowledge to what has already been done in the country.

1.2 Hypothesis

The study has hypothesised that integrating hydrochemistry and tracer techniques may reveal seepage mechanisms to underground mine workings and flow paths

1.3 Research Questions

The study is guided by the following main research question: ***What are the possible source(s) of seepage water at SDGM?*** However, to answer and/ or investigate the source of seepage at SDGM the following key research questions have been formulated:

- What are the hydrogeochemical characteristics governing the chemical evolutions within SDGM and what is the residence time for seepage water?
- What are the hydrogeological and/ or geological structures controlling/governing the occurrence of seepage?

1.4 Research Objectives

The study aims to promote sustainable mine water management through a better understanding of the source of seepage by utilising integrated hydrochemical and tracer techniques. A better understanding of the sources of seepage at SDGM will assist the mine with strategic planning and design, and rock-support replacements.

The main objective of this research work is "***To investigate the source(s) of seepage water at SDGM***" and to achieve this specific objective, the following key objectives were considered:

- To investigate the hydrogeochemical characteristics governing the chemical evolutions; and
- To investigate hydrogeological and/ or geological structures governing the occurrence of seepage.

1.5 Research Limitations

The extent to which the study is completed is limited to data availability. Data include accessibility of the underground sampling points (with seepages) due to the safety of personnel in the study area. Limitations of data (e.g isotope data) from groundwater monitoring boreholes and the extent to which the data covers. There was no data available for boreholes tapping into the deeper dolomite in the area, and such information was not collected for sampling, thus this study will rely on the old reports on the deeper aquifer. There was also no groundwater isotopic data in the study area. Covid 19 also had an impact on data collection and submission to the labs for analysis due to lockdown regulations. Laboratory costs for sampled water analysis resulted in a limited number of samples that were collected and analysed.

CHAPTER 2

LITERATURE REVIEW

2.1 Introduction

Seepage water investigations in underground mines have been conducted globally. Various studies have revealed varying results due to variable site characteristics, including seepage or base-flow from nearby rivers, groundwater ingress/inrush, and surficial sources (Water Return Dams/ Pollution Control Dams/ Sumps / Tailings Dams / Ponds) from mining activities (Rubio et al., 1998, Mulenga 1993; Mengistu et al., 2015). Furthermore, various studies also revealed that seepage water can be generated or caused by the cessation of dewatering activities (DWAF, 2008).

Seepage investigation in underground mines is well known and various investigations have been conducted throughout the world (Duan et al., 2019). Various techniques have been applied from one mine to another depending on the nature of seepage. However, understanding and quantification of seepage in underground mines is very challenging due to the complex nature of seepage occurrence and varying hydrological and hydrogeological characteristics. Therefore, these data need to be assessed to provide a better understanding of seepage occurrence as well as to accurately quantify seepage flow.

The section below provides an in-depth understanding of (i) seepage occurrence in underground mines, (ii) an overview of the commonly used techniques to assess seepage occurrence in underground mines, (iii) a summary of the commonly used techniques to assess seepage occurrence and the most feasible techniques to assess seepage occurrence in underground mining areas. The last section of this chapter evaluates seepage investigation techniques utilised (integrated hydrochemical and tracer techniques) at SDGM.

2.2 Definitions and Concept of Seepage Occurrence in Underground Mines

Seepage occurs when the mine cuts through aquifers and/ or when mining occurs below the piezometric surface (Fernandez et al., 1988). Furthermore, seepage can occur through mining-induced activities such as permanent and temporary engineering openings. Permanent engineering openings include shafts (inclines and decline (Figure 2-1)), conveyor excavations, escape ways and so on. While temporary openings include opening such as stopes, drill drives, and ventilation rises.

Several sources contributing to seepage/ingress into underground workings have been identified (Scott, 1995; Krige, 1999; Horstman et al., 2004a and 2004b). These sources can be summarised as follows: (i) direct rainfall onto open mine workings, stopes, and old surface workings; (ii) groundwater seepage into mine workings due to disturbance of natural groundwater conditions by mining activities; (iii) water from nearby old or decanting mines; (iv) poor service water management underground; and/or (v) base-flow from streams and rivers overlying mine workings. Such streams seep water directly into mine openings and to the shallow groundwater system above zones of shallow undermining and historical surface operations. DWAF, (2008) identified different sources of seepages:

- Underground void contact with surface water (pond, river, canal, or stream).
- Underground void contact with surface unconsolidated deposits-glacial or organic.
- Strata water entering underground workings.
- Shaft sinking.
- Clearing old shafts.
- Neighbouring mines that are hydraulically connected.

DWAF (2008) characterised water ingress pathways associated with different mining methods. According to the study, it concluded that shallow mines often experience ingress into mine workings from surface water sources or outcrop openings and shafts (vertical and incline shafts) or either through storm water runoff or through riverbed loss where these features intersect watercourses. Furthermore, the study concluded that direct rainfall infiltration through weathered zones and outcropping fractures are one of the common sources of ingress into mine voids especially in shallow open cast mines. Direct rainfall recharge is normally prevalent in open cast mines. However, this is also possible in deep underground mines where water-bearing formations are exposed on the surface and there is a high structural density that acts as conduits for rainwater.

Apart from direct rainfall infiltration and/ or direct rainfall recharge, particularly in deep underground mines that are below groundwater aquifers, significant groundwater ingress can drain into the underground workings, especially if the aquifer is closer to the void. In contrast, aquifers may be far from the mine void and not be directly disturbed by mining activities, but the mine still experience observed seepage inflows due to poor mine water management within the operations. Experience shows that poor underground mine water management is one of the common causes that can lead to seepages in a mine.

Unmanaged water may seep through openings into other working areas resulting in the damage of rock-support and machinery. As an example, unmanaged water from backfilling processes may run down the ramp and/or declining surfaces and if there are openings –geological structures, mining-induced openings or subsidence related openings, between mined out areas or levels, water can seep through and be observed on the current active stope (DWAF, 2008). Backfill water can be mistaken as groundwater and needs to be scientifically proven/defined through chemical analysis.

Poor underground mine service water management (from backfill, damaged pipes or overflowing water dams) can contribute to excess water in a mine. Furthermore, underground workings in contact with abandoned old workings and failure of the underground dam, seal, or leakage of a borehole can contribute to excess water if not properly managed.

It is clearly evident that seepage occurrence is the result of various surface and subsurface complexities. Apart from surface and subsurface complexities, it is also been observed that various mining techniques and other mining activities have the potential to facilitate seepage occurrence or generation through permanent and/ or temporary openings that can act as a conduit to flow and also connect the subsurface layer. This makes it extremely challenging to assess seepage occurrence accurately and precisely.

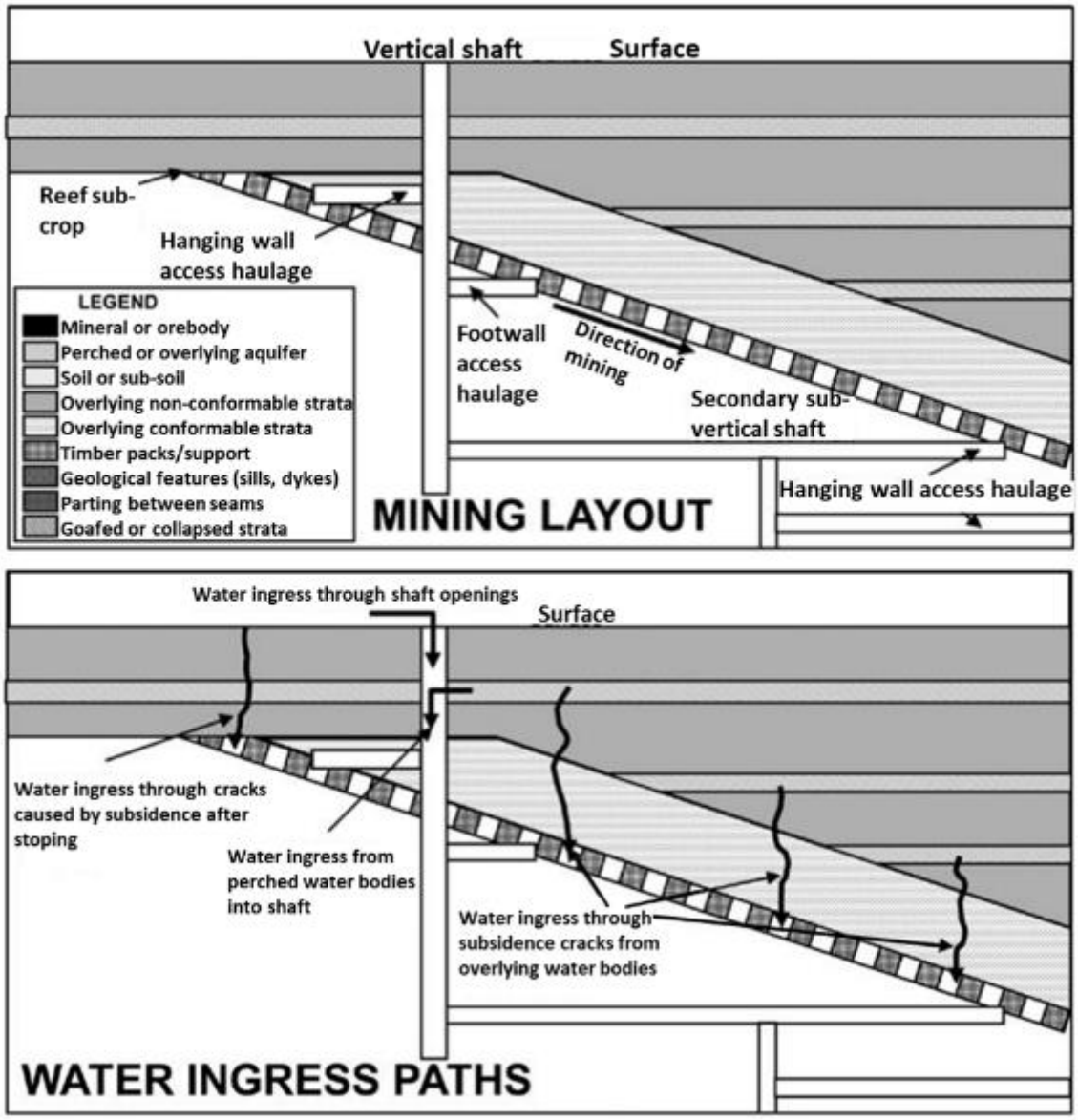

Figure 2-1: Cross-section through a typical deep reef mine showing water ingress through subsidence cracks from overlying water bodies (Source: DWAF, 2008)

2.3 An overview of the commonly used techniques to assess seepage occurrence in various mining areas

Several methods have been applied to assess seepage occurrence. Various hydrogeochemical and tracer techniques (pH, EC, DO, redox, alkalinity, trace metals, major anions, and total element concentrations) have been utilised to assess the source of seepage globally.

Mengistu et al. (2015) investigated the source of excess water at a pumping shaft using the environmental stable isotope (ESI). To supplement the results, the water samples were further analysed for tritium. The results confirmed that recent recharge is taking place through open

fractures as well as man-made underground workings and the hydrochemistry data illustrated the presence of mine water signatures. The results illustrated excess water was mostly coming from seepage of a closer mine tailings dam and the local aquifer Tritium data illustrated that recent recharge is through open fractures as well as artificial (man-made) underground workstations.

Similar to Mengistu et al. (2015), Majumder and Shimada (2016) utilised integrated hydrochemistry and environmental Isotopes to identify the origin of water ingress at Barapukuria Coal Mine in North-western Bangladesh. According to the study, the $\delta^{18}O$, and $\delta^{2}H$ results showed that the groundwater and mine inflow water originates from local rainfalls. Further, the results showed good hydraulic connectivity between the fractured coal seam aquifers and the covering Dupi Tila aquifers.

Cozma et al. (2016) used natural tracers ^{222}Rn, ^{226}Ra, $\delta^{18}O$, and $\delta^{2}H$ to determine the source, mixing and dynamics of waters while Kusumayudha et al. (2018) analysed fissure/fracture structures to unravel groundwater inflow problems in a gold mine site located in the Pongkor area of West Java, Indonesia. The analytical assessment was done using secondary and primary data, compiled with some fieldwork, such as surveys, observations, and mappings. Furthermore, information from remote sensing by satellite imagery analysis was used. The results illustrated that different pathways, residence times, and geochemical processes exist. Groundwater recharge in the particular study area was discovered to come from atmospheric precipitations, submitted to a longer or shorter path, and it is subjected to interact with the host rocks (Water rock interaction). Guan et al. (2019*)* applied hydrogeochemical (fuzzy comprehensive evaluation method and cluster analysis method) and isotope analyses to detect the inrush water sources of the Mindong No. 1 mine, situated in north-east Inner Mongolia of China. The results indicated the presence of river leakage into the fracture scheme cutting through the tunnel, triggering floods in the tunnel.

Mulenga (1992) used a combined study of the historic, dewatering and mining records, structural geology, surface hydrology, rock chemistry, groundwater chemistry, river/surface gauging, evaporation measurements and groundwater flow numerical modelling at Konkola mine to find and solve their water inflow problems. The study concluded that the water originates from surface recharge close to the mine and the regional aquifers at greater depths.

Various techniques exist to assess seepage occurrence. It is evident that environmental tracers (e.g., isotopes of oxygen, hydrogen) and radioactive elements (e.g., radium and radon) are predominantly used in hydrological investigations for a complete view of the water cycle, groundwater recharge, water-rock interactions, and geochemical processes. In summary, the most used methods are environmental tracer techniques, artificial tracers, hydrochemistry, hydrology, and models.

2.4 Application of Integrated Hydrochemical and Tracers Techniques

2.4.1 Hydrochemical Tracers

2.4.1.1 ***Chemical composition/species in groundwater***

Wide varieties of dissolved inorganic and organic constituents exist in groundwater. This is due to chemical and biochemical interactions that occur between the groundwater and the geological materials of rock surfaces and soils (Hiscock, 2009). Other contributing factors may be from a varying composition of rainfall and atmospheric deposition on groundwater recharge areas or mixing with seawater in coastal regions.

2.4.1.2 ***Factors that influence the chemical composition of groundwater***

Both geogenic and anthropogenic sources may contribute to the alteration of groundwater chemistry. Various hydrochemical techniques that can alter water quality are ion exchange, rock-water interaction, and reduction-oxidation (Singhal and Gupta, 2010). The water composition can additionally provide records of water-rock interactions and microbial procedures in the water. The chemical composition of groundwater can give information about the mineral composition of the host rock. This information can be used to determine recharge areas and the origin of groundwater (meteoric, marine, fossil, magmatic and metamorphic water) and of individual chemical components (e.g., carbonate, sulphate, nitrate, and ammonium) as suggested by Mook (2000). The work further states that the dissolution of host rock or aquifer may cause increased concentrations of toxic substances and heavy metals like Fluoride, Arsenic and Iron, which change the groundwater chemistry drastically.

Singhal and Gupta (2010) indicated that, in addition to the dissolution of rock material, other processes such as ion exchange, membrane filtration and sulphate reduction can modify the chemical composition of groundwater. When groundwater interacts with the rock matrix, it

tends to exchange ionic constituents through reactions such as sorption, adsorption, absorption, and desorption. The reduction of SO_4^{2-} to HS^- is a common reaction in groundwater and takes place in the presence of bacteria $SO_4^{2-} + CH_4$ (bacterial) $\rightarrow HS^- + H_2O + HCO_3^-$. Waters that have gone through sulphate reduction are characterised by the presence of HS− and high content of HCO_3^- (Singhal and Gupta, 2010). Other naturally occurring systems may contribute to elevated dissolved ions in groundwater.

Carbonate systems naturally exist and can contribute to elevated values of carbon in groundwater (Hiscock, 2009). Other inputs may be from the varying composition of rainfall and atmospheric deposition on groundwater recharge areas or mixing with seawater in coastal regions. Mook (2000) highlighted that, mixing of different groundwater is another factor that can influence its chemical composition and can be determined by using δ^2H, $\delta^{18}O$, $\delta^{34}S$ values and the $^{87}Sr/^{86}Sr$ ratio.

Human activities such as agricultural practices, mining activities and municipal wastes may also alter the chemistry of groundwater. Industrial activities have much influence on the chemistry of groundwater in their surrounding areas. The wastewater released from industries contains several dissolved and suspended impurities according to the industry and processes used (Gupta, 2010). For example, mining industries are responsible for groundwater contamination due to acid mine drainage, leachate from mine waste and tailing. Like the mining industry, (in certain regions/areas), agriculture is one of the biggest contributors to a country's economy. Other factors that can contribute to groundwater chemistry changes include seawater intrusion and groundwater mixing.

Hiscock (2009) summarised the common changes in hydrochemical facies along a groundwater flow-path, where dilute rainwater comprised of NaCl water type and dissolved CO_2 dissolved in the infiltrating water as indicated in Figure 2-2.

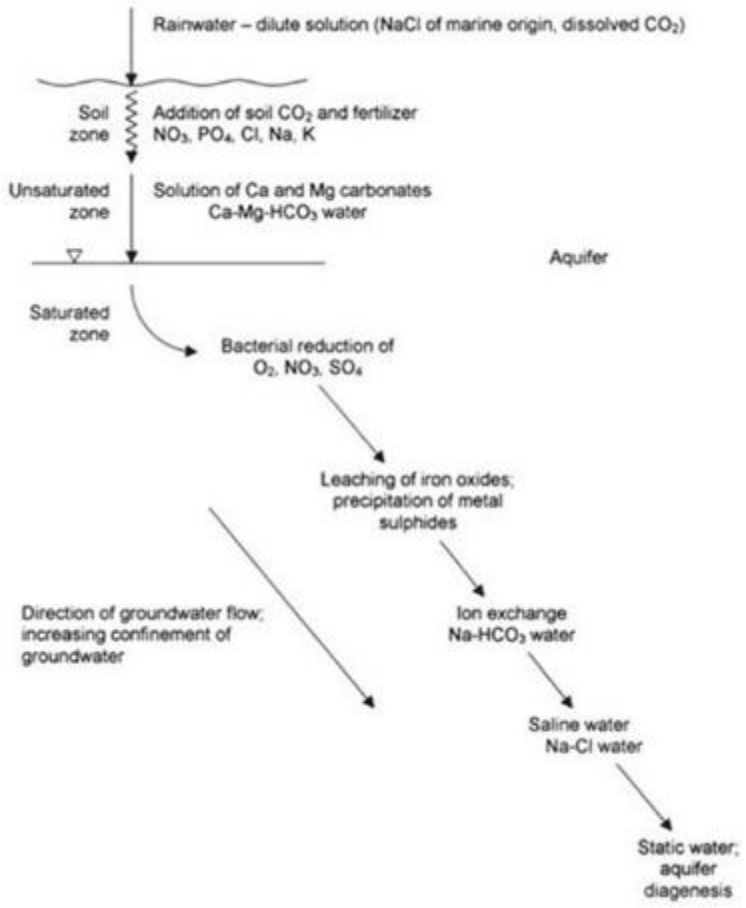

Figure 2-2: Schematic diagram summarising the common changes in hydrochemical facies along a groundwater flow-path (Source: Hisckock, 2009)

2.4.2 Environmental Tracers

Tracer techniques contributed to the advancement of hydrology by improving hydrological investigations of subsurface examining methods. This entails an assessment of water in all its different phases/forms, behaviours and characteristics in different mediums and cycle (Sieber and Uhlenbrook, 2005).

In South (ern) Africa, tracer studies are becoming common tools of hydrological investigations (Talma and Van Wyk, 2013). According to Sieber and Uhlenbrook (2005), tracers are substances with the potential to be detected at very low concentrations and they make it simpler for water flow to be traced through different systems. Tracers should be non-reactive (conservative) and easily measurable, mobile, soluble, and not retarded by soil or aquifer matrix (Mook and De Vries, 2000). This character allows the substance used to not interfere with the condition of the water investigated, thus, real representation of the water/study is evaluated.

Tracers have been successfully used in understanding the groundwater flow dynamics, mixing and recharge conditions (Sami, 1992; Adams and Younger, 2001; Abiye et al., 2015). The ability to trace the flow of water is imperative in understanding groundwater flow systems of an area, and studies have revealed that this is best done by environmental tracers.

Understanding the water flow systems of an area can help in the identification of potential sources of seepage that might be present in that area. Moreover, predictions of water quality for health reasons, climate or land-use changes and many other motives can be aided with the understanding of the dynamics of water in an area.

2.4.2.1 ***Isotopic Species in Groundwater***

Water in its natural state contains mainly Hydrogen (H) of mass (^{1}H) and Oxygen (O) of mass 16 (^{16}O). Additionally, it contains small amounts of Deuterium (^{2}H), Tritium (^{3}H), and isotopes of oxygen (^{17}O and ^{18}O) as expressed by Singhal and Gupta (2010). Abiye (2013) explained the term environmental isotopes as the measurement of isotope proportions of the elements making up the water molecule and of constituents dissolved in water that can give rise to hydrogen and oxygen. This study utilises environmental stable (^{2}H and ^{18}O) and unstable (^{3}H) isotopes of oxygen and hydrogen to assess and characterise seepage underground.

According to Mook and Rozanski (2000), the most important and commonly used atomic components of the water molecule are ^{16}O and ^{18}O ($\delta^{18}O$) and ^{1}H and ^{2}H ($\delta^{2}H$). They are widely applied in groundwater studies, for example, to trace the origin of water, groundwater mode of recharge and residence/ calculation time (^{3}H). Tracing of groundwater utilising natural isotopes gives supplementary prove on the origin and development of groundwater and its dissolved constituents.

Isotopes further make it possible to evaluate whether there are any mixing and other physical processes or isotopic exchanges in systems. As explained by Clark and Fitz (1997), certain isotopes are stable while others are radioactive. Six isotopes of hydrogen and oxygen exist, (^{1}H, ^{2}H, H^{3}, ^{16}O, ^{17}O and ^{18}O), five are stable, while Tritium (^{3}H) is radioactive with a half-life of 12.3 years (Singhal and Gupta, 2010). According to Mook and Rosanski (2000), secondary water-rock interactions can be studied, and groundwater residence time can be calculated by using unstable radioactive isotopes, ^{14}C or ^{3}H as an example.

Furthermore, the stable isotopes (^{18}O and ^{2}H) in rainwater provide unique signatures, evidenced by atmospheric processes, altitude and latitude, and the characteristic weather pattern throughout the year (Baqa, 2017). These stable isotopes are also used to provide an insight into the processes and/ or mechanisms under which water was recharged into the aquifer and possibly to estimate the recharge. Craig (1961) concludes that even though isotopic content varies exceptionally in precipitation, precipitation that has not suffered from significant evaporation shows a specific relationship between Oxygen and Deuterium (^{2}H) as illustrated by Equation 1.

$$\delta^{2}H = 8 * \delta^{18}O + 10 ‰ \qquad \textbf{Equation 1}$$

On a global scale, the isotopic composition of ^{18}O and ^{2}H is mostly driven by evaporation from the oceanic surface and the progressive rainout from the ocean to the inland regions. Therefore, from the analysis, it can be determined whether significant evaporation occurred before the water was recharged into the aquifer, and if it is possible, it can be assumed that direct rainfall-infiltrating or preferential flow mechanism was/is not the dominant process controlling recharge (Mazor, 2004).

Radioactive isotopes are important in groundwater studies and their main role is isotopic dating (Cook, 2020). The time unit is given by half-life $T_{1/2}$ where any movement of a particular isotope deteriorates by 50%. Various environmental isotopes have distinctive half-lives and decay rates. For illustration, Mook and Rozanski (2000) show that, half-life range from 300 000 yr (^{36}Cl) to 5 730 yr (^{14}C) and 12.43 yr (^{3}H). They further highlighted that two primary standards of groundwater dating exist, and these are cosmogonic and dating of groundwater using input functions in time.

Cosmogonic radionuclides are calculated using Equation 2 where initial motion A_{init} is known or can be evaluated and $T_{1/2}$ is the half-life of the given radionuclide (Mook and Rozanski 2000). The second standard of groundwater dating by means of input functions in time requires input function to be known or determined (Clark and Fitz, 1997). This incorporates anthropogenic radionuclides created by atomic weapon tests (Mook and Rozanski, 2000 and Leibundgut and Seibert, 2011). Examples of these are ^{3}H, $^{3}H/^{3}He$, ^{14}C and ^{36}Cl and ^{86}Kr produced by the nuclear energy industry.

$$t = \frac{\ln 2}{T1/2} \ln\left(\frac{Ainit}{Aspl}\right)$$ **Equation 2 (Mook and Rozanski, 2000)**

Integrated hydrochemical and tracer techniques (tracer hydrology) helps to address important questions in hydrogeology and give an understanding of the complex processes in hydrological systems.

2.4.3 Application of Integrated Hydrochemical and Tracers Techniques

Hydrochemical assessment is one of the commonly used techniques in hydrogeology to classify groundwater characteristics (Hiscock, 2009). Furthermore, the distribution of hydrochemical factors (such as physical parameters, pH, EC, TDS etc.) in groundwater can assist in providing an understanding of the hydrogeochemical evolution as well as to aid decisions relating to drinking water quality condition.

Tracers play a significant role in hydrogeology in that they provide an improved understanding of hydrological systems such as aquifers, catchments, and streams (Singhal and Gupta, 2010). Each tracer method has its strengths and weaknesses and hence, understanding the concept, assumption, limitation and applicability of each technique is of significant importance. One of the key advantages of using environmental tracers is the ability to cover wide (area) range/scale, and the ease at which they can be injected for longer periods, however, environmental tracers can be expensive to analyse and therefore require enough budget.

Leibundgut and Seibert (2011), Abiye (2013) and Mengistu et al. (2015) emphasized the use of multiple independent methods and techniques simultaneously in hydrological investigations and the benefits as it mitigates the risks of producing unreliable results. This limits one tracer from swaying the characterisation of the hydrological system. Integrated hydrochemical and isotopic tracer techniques can provide valuable complementary information.

The advantage of integrating techniques is the weight/value of the combined results obtained from different independent methods for general and confident conclusions. Integrating techniques further allows one to reduce uncertainties of individual methods.

In this project, integrated hydrochemical and environmental tracer techniques are utilised to provide a better understanding of the source of seepage at SDGM. The stable isotopes of Oxygen (^{18}O) and Hydrogen (^{2}H) are utilised to characterise the source of seepage occurrence in underground workings. Tritium (^{3}H) is utilised to distinguish between old groundwater and

the recent recharge water, and as well as for dating such groundwater samples. Additionally, chemical compounds are assessed for a definite interpretation of isotope results (Mook, 2000). Studies show that these techniques have been applied in several investigations with success. Hydrogeochemical analyses are widely used in mining for seepage source identification (Zhang et al., 2018).

Hydrogeochemical tracers and environmental isotopes have been successfully integrated to identify the source of seepage and pollution in the mining industry (Abiye et al., 2015). The hydrochemical analysis gives an understanding of the hydrological system in a study area, and how groundwater changes with time due to geology (rock-water interactions, dissolution of the host rock, ion exchanges). The analysed data can be plotted on several diagrams that characterise the water. Once the water type is established, it then becomes possible to work out the type of system and/or processes that the water went through. Moreover, water mixing, and possible flow paths can be understood by the assessment of selected inorganic chemical constituents. This information is then integrated with isotopic analysis to work out the source of seepage at SDGM.

2.4.4 Summary

An overview of integrated hydrochemical and tracer techniques was evaluated. Furthermore, the review on the application of integrated hydrochemical and tracer techniques to investigate the source of seepage in underground gold mines was undertaken. The review included (i) seepage occurrence in underground mines, (ii) an overview of the commonly used techniques (^{18}O, ^{2}H and ^{3}H) to assess seepage occurrence in underground mines, (iii) a summary of the commonly used techniques to assess seepage occurrence and the most feasible techniques for seepage investigation in various mining areas. The last section of this chapter evaluated seepage investigation techniques utilised (integrated hydrochemical and tracer techniques) at SDGM

CHAPTER 3

STUDY AREA

3.1 Description of the study area

South Deep Gold Mine (here-in-after SDGM) is located approximately 15 km (South of South-East) of Westonaria town, near the intersection of N12 (national road) and the R28 (provincial road) in the West Rand, Gauteng Province (Figure 3-1). The area is characterised by hills with gentle undulating slopes and tailing dams due to the existence of several gold mines. Westonaria is largely characterised by residential areas, farms, wildlife reserves, and several gold mines.

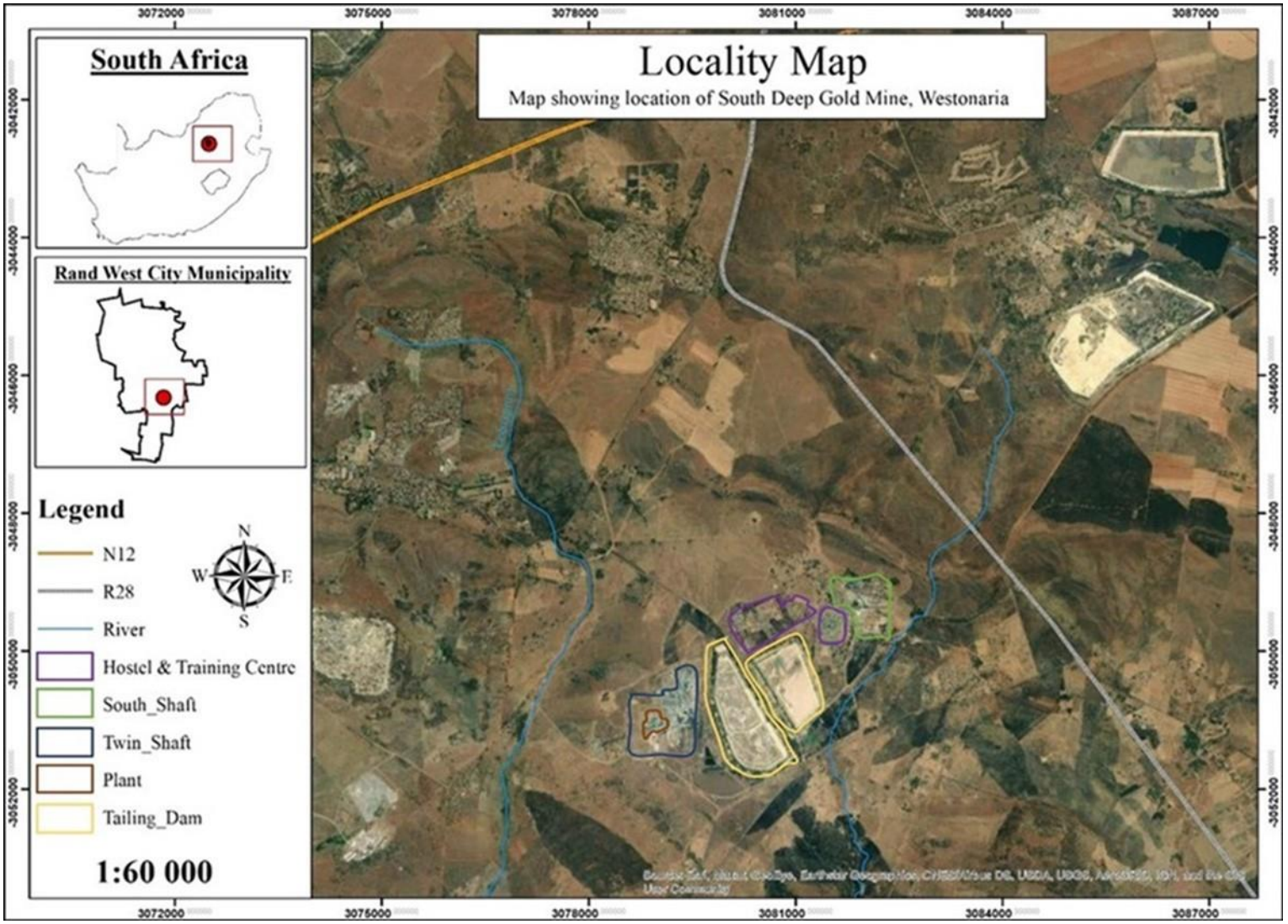

Figure 3-1: South deep locality map showing major access roads to the mine and main infrastruct

3.2 Climate

3.2.1 Regional Climate

The mine is situated in the Highveld region of South Africa and experiences typical semi-arid climate conditions (WRDM, 2017). Summer months (October to March) are characterised by warm to hot temperatures (approximately 24°C-28°C), with maximum temperatures up to 32°C experienced in the late summer months between January and February. Winter months (April-September) are characterised by moderate to cool temperatures (10°C-20°C). Rainfall largely occurs in the summer months, with most of the rainfall largely experienced between November and March. Winter months are characterised by dry cold weather conditions with little to no rainfall. Extreme weather events have been rare in the West Rand District; however, this may change due to climatic conditions (WRDM, 2017).

3.2.2 Precipitation: Mean Monthly and Annual Rainfall for the Site

The mine receives its rainfall data from the South African Weather Service`s Westonaria Kloof Mine station. This weather station is the closest station to the site with the longest rainfall record and has a similar elevation to the mine. According to Barnard (1999), SD EMP (2011) and Golder (2018), the mean monthly rainfall in the region that hosts the mine ranges between 3 mm to 119 mm (Table 3.1), annual rainfall ranges between 390 mm to 1800 mm (Figure 3-2) with mean annual precipitation (MAP) ranging between 632 mm- 683 mm. Most rainfall (92%) is observed between October and April, and 8% of the rainfall between May and September (Table 3.1 and Figure 3-2).

A cumulative rainfall departure (CRD) graph for SDGM is shown in Figure 3-3. CRD is a recharge estimation method applied in the semi-arid region (Southern Africa) by subtracting monthly rainfall and the average monthly rainfall (Xu and Beekman, 2003). Increasing trends indicate rainfall above average rainfall events, which possibly contribute to the groundwater recharge (the rising water levels) in the area while declining CRD trends indicate rainfall below-average rainfall events, which implies less groundwater recharge from rainfall (declining water levels).

Table 3.1: Monthly Rainfall, Evaporation Data and Average Temperatures (Source: Modified after South Deep Mine Environmental Management Programme, 2011)

Month	**Mean Monthly Rainfall (mm)**	**Mean Monthly Evaporation (mm)**	**Average Number of Rain days (/month)**	**Average Max Temp (°C)**	**Average Min Temp (°C)**
Station	**Kloof**	**Zuurbekom (S-pan)**	**Kloof**	**Krugersdorp**	**Kroningspark**
January	119	169	10.6	26.1	14.6
February	86	139	8.4	25.5	14.2
March	85	131	7.9	24.3	12.9
April	49	103	5.4	21.3	9.4
May	13	87.1	2.5	19.1	5.6
June	5	70.4	1.5	16.3	2
July	3	79.3	1.4	16.9	2.4
August	9	112	1.7	19.4	4.7
September	22	149	3.7	22.9	0.7
October	72	168	8	24	10.9
November	101	166	10.2	24.6	12.5
December	119	172	11.5	25.7	13.7
Annual	683	1545.8	6.1	22.2	8.6

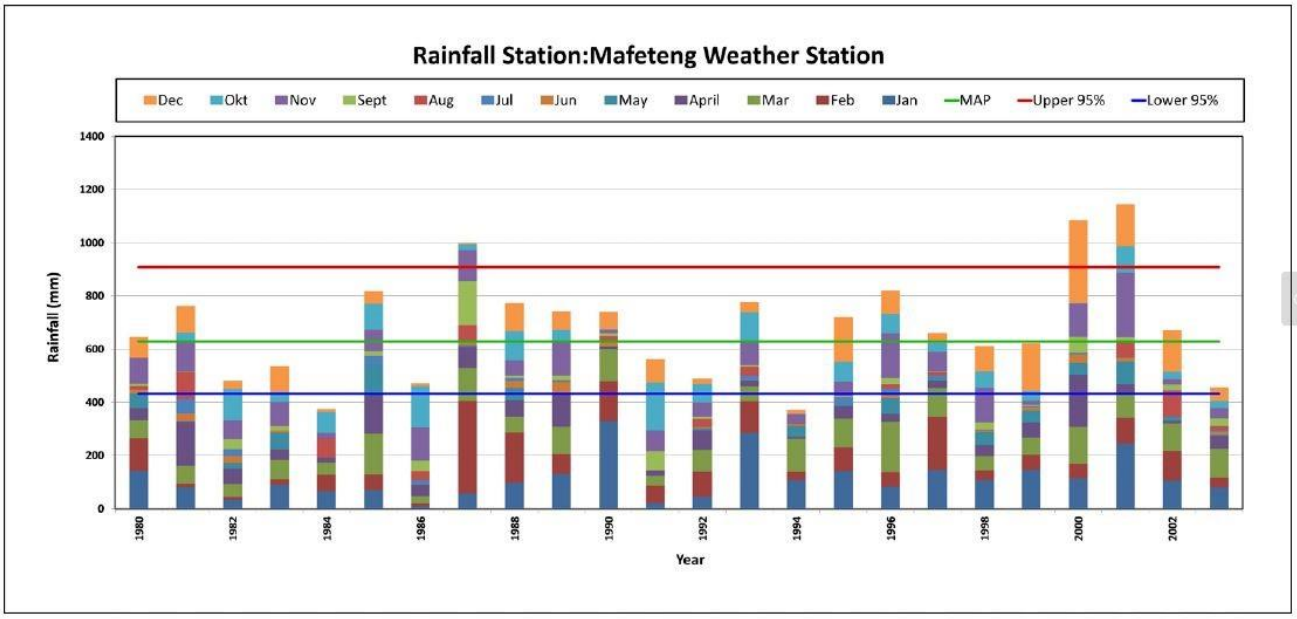

Figure 3-2: Annual rainfall for SDGM (1958-2018) (Source: Golder, 2018)

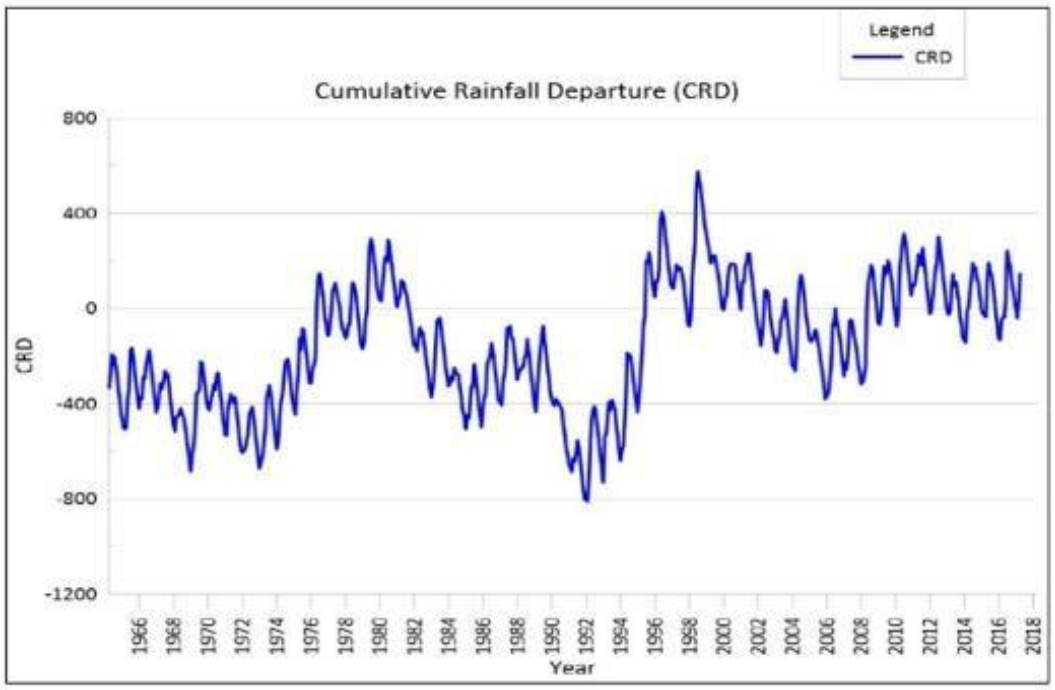

Figure 3-3: Cumulative Rainfall Departure (CRD) for SDGM (Source: Golder, 2020)

3.2.3 Mean Monthly Evaporation

Evaporation data is sourced from the Zuurbekom station. Rainfall and evaporation data are represented in **Error! Reference source not found.** The average S-pan evaporation is approximately 1 546 mm per year (SD EMP, 2011). Evaporation reaches a peak in December with lower evaporations occurring in May, June and July **(**Table 3.1). SDGM is in a region where the rate of evaporation exceeds the rate of precipitation.

3.2.4 Drainage and Surface Topography

The topographical elevation of the study area varies from 1 700 m above mean sea level in the north to 1 580 m above mean sea level in the south. The topographical elevation varies by approximately 220 m. The topography varies from topographical high in the north to topographical low in the south. The landscape in the northern side of the mine is characterised by quartzitic ridges of Gatsrand topographical high while the southern side is characterised by gentle slopes. Gatsrand topographical high occurs across the study area from the west to east direction as shown in Figure 3-4. The mine area is drained by the Leeuspruit, Loopspruit and Rietspruit surface water streams, which run in the north to south directions across the area. The groundwater flow is towards the south as indicated on Figure 3-5.

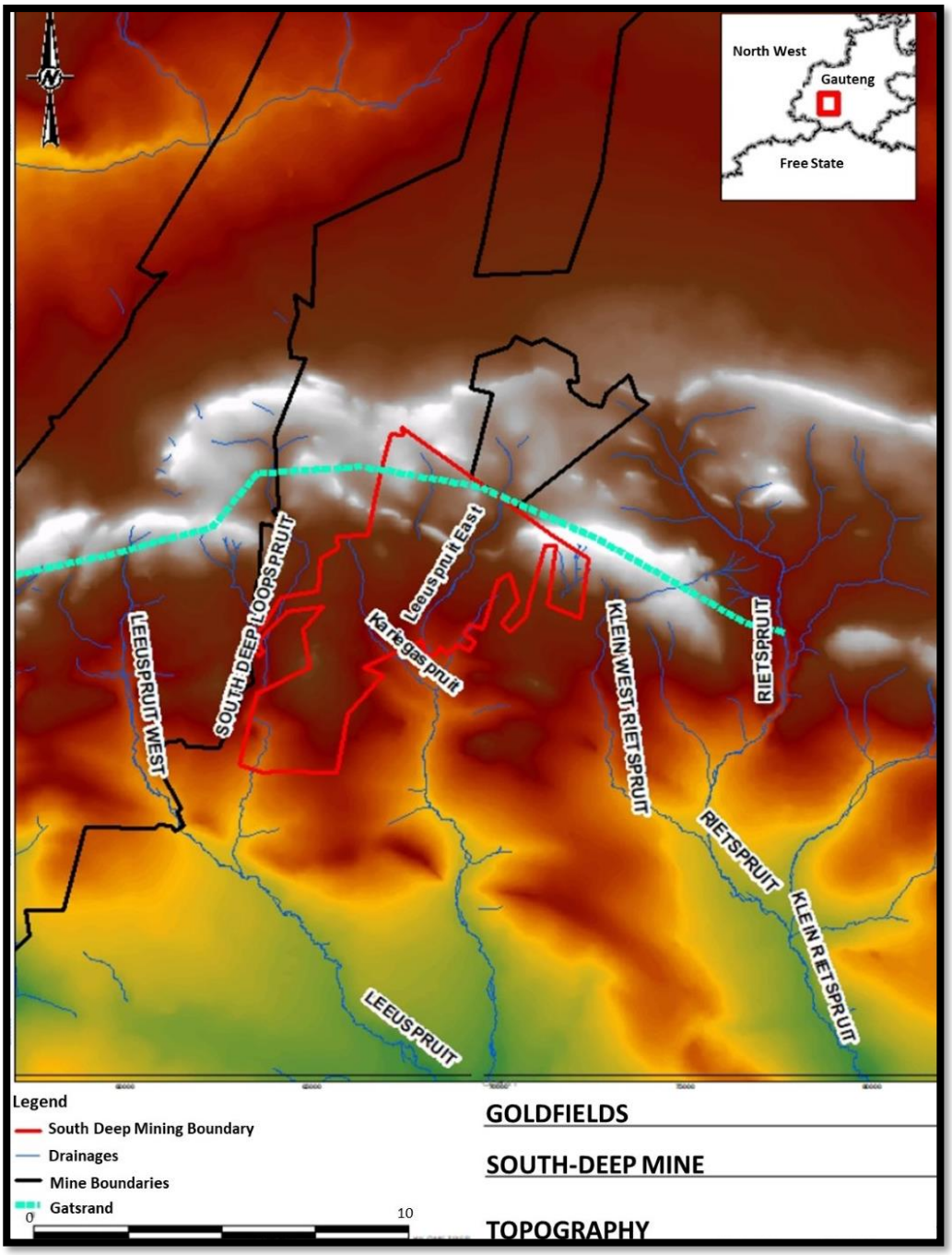

Figure 3-4: Topography map (Source: Modified after Golder, 2020)

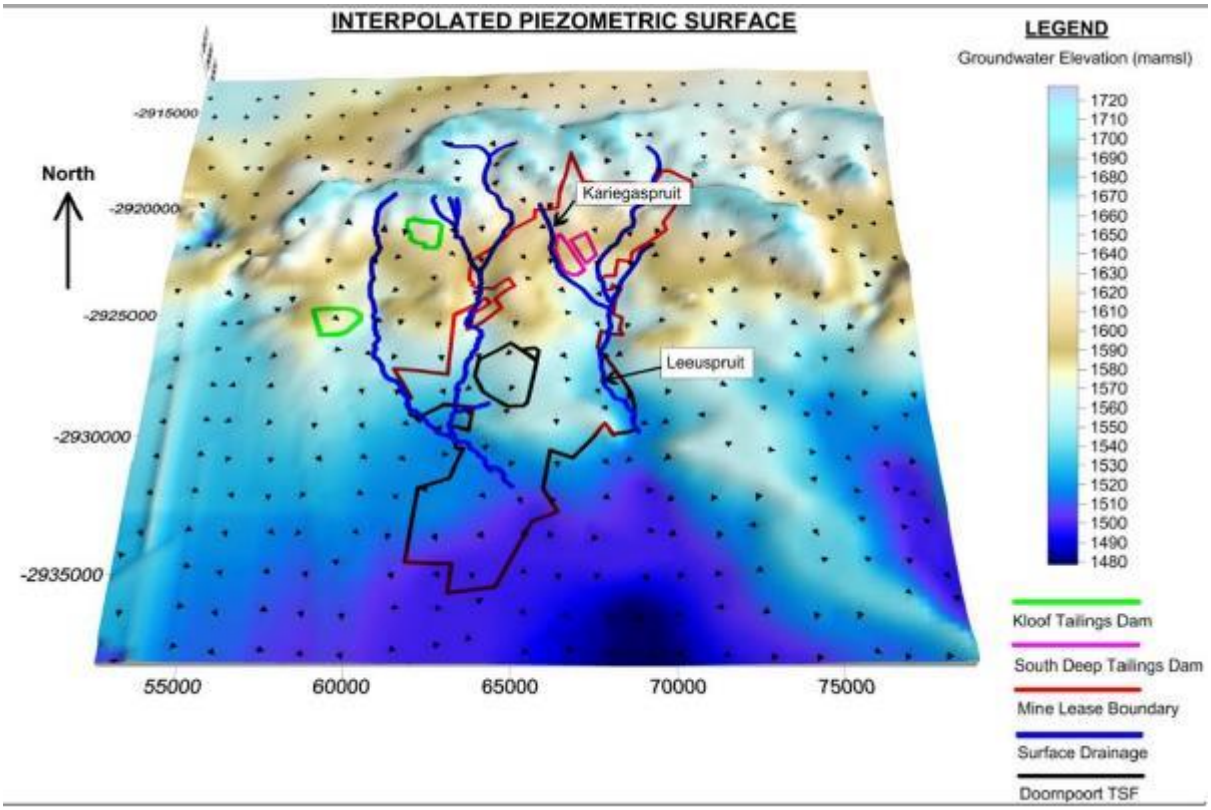

Figure 3-5: Interpolated regional piezometric surface and groundwater flow at SDGM. (Source: Prinsloo 2019)

3.2.5 Land-use, land-cover and Soils

The land use of the study area ranges from rural (undeveloped land) to semi-developed land (rural-urban transition zone) in and around the West Rand District Municipality. The SDGM area can be characterised as rural with disseminated villages associated with agricultural farming activities. The land use within the study area is mainly crop production and smaller parts as livestock farming. These farming activities largely depend on groundwater abstraction through private boreholes, while some depend on rainfall (rain-fed).

3.3 Geology

3.3.1 Regional Geological Setting

SDGM is located in the North-western rim of the Witwatersrand Basin in the Central Rand Group (Goldfields, 2012). The Witwatersrand basin, shown in Figure 3-6, is the biggest gold province worldwide (Dankert and Hein, 2010). According to Tucker et al. (2016), the Witwatersrand basin was formed from a series of crustal plate movements and the sediments that are understood to be

deposited between 2,895 and 2,849 million years ago. They further argue that the Witwatersrand basin was reshaped by three major events, namely; the lateral movement of crustal plates that resulted in severe faulting and folding, the Vredefort meteorite impact that hit the centre of the basin, and lastly the setting of the Bushveld complex, which is the largest unique layered igneous intrusion worldwide.

Gold mineralisation in the Witwatersrand basin is found within conglomerate beds called reefs. The reefs occur within seven dispersed goldfields known as Evander, East Rand, Central Rand, West Rand, Far West Rand, Klerksdorp, and Free State Goldfields as indicated in Figure 3-6. The Goldfields are not continuous due to faulting and other primary mineralisation controls (Robb and Meyer, 1995; Frimmel and Minter, 2002). The SDGM orebody is in the Witwatersrand Supergroup. The Witwatersrand Supergroup is subdivided into the lower West Rand Group (WRG) and the upper Central Rand Group (CRG) as reported by SACS (1980). According to Tucker et al. (2016), the deposition in the Witwatersrand basin originated in a shallow marine setting with quartzite and protruding the iron-rich shale horizons establishing the West Rand Group (WRG).

CRG overlaying the WRG is dominated by the arenaceous quartzite and conglomerate beds quartzwackes and minor shales that were deposited in a braided system of rivers associated with a shallow marine delta (Tucker et al., 2016). Most of the gold mineralisation occurs at the CRG, which is exploited by SDGM. The orebody (CRG) is overlain by the Klipriviersberg Group volcanic rocks (Ventersdorp Supergroup), which are further overlain by the Chuniespoort Group (Transvaal Supergroup). Above the Chuniespoort Group lies the Pretoria Group sediments and outliers of Karoo Supergroup shales and sandstones. Figure 3-7 shows a general stratigraphy of the Witwatersrand basin around Johannesburg. The Witwatersrand rocks are unconformably overlain by the Ventersdorp Supergroup lavas (Osburn et al., 2014).

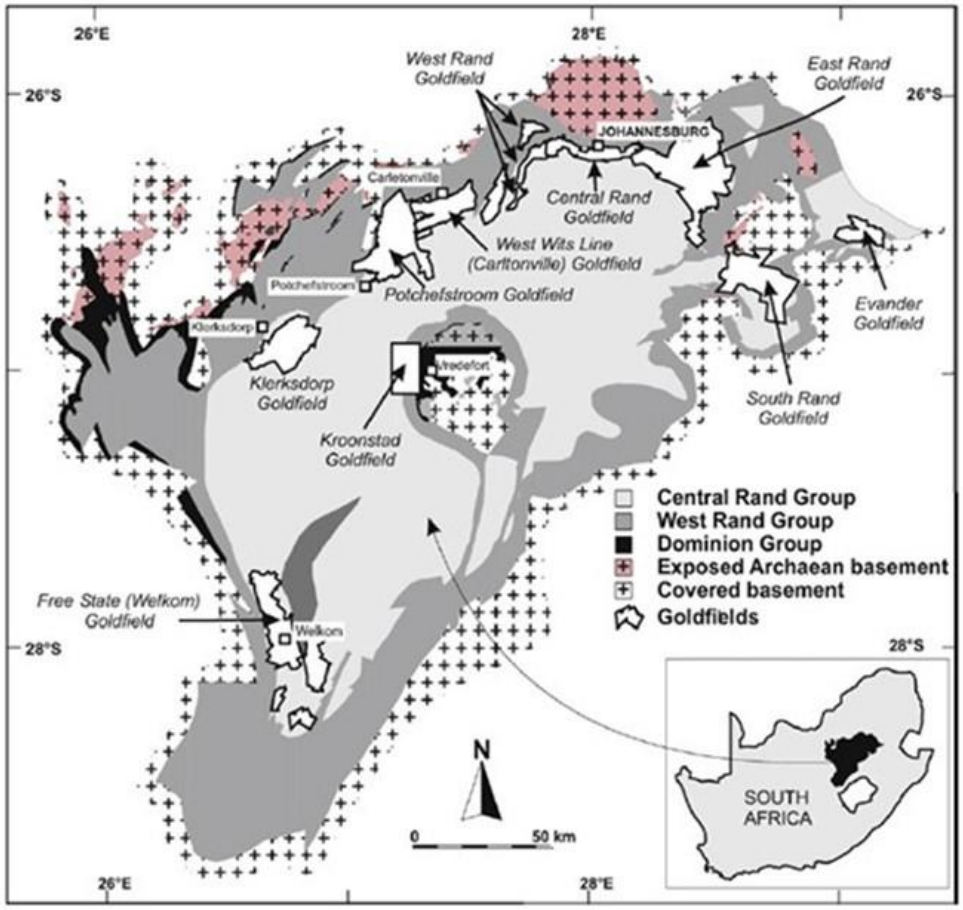

Figure 3-6: Geological map of the Witwatersrand Basin (Source: Dankert and Hein, 2010)

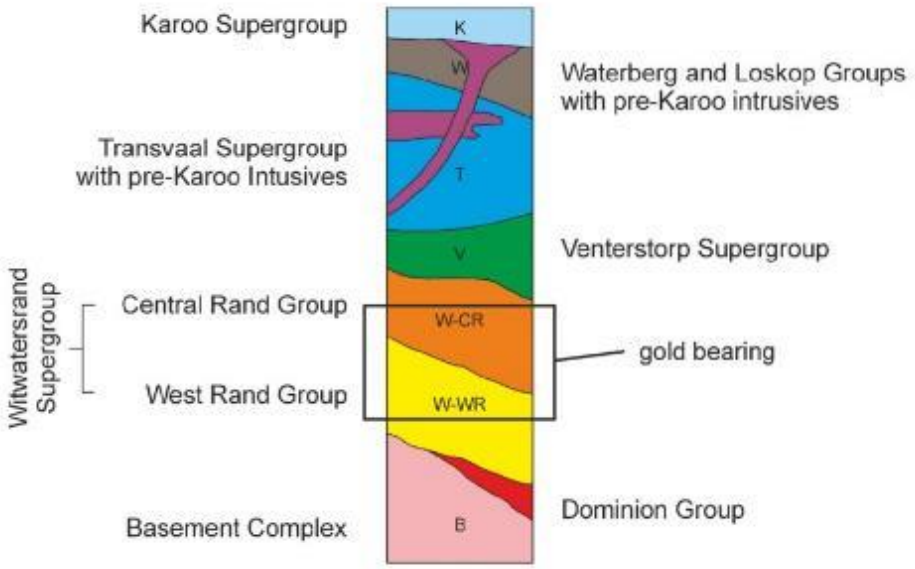

Figure 3-7: General stratigraphy of the Witwatersrand basin around Johannesburg (Source: Menschik, 2015 after Guilbert and Park 1986)

3.3.2 Local Geology

The geology of SDGM is shown in Figure 3-8, whereas Figure 3-9 shows a schematic 3D section through the mine, and Table 3.2 outlines the Lithostratigraphy (groups, subgroups, and formations) of the Dominion Group, Witwatersrand, Ventersdorp Supergroup, and the Transvaal Basin sequences in the study area. Mining right surface area is characterised by sedimentary strata of the southerly dipping Transvaal Supergroup (Timeball Hill Formation quartzite, shale and siltstone of the Pretoria Group) (Figure 3-9). The Chuniespoort (Malmali) dolomite outcrops in the northern side of the study area (Golder, 2013). Outcrops of Mudstones and quartzites belonging to the Timehill Formation cover a larger portion of the mine property (Golder, 2020). An outcrop of Andesitic lava belonging to the Hekpoort Formation is observed in the southern extent of the property.

The Chuniespoort dolomites are below the Pretoria group sediments, which comprise of ~6-7 km thick intercalated mudstone-sandstone units, andesites and conglomerate beds, diamictite and carbonate units (Manzi et al., 2013). They further explained that the dolomites are underlain by the Ventersdorp Supergroup comprising of ultramafic and mafic meta-volcanic rocks together with metasedimentary rocks. The Ventersdorp Supergroup is underlain by the Ventersdorp contact reef (VCR), which consists of a thin auriferous conglomerate reef. The VCR is an erosional surface that formed at the end of the deposition of CRG.

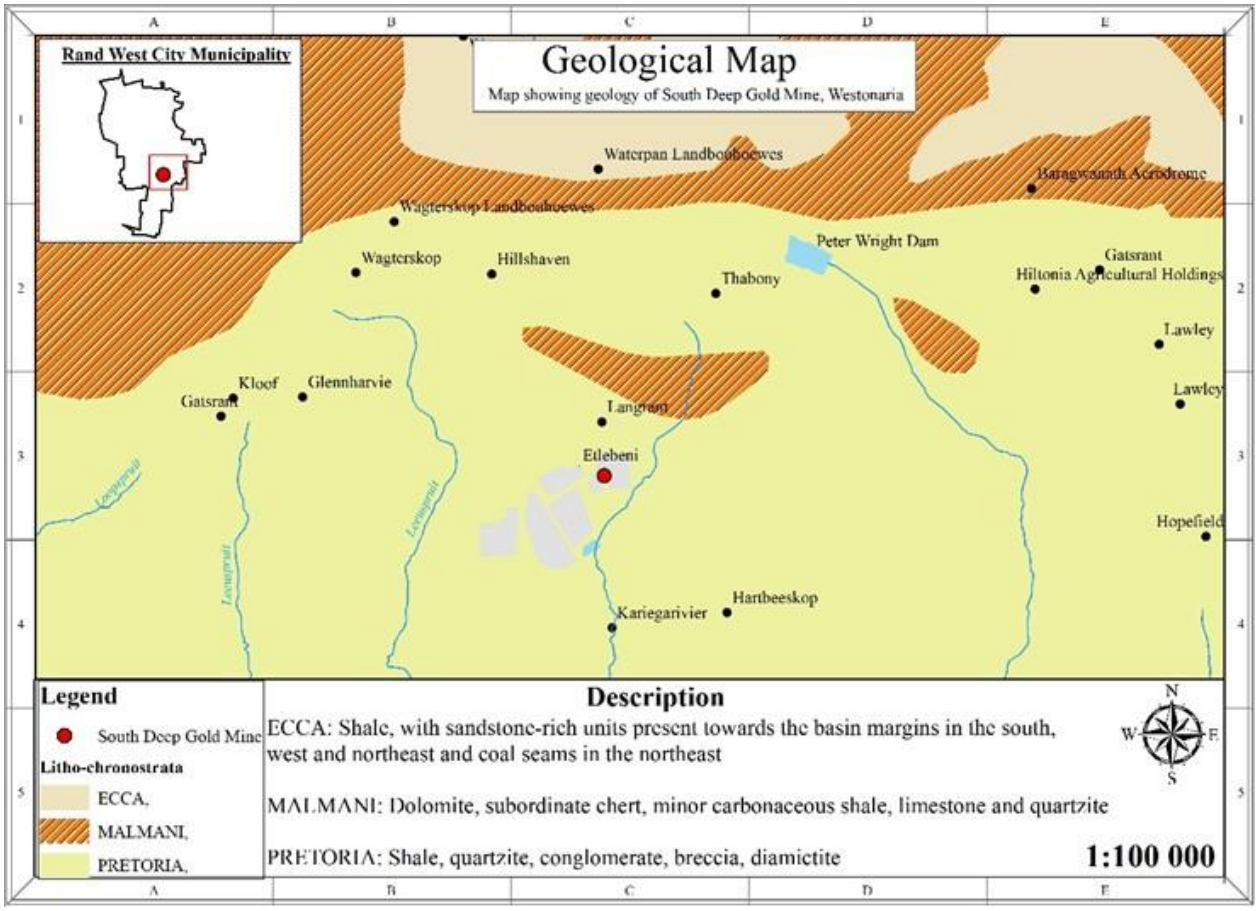

Figure 3-8: Map showing the geology of SDGM

Table 3.2: Regional Stratigraphy at South Deep Mine (Source: Dankert and Hein, 2010)

Thickness	Unit	Informal	Unit Member	Formation	Sub Group	Group	Super Group
200 - 500m				Hekpoort Andesite		Pretoria	TRANSVAAL
50 - 200m				Timeball Hill			
				Rooihoogte			
300m				Eccles	Malmani	Chuniespoort	
150m				Lyttleton			
500m				Monte Christo			
100m				Oak Tree			
10 - 20m				Black Reef			
400 - 500m				Edenville		Klipriviersberg	Ventersdorp
				Lorraine			
				Jeanette			
100m				Orkney			
250m				Alberton			
0-40m				Westonaria			
0-6m	VCR	Ventersdorp Contact Reef		Venterspost			
Approx. 700 metres	MB	Elsburg Massives	Modderfontein	Mondeor	Turffontein Sub-Group	Central Rand Group	Witwatersrand
	MI						
	MA						
	ED	Elsburg Individuals	Waterpan				
	EC						
	EB						
	UE6/EA		Doornpoort				
	UE5						
	UE4		Bekkersdal	Elsburgs			
	UE3						
	UE2						
	UE1		Gemsbokfontein				
	UE1A						
	E9		Panvlakte	Kimberley			
	E8						
	E1-7		Gemspost				
	K11		Vlakfontein				
	K10						
	K9						
	K8	K8 Shale	Rietvalei				
	K7						
	K6						
	K5						

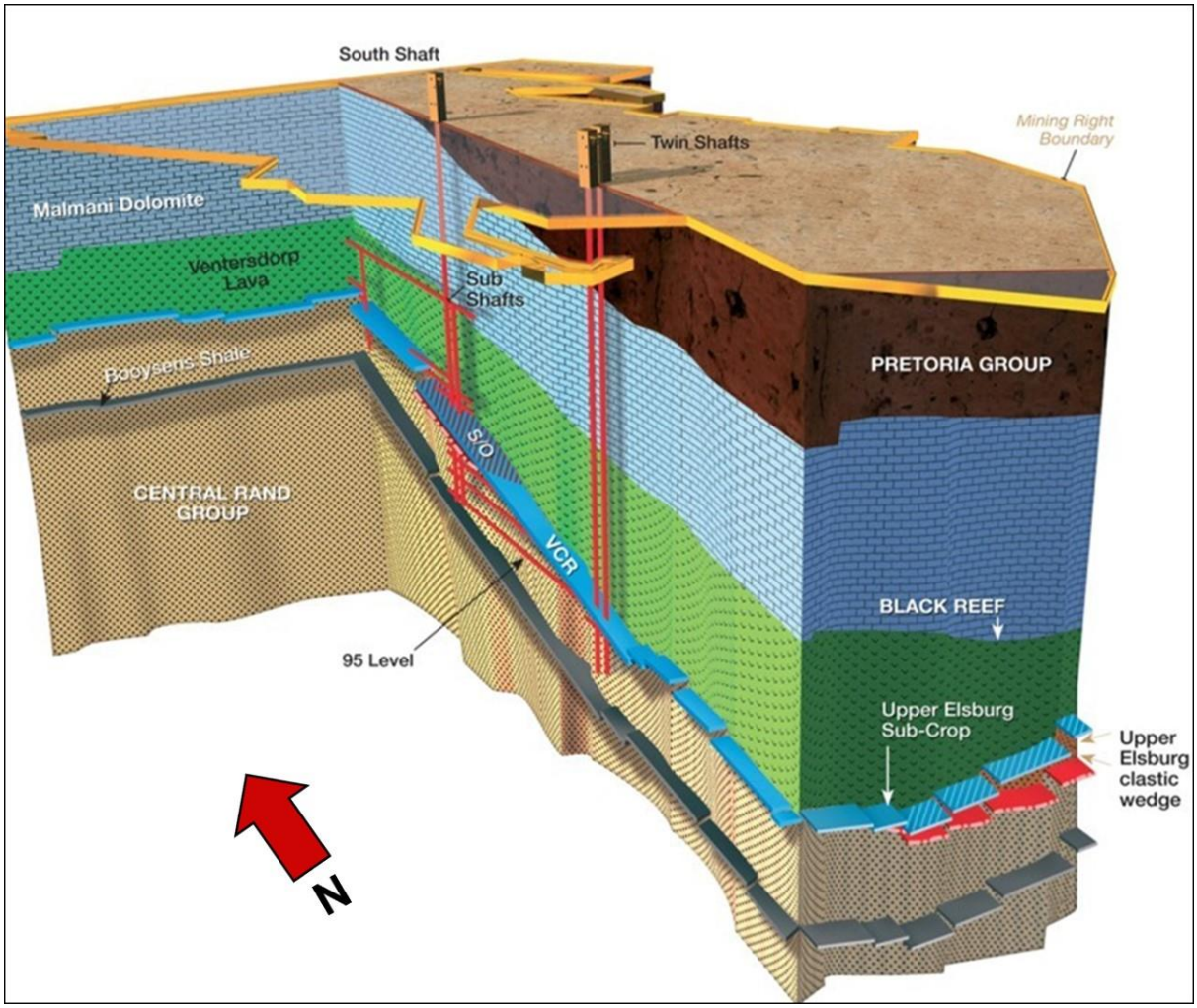

Figure 3-9: A schematic isometric diagram illustrating the geological sequence at South Deep Gold Mine (Source: Gold Fields, 2011)

3.3.3 Underground Mine Geology

SDGM exploits mostly the reef horizons from the Ventersdorp Contact Reef (VCR) and the Upper Elsburgs of the Mondeor Formation (CRG). VCR is well developed on the western side of the Upper Elsburg subcrop (buried rocks that were exposed at ancient erosion surfaces). These are found at a depth of between 2 000 m and 3 500 m below the surface. The Elsburgs reef units are divided into Massives and Individuals (Osburn et al., 2014). The Upper Elsburg Massives (MB`s, MI`s and MA) and Individuals (EA`s, EB`s, EC`s and ED`s) of the Waterpan and Modderfontein Members constitute the upper portion of the Mondeor Formation (Turffontein Subgroup) and are the main mining target at South Deep.

The Upper Elsburg appears as a clastic wedge composed out of 15 units with a rotational on-lap and disconformity between each unit (Osburn et al., 2014). The wedge diverges from the western

side of the mining area (against the VCR) to a vertical thickness of around 130 meters at the eastern boundary of the mine, (Figure 3-10: A schematic West-East section through the Upper Elsburg`s at South Deep (Source: Osburn et al., 2014)

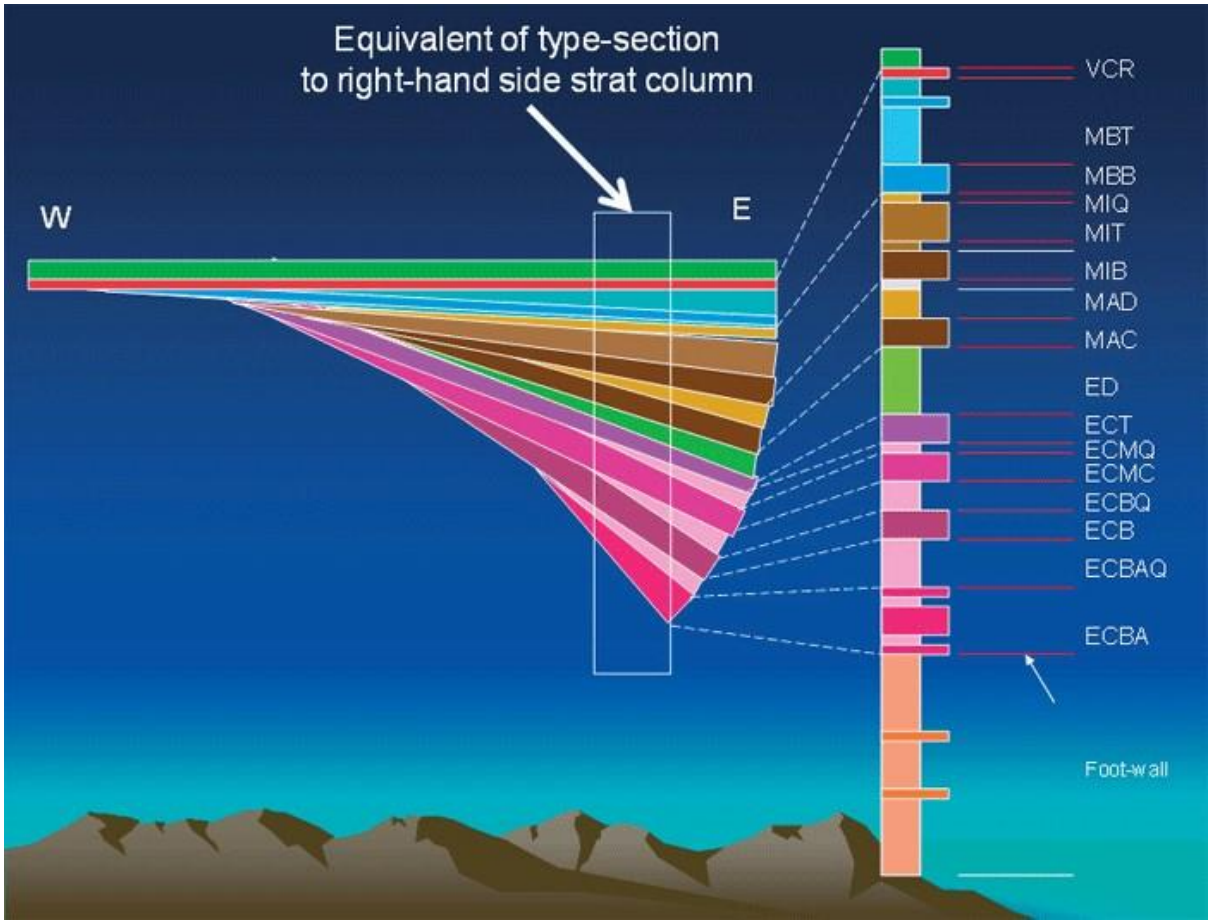

Figure 3-10: A schematic West-East section through the Upper Elsburg`s at South Deep (Source: Osburn et al., 2014)

3.3.4 Structural Setting

Geological structures influence groundwater flow at various scales by either acting as barriers or channels of flow (Anna, 1986). In underground hard rock mines, most of the groundwater flow occurs through fractures produced by geologic structures (Zabidi et al., 2019). In mechanised mines like SDGM, where massive (large bulk) mining occurs, mining-induced fractures occur and serve as secondary mediums of water, increasing the structural (geological) intensity (DWAF, 2008). Once the fracture-controlled flow system is understood, it may be possible to develop measures to mitigate water flow into underground mine workings (Kipko et al., 1984; Kipko, 1988).

According to Osburn et al. (2014), several major faults and folds define the structural character of the West Rand Goldfield. The regional structure of the Witwatersrand basin is shown in Figure 3-11 where different populations of dykes form networks across the mine lease area. Understanding the regional structural setting of the area and dominating structural features underground can assist in determining the source of seepage at SDGM. The data collected from underground drilling, logging, and mapping in conjunction with data derived from surface boreholes can be useful for structural modelling at SDGM.

The 3D structural model (Figure **3-12**) shows that the orebody is fractured/faulted, thus possible water movement in the orebody is expected through geological openings. Golder (2018) recommends mapping of visible seepage/fissure flows whenever observed at South Deep underground working areas. This project will provide several sampled points of seepage and major faults intersected underground.

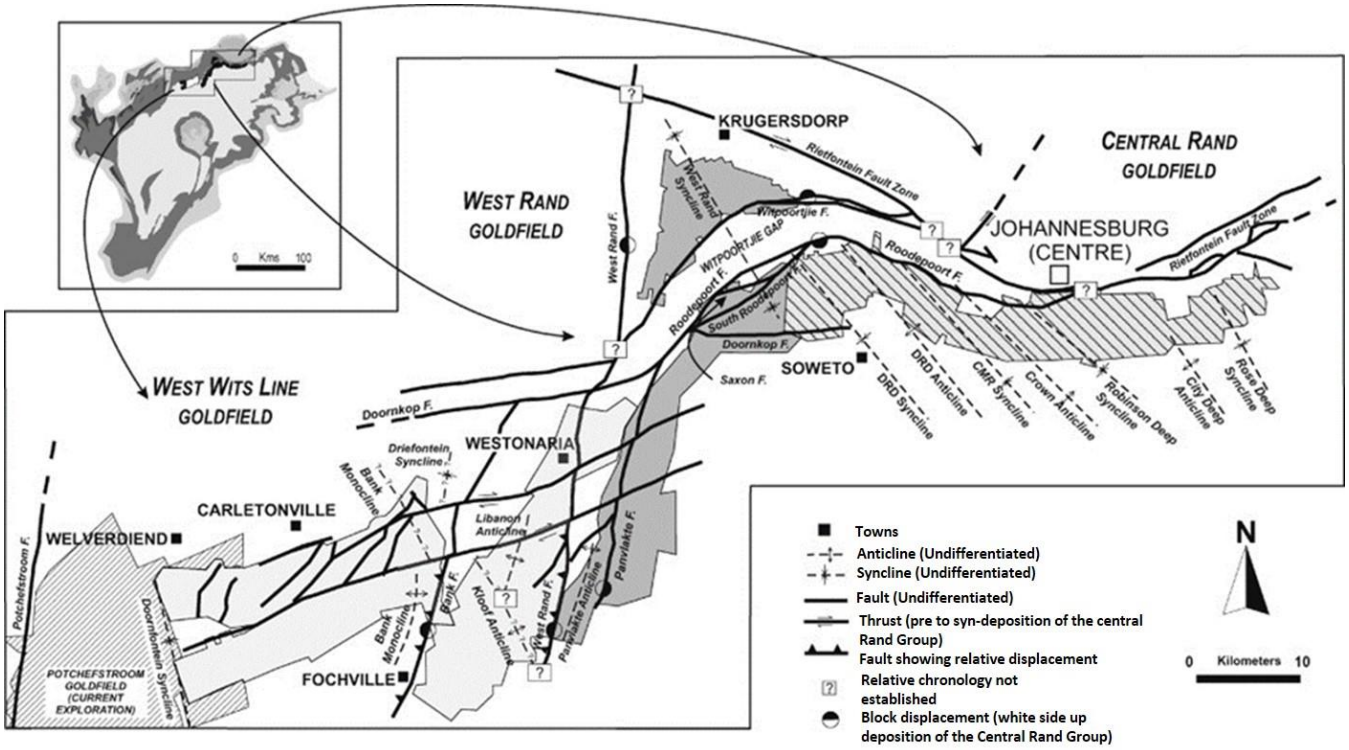

Figure 3-11: Regional structure of the Witwatersrand Supergroup (Source: Dankert, and Hein, 2010)

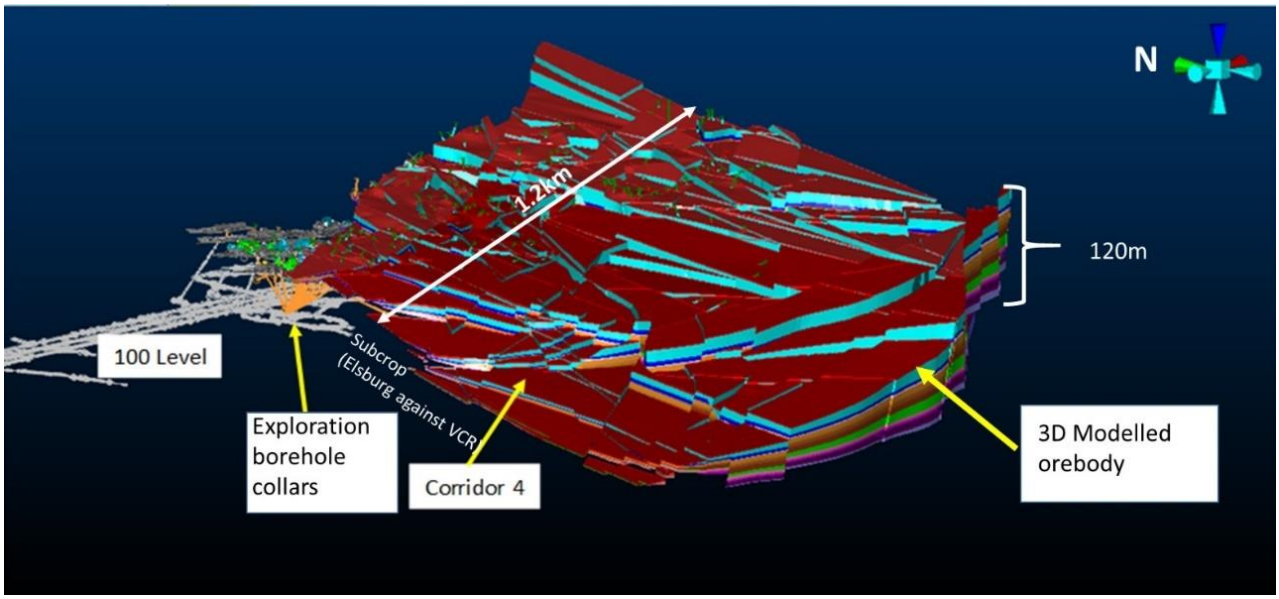

Figure 3-12: Isometric view of the geological model at SDGM, based on the exploration boreholes and 3D seismic modelling inputs, with modelled geological structures(Source: Goldfields,2012)

Faults

The regional faults include the north-south trending primary fault systems, which include the regional faults such as the West-North-West (WNW) trending extension of the Rietfontein fault zone, the arcuate Witpoortjie and Roodepoort–Saxon–Panvlakte faults, the north-trending West Rand fault, the West-South-West (WSW)-trending Doornkop fault, and WSW-trending faults south of Westonaria as shown in Figure 3-13 and Figure 3-14 (van Biljon, 2006; Osburn et al., 2014).

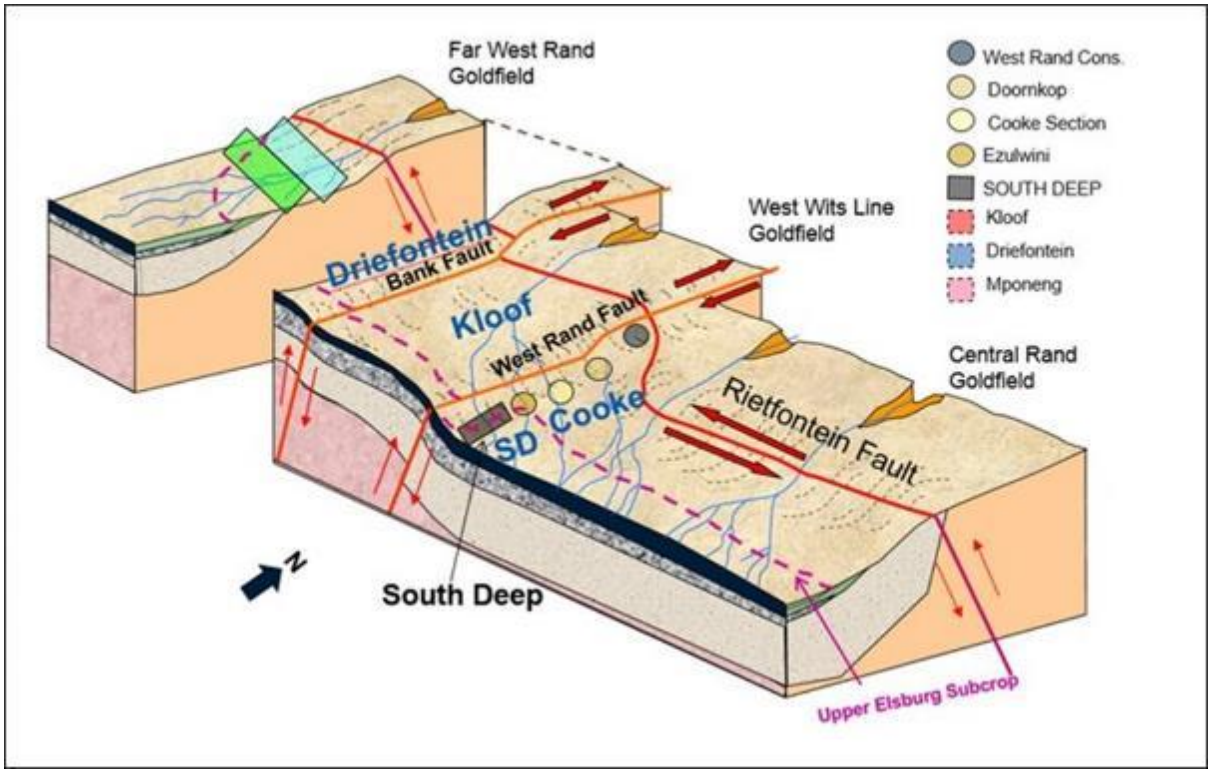

Figure 3-13: Isometric view of the Major Structures in the Far West Rand Goldfield and the Central Rand Goldfield about SDGM (Source: South Deep Gold Mine, 2010)

The activated West Rand fault behaves as both normal and strike-slip fault (s) and has a throw of ~2200 m (Goldfields, 2011). Another significant fault in the study area is the fault in the southern part of the mine called the Wrench fault. According to Osburn et al. (2014), this massive (wrench) fault, shows a right lateral movement of ~350 m and a northward down throw ranging between 80 m and 140 m. They further highlight that the north-trending faults (West Rand and Panvlakte) are older and the east-trending dextral wrench faults (Waterpan and Wrench) are the youngest. Faulting in this area has caused the development of structural blocks dominated by the West Rand (or Witpoortjie) and Panvlakte Horst blocks that are superimposed over wide folding related with the southeast-plunging West Rand syncline.

Folds

Regional folds incorporate the NW-trending West Rand syncline and the NNE-trending Panvlakte Anticline as shown in Figure 3-11 (Dankert and Hein, 2010). The West Rand syncline in the meta-sedimentary rocks of the Witwatersrand Supergroup comprises a refolded double plunging, asymmetric syncline (Toens and Griffith, 1964). This syncline forms the boundary between the West Rand and Central Rand goldfields. Toens and Griffith (1964) summarised these folds to have resulted from a series of events, including:

1) Fold–fault formation during deposition of the Central Rand Group with excision of the folds.
2) Listric fault and/or drag fold (rollover) formation and excision before emplacement of the Klipriviersberg lavas.
3) Fault (normal) and/or fold (rollover) formation during deposition of the Platberg Group.
4) Thrust–fold formation during or after deposition of the Transvaal Supergroup.
5) Fault formation during the Vredefort impact event.

Dykes

Different dykes exist across the mine lease area. Some of these are orientated roughly north-south, near-vertical, and attain thicknesses up to 30 m (Golder, 2018). South Deep Gold Mine (2011) indicates that the younger post-Black Reef age dykes (Gemsbokfontein No.1 and 2 Dykes) separate the overlying dolomites into different water compartments as shown in Figure 3-14.

The Gemsbokfontein dykes are north-south orientated and crosscut the SDGM property. Dykes having a north-south trend, which includes Transvaal rocks of the West and Far West Rand, are regarded as being of Pilanesberg age (±1300 Ma). These dykes were emplaced in faults and fractures induced in Transvaal and older rocks during a period of crustal extension. These dykes are of importance in the mining on the Far West Rand as they compartmentalise the Transvaal dolomites into different groundwater zones.

Some faults and dykes have acted as conduits permitting high inflows of groundwater into the underlying mine workings (Golder, 2018). Highly jointed dykes turn to act as conduits for groundwater flow while unjointed dykes prevent groundwater flow by acting as impervious boundaries, redirecting the direction of groundwater movement (Cook, 2003).

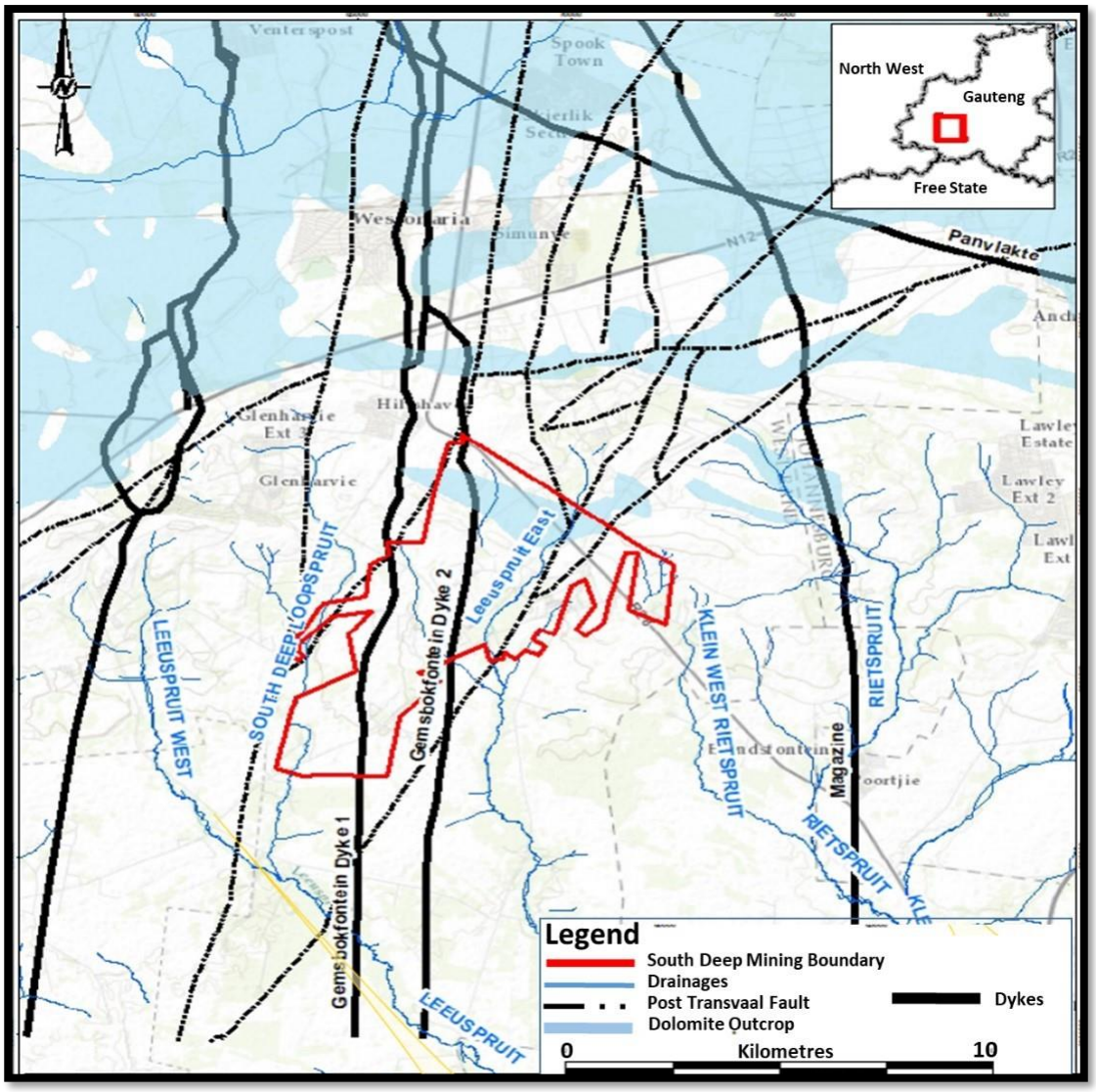

Figure 3-14: Major Geological structures across around the study area (Source: Golder, 2020)

3.4 Hydrogeology

SDGM is located in the Rietspruit Quaternary Catchment C22J with an area of 669 km^2, getting 632 mm- 683 mm of rainfall yearly, and average yearly evaporation of 1546 mm. The general groundwater flow direction in the area follows the topography towards the south in the direction of the Leeuspruit, situated about 5 km south of the study area.

The mine lease area is in the Gemsbokfontein compartment of the Chuniespoort group. The Gemsbokfontein dolomitic groundwater is situated 15 km south of Randfontein town, with a trapezoidal shape and a surface area of 114.7 km^2 (De Roer, 2004). According to SRK (1985), the Gemsbokfontein dolomitic groundwater is bound by the Panvlakte dyke to the north, the Gemsbokfontein dyke to the west, Klip River dyke to the east and the Pretoria series to the south.

The dolomitic aquifers in the West and Far West Rand of Johannesburg, Gauteng Province are of great importance due to their high storage capacity and regular to high permeability (Barnard,1999; De Roer, 2004 and Dill et al., 2007). However, this region houses several gold mines and many other industries that demand a lot of groundwater for their operation. Mining has had a great effect on the amount and the quality of the resource (Jhariya et al., 2016).

The Chuniespoort dolomite aquifers are not continuous due to several vertical and sub-vertical dykes. Drill et al. (2007) state that these dykes have very low permeability and can be defined as impermeable rocks. The dykes within the dolomites act as barriers to the movement of groundwater and as a result, several compartments exist within the dolomite.

3.4.1 Aquifers

According to Prinsloo (2019), the groundwater occurrence in the study area can be divided into two distinct aquifers as described below:

1) **Shallow perched aquifer (weathered and fractured)**:

A shallow weathered zone of the Timeball hill shales, ranging from 0-30 m with a deeper fractured aquifer system to ~70 m depth was formed by the geological strata near the centre of the mine (Golder, 2018). The study further ascertains that the weathered aquifer has low transmissivity and storativity, causing the groundwater movement to be slow, likely due to its silty sand and clay material. The aquifer is of low potential, but where faults and dykes are intersected, significant groundwater yields are possible (Golder, 2020). This aquifer zone is regarded as the secondary aquifer zone in the study area, with water levels varying between 0 and 56 mbgl (Prinsloo, 2019).

2) **Deep dolomite aquifer (weathered and karstified)**:

Below the shallow weathered aquifer lies a Malmali dolomitic aquifer, outcropping north of the mine lease area (Golder, 2020). The shallow aquifer is detached from the underlying dolomite by a thick impermeable shale layer, approximately 400 m in thickness (Prinsloo, 2019). This primary (dolomitic) aquifer is considered the major water-bearing aquifer in the area and it is known as the Gemsbokfontein west compartment. Parsons (1985) mentions that the Chuniespoort dolomite

attains a thickness of up to 1 000 m within the study area. The dolomite aquifer constitutes the upper weathered or karst dolomite.

The weathered and karstified zone extends to a depth of ~35m, and it behaves like a fractured rock aquifer with depth (Golder Associates Africa, 2008). Significant fracturing is at 150-200 m below surface level. The dolomite aquifer is considered minor, as groundwater occurrence is intergranular and occurs within fractures. Groundwater depth is approximately 10-20 m below ground level (bgl). The two aquifers (shallow perched and deep dolomite) are not hydraulically connected – thus, they act independently. This was proven when dewatering the dolomite, and no effect was observed on the fractured aquifer water level (Golder, 2020).

Although, the dolomites extent to about 900 m to 1100 m thick, it is unlikely that significant groundwater occurs at depth near the mine void (Golder Associates Africa, 2008). Groundwater flow in these dolomite units is limited, except for large fracture zones which traverse the area, that act as conduits for groundwater flow between the karstic dolomites and the mine workings at depth (Golder Associates Africa, 2008). Also, Van Biljon (2006) suggests that the presence of a 50 m Ventersdorp lava thickening towards the south prevents groundwater inflow. The Ventersdorp lava lies between the dolomite and the mine voids as shown in Figure 3-15. The figure also shows a conceptual hydrogeological model across the mine, highlighting possible seepages. The conceptual model shows the relation of the sample location (levels) in relation to surface infrastructures and mine main tailings dams (TSF). There is no relationship between the two.

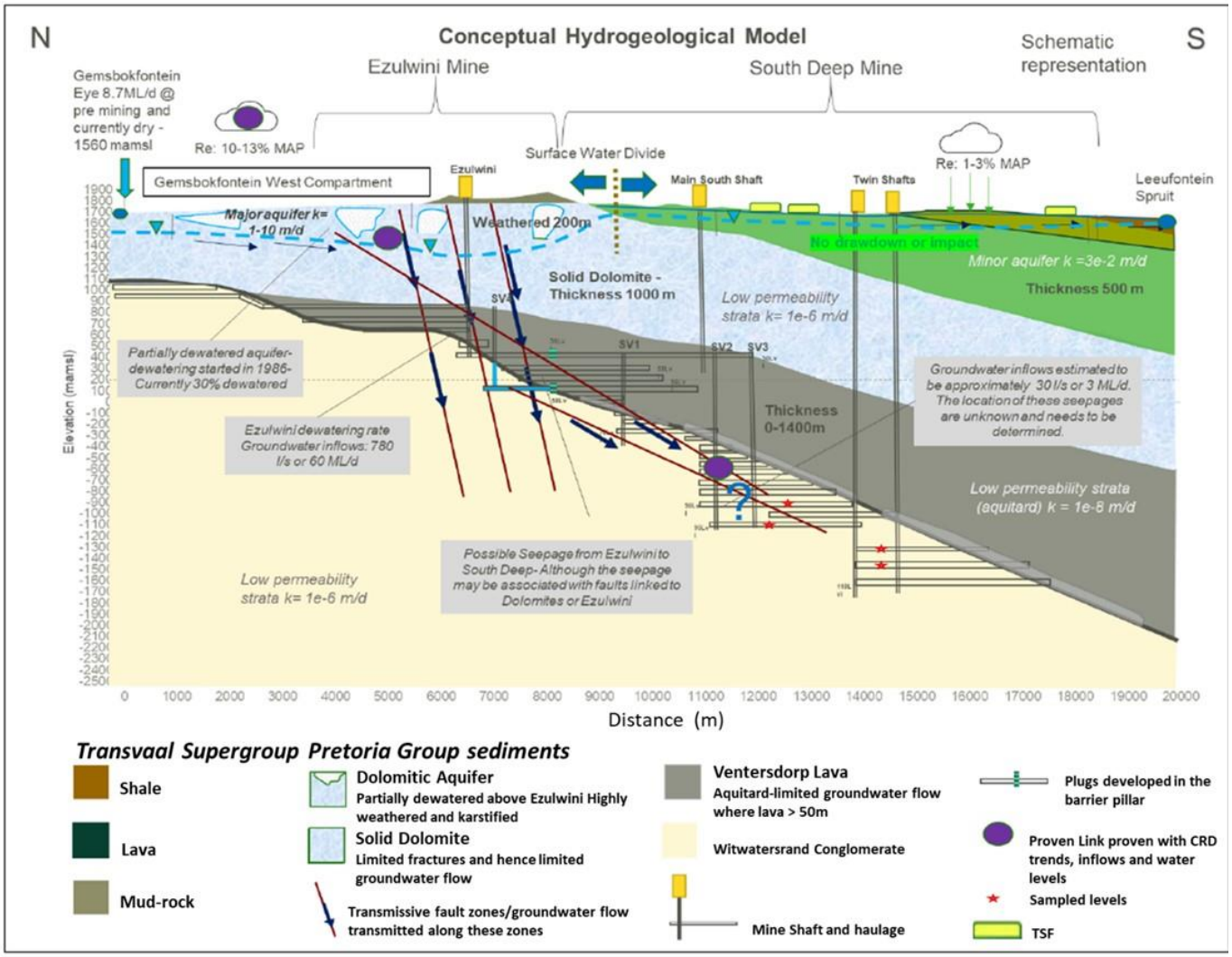

Figure 3-15: SDGM`s conceptual model (Source: Golder, 2018)

According to Golder (2020), the Ventersdorp lava serves as a barrier limiting the groundwater movement from the dolomite into the mine workings. Most of the extensive underground groundwater intersections happened in areas where the lava is either absent or less than 50 m in thickness (towards Ezwilini shaft). However, any drilling of the Ventersdorp lavas to access the SDGM ore body can result in water percolation to the mine voids if holes are not properly sealed and there is the existence of geological structures connecting the aquifers and the mine voids through the lavas.

When the mine's south shaft was sunk, large quantities of groundwater were intersected. Groundwater from deep fractured aquifers has an impact on mining operations in that groundwater inflow into mine workings results in nuisance water that has to be sealed and/or pumped out (Prinsloo, 2019). Additionally, several haulages underground are developed, and this may mean

blasting the lavas; it is possible that groundwater can seep if the openings are not properly plugged and grouted. Several boreholes were drilled to evaluate the aquifer underlying the mine lease area aiming to intersect both the weathered and fractured aquifers (Van Biljon, 2006). The drilled boreholes were tested, and hydraulic conductivity was determined that ranges between 0.37 m/d for the weathered aquifer and 3.14 m/day for the fractured aquifer.

Van Biljon (2006) further notes that groundwater gradients are generally towards Leeuspruit to the east at a shallow angle of 2° and that the Gemsbokfontein dykes have an influence on groundwater flow paths. Groundwater flow through the weathered aquifer is generally slow at a rate of 0.029 m/day (10.6 m/annum) and 0.025 m/day (9.125 m/annum) through the fractured aquifer. Table 3.3 and Table 3.4 highlight the aquifer parameters in the fractured aquifer at SDGM and the hydraulic conductivity values in the geological units, respectively. Figure 3-16 present the locality of all monitoring boreholes around South Deep Mine.

Table 3.3: Aquifer parameters in fractured aquifer at SDGM (Source: Golder, 2016 after Van Biljoen, 2006)

BOREHOLE	TRANSMISSIVITY (m2/d)	HYDRAULIC CONDUCTIVITY (m/d)	AQUIFER
RGC01	0.75	0.02	Dyke contact-fractured aquifer
RGC02	1.12	0.12	Weathered sandstone, overlying dolerite
RGC02d	0.39	0.02	Fractured dolerite
RGC03	0.42	0.01	Dyke contact-fractured aquifer
RGC04	0.63	0.06	Weatherd sandstone, overlying dolerite
RGC04d	0.43	0.02	Fractured dolerite
BH0	0.49	0.01	Fractured shale, quartzite
SD1	1.35	0.0604	Weatherd shale
SD4	0.65	0.0078	Weatherd shale
SD6	0.04	0.0015	Weatherd shale
SD7	0.38	0.0216	Weatherd shale
SD11	0.1	0.0068	weathered lava
SD12	3.39	0.2827	Weatherd shale
GEOMETRIC MEAN	0.5	0.02	

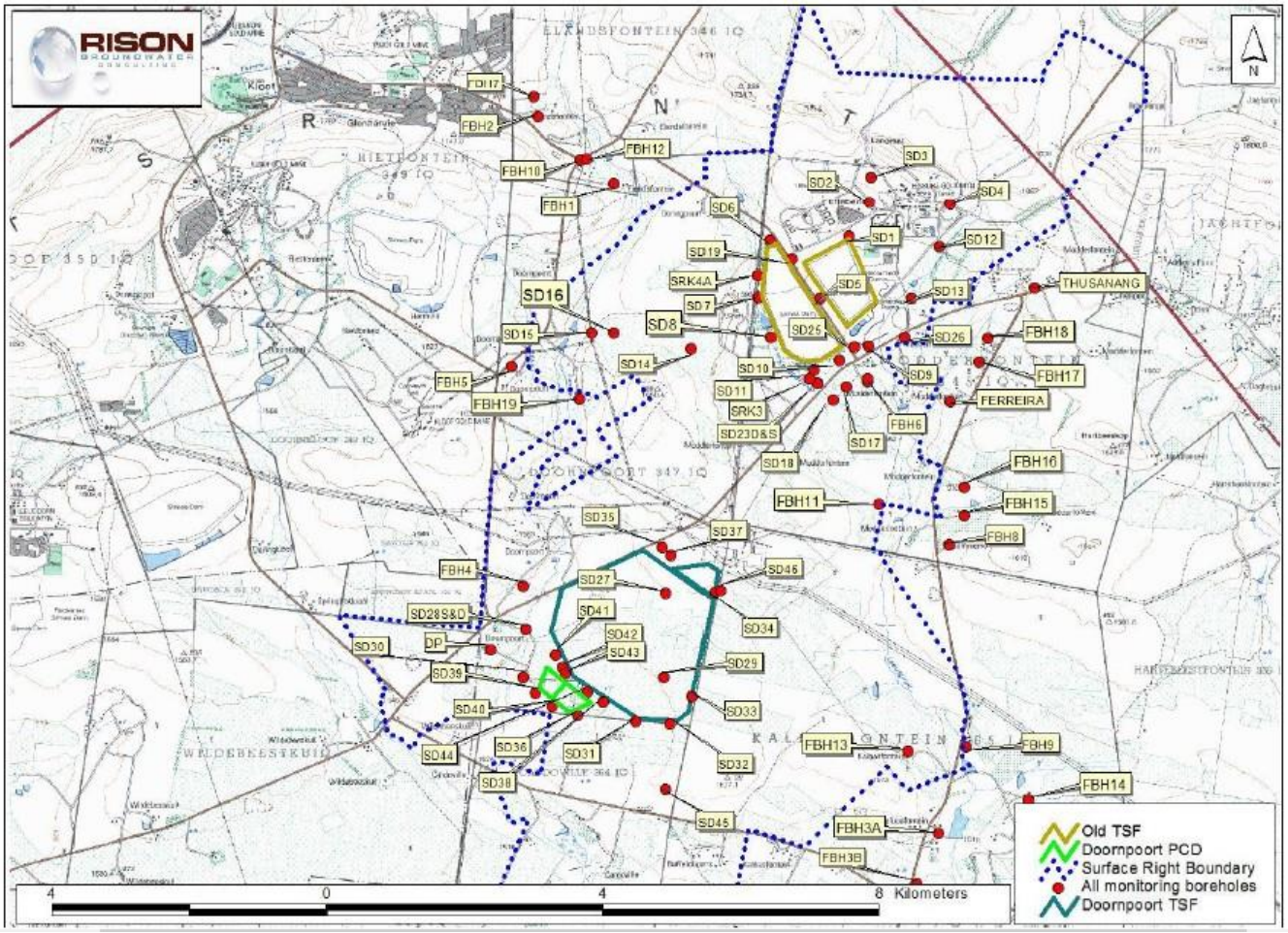

Figure 3-16: Locality of all monitoring boreholes around South Deep Mine (Source: Prinsloo, 2020)

Table 3.4: Hydraulic conductivity values in the geological units (Source: Golder, 2016)

GEOLOGICAL UNIT	HYDRAULIC CONDUCTIVITY (m/d)
Transvaal, Witwatersrand & Ventersdorp supergroup	1
Karoo	0.6
Black Reef Quartzite	11
Oaktree formation	12
Monte Christo Formation	40
Lyttelton Formation	26
Eccles Formation	40

3.4.2 Underground Workings

The Witwatersrand conglomerates reefs, mined by South deep mine have low permeability, with $k = 10^{-6}$ m/d. The VCR lava is also considered to have a very low permeability of approximately $k = 10^{-8}$ m/d. Possible seepage routes from the neighbouring mine are highlighted on the conceptual model (Figure 3-15), and they may be associated with geological structures which are

linked to the dolomites. Investigations made by Golder Associates (2018), show a recorded groundwater make of approximately 3 ML/day.

The 1000 m layer thickness of the VCR lavas above SDGM underground workings are considered aquitards because they do not allow the flow of water, hence limited flow from the upper aquifer zones. Golder (2018) highlights a gap in the understanding of ingress/fissure flow where there is about 3 ML/day of ingress that cannot be located underground.

The figures below, including Figure 3-17, Figure 3-18 and Figure 3-19 illustrate the fissure flows at SDGM compared to Cumulative Rainfall Departure (CRD). According to Golder (2018), there is a correlation between underground fissure water and rainfall, which suggests a link between SDGM and weathered karstified dolomitic aquifer above the neighbouring mine as indicated in Figure 3-15 above. About 2 980 m^3/day of fissure flow with a TDS of 598 mg/L was modelled. Golder (2018) highlighted level-AA and Level-CC as the two locations/sources where fissure water exists. This water can travel down to active mine working areas through the geological structures.

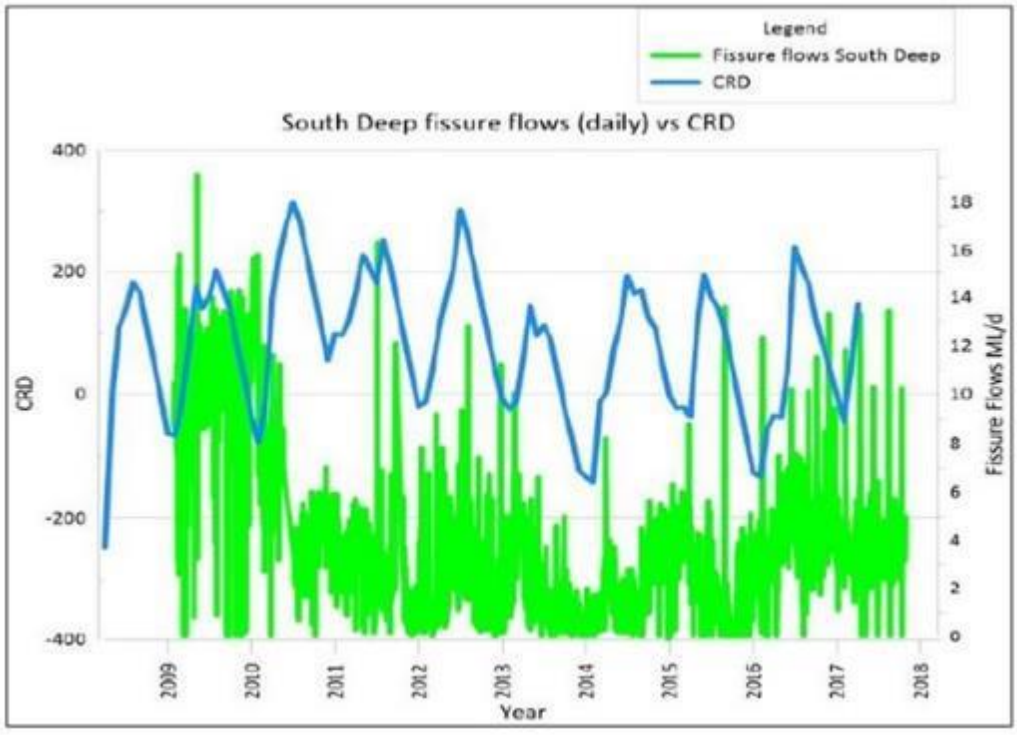

Figure 3-17: SDGM daily fissure flows with CRD (Source: Golder Associates, 2018)

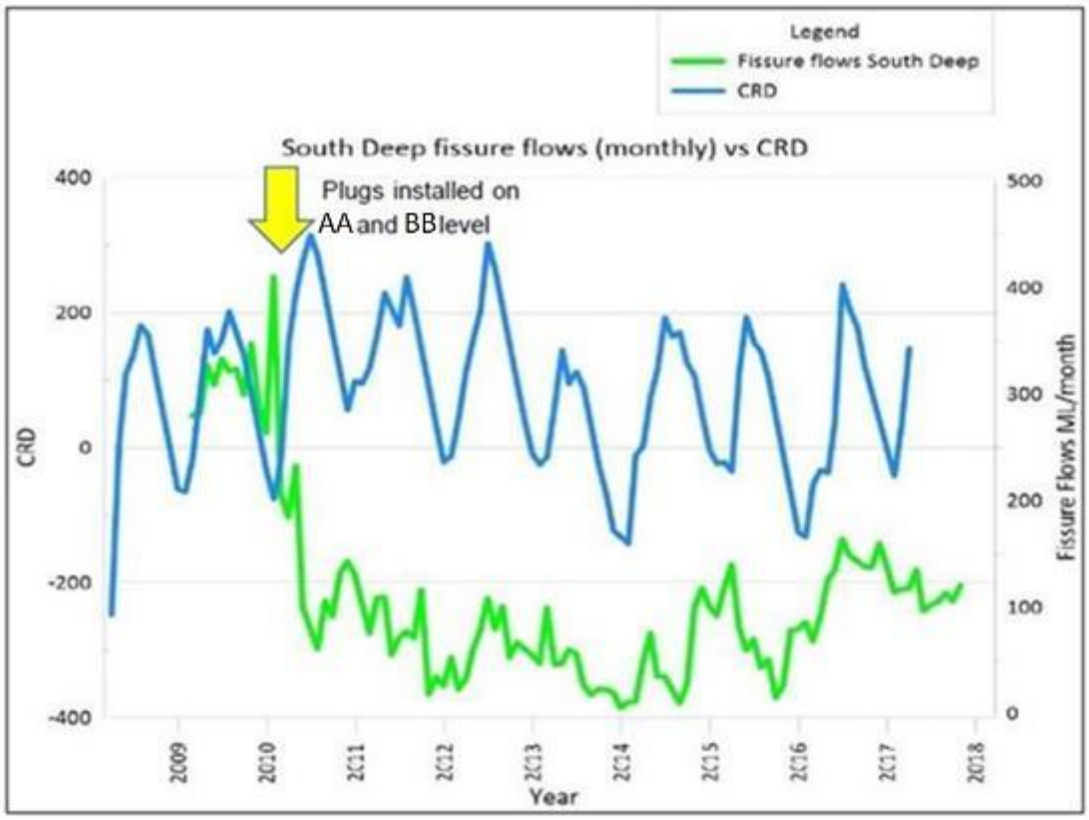

Figure 3-18: South Deep total monthly fissure flows with CRD (Source: (Golder, 2018)

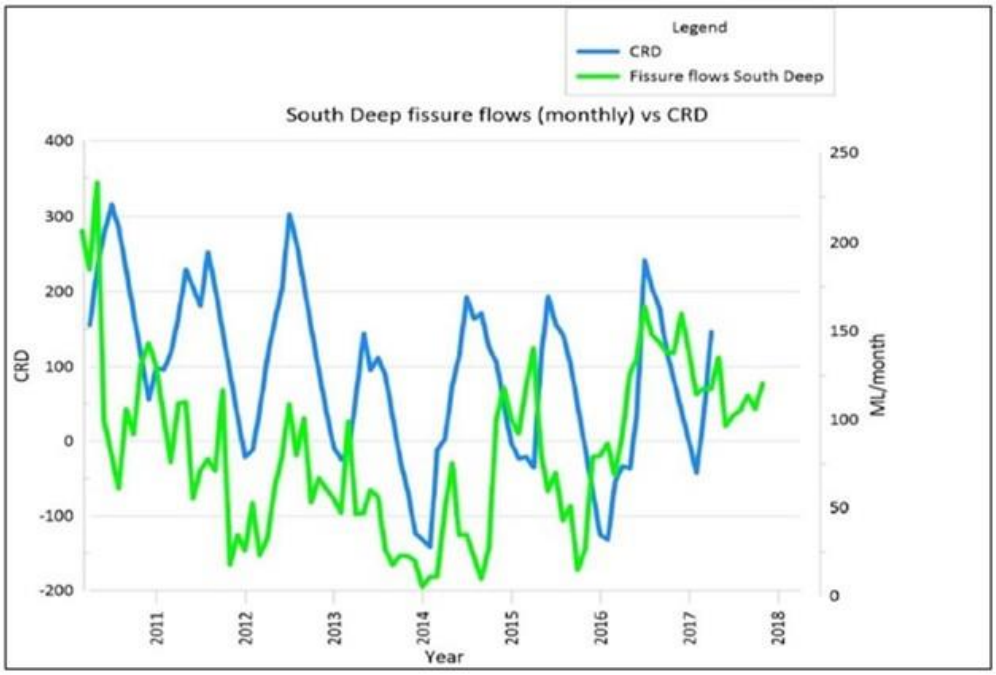

Figure 3-19: South Deep monthly fissure flow after plugs vs CRD (Source: (Golder, 2018)

..

CHAPTER 4

METHODOLOGY

4.1 Research Design

Methods used in this project include verbal communication with underground mineworkers, field observations, the use of computer software to model hydrochemical variations in the collected samples, review of maps, and review of literature on/around the mine.

The following strategic phases are implemented in the study:

- Desktop survey
- Fieldwork
- Presentation of the results and analyses

4.1.1 Desktop Survey

The survey was done based on reviews of existing literature on the geology of the Witwatersrand Basin and the dolomite aquifers in the Gemsbokfontein compartment of the Chuniespoort Group. Additionally, the geology and hydrogeology of (SDGM) Modderfontein Farm and surrounding areas were assessed. This included geological data of SDGM and of the nearby mines. The mine plans and survey data, hydrological maps, aerial photographs, and reviewing hydrogeological work done by consultants at SDGM. Computer software was used to create the structural model of the orebody and plans underground, especially where seepage samples were collected.

ArcMap (version 10.6)software is used to produce a locality map of the Westonaria (SDGM) Figure 3-1, Gauteng, South Africa, and the geologic map of the study area Figure 3-8. These maps highlight important information such as possible major faults and the geological formations across the study area.

MineCad software and Datamine software was used to create underground plans (indicating sampled points and the mapped geological structures), a cross-section of the orebody with exploration borehole (sample SD1 and SD2) and a structural model of the orebody (Figure 3-12). This information provides a clear picture of structures across the mine, possible water pathways, and activities happening around the observed seepages. From these, we can link information to conclude on the possible seepage sources and water pathways underground.

Windows Interpretation System for Hydrogeologist (WISH) software was used to construct hydrogeochemical data to represent results (Piper, Stiff and Expanded Durov diagram), Figure 5-1 to Figure 5-3. This survey assisted in understanding the hydrological setting of the area, the main water resources, identifying the main possible sources of water in such an underground setting, and finding the appropriate techniques to trace the water.

4.1.2 Sampling Method

A quota sampling method was used to select relevant underground employees based on their profession. Quota sampling is a type of purposive sampling whereby the number of people to be included as participants is decided in the designing stage of the research (Moriaty, 2011). The researcher knows all the participants. A verbal communication inviting and informing the potential participants was done before conducting an interview.

Underground sampling was based on convenience sampling. This refers to non-random sampling whereby sampling stations meet certain criteria such as easy accessibility, availability or certain geographical proximity at a given time of the study (Etikan et al., 2016). Seepage sampling sites are based on the known seepages of which the locations are safe to access and are well-defined by the existing underground plans.

4.1.3 Data Collection

Qualitative research is non-experimental but expressive and is implemented in a way that resembles daily routines (Drummond and Camara, 2007). In this study, five employees with different roles were approached, based on their experience and occupation. The underground employees were approached for short interviews or conversations to get their views and understanding regarding seepage at SDGM. This involved mine Surveyors, Rock Engineers, drill rig operators and Mining Engineers. The interviews involved important questions which created a continuous discussion with responses that led to an understanding of other possible sources of seepage water underground. The answers were drafted on a book while noting down keywords.

The quantitative approach involved the collection of ten seepage water samples underground in September 2020 (Figure 5-10 to Figure 5-16) from different levels and corridors underground. The samples are labelled SD1, SD2, SD3, SD4, SD5, SD6, SD7, SD8, SD9 and SD10. Samples were sent to the DD SCIENCE laboratory in Randfontein for chemistry analysis. For isotopic analysis, the samples were sent to the University of the Witwatersrand School of Geosciences and

iThemba Laboratory, Johannesburg. Table 4.1 presents the location of seepage samples while the plans and surveyed cross-sections indicating the sampling points are presented in Chapter 5.

Table 4.1: 2020 SDGM underground seepage-sampling points

Sample ID	Level/ Location	Physical appearance
SD1	Level-F MIH 1 LIB X (exploration BH)	Cloudy
SD2	Level-E (exploration BH)	Cloudy
SD3	Level-E 1BW CUT4 MAD4W	Brownish in colour
SD4	Level-E 1BW CUT4 MAD4W	Brownish in colour
SD5	Level-E 1BW CUT4 RAMP	Brownish in colour
SD6	Level D 01W HAULAGE	Brownish in colour
SD7	Level-E 04W CUT 04 LAT 02 ACC2	Clear water
SD8	Level A 01W CUT 01	Brownish in colour
SD9	Level A 01W CUT02	Brownish in colour
SD10	Level-E 04W CUT4 BACKFILL	Cloudy

4.2 Sample Collection

4.2.1 Preservation and Analytical description

Prior to sampling, bottles were washed with de-ionised water provided by the laboratory. Samples were collected to represent the in-situ seepage condition. The location of the sampling point is mapped/plotted, and photographs were taken. For sample quality assurance and control, one sampling site is duplicated (SD 03 and SD 04 are from the same point).

Chemical (Major Ion) Analyses

For the determination of major ions, water samples for cations and anions analysis were collected with 2L polyethene bottles provided by the DD SCIENCE laboratory. Samples were marked and named accordingly and water condition (clear, cloudy, colour, smell, foam) was noted down. Samples were kept under dark and cool temperatures until submitted to the DD SCIENCE laboratory in Randfontein, Gauteng Province, within 24 hours of collection.

Samples were analysed for major ions: Ca^{2+}, Mg^{2+}, Na^{+}, Total Alkalinity (TAlk), Cl^{-} and SO_4^{2-}. Some minor constituents: K^{+}, Fe^{2+}, F^{-}, NH_4 and trace elements: Al^{3+}, Mn^{2+}, were also analysed. Furthermore, physio-chemical parameters (pH, electrical conductivity (EC), temperature (°C), and oxidation-reduction potential (REDOX) readings were also measured using Digital Crison MM 40 and YSI 550A multimeter. One set of duplicates (SD3=SD4) were sent to the laboratory for evaluation of the results, as a quality control check.

Stable isotope analyses

A total of 10 samples were collected in 10 ml glass bottles and were placed in a dark place to avoid isotopic fractionation from the sun. The samples were analysed at the University of the Witwatersrand, Johannesburg (Hydrogeology Laboratory), South Africa. The samples were analysed using the Liquid Water Isotope Analyser-model 45-EP as described in Abiye et al. (2018). The Liquid Water Isotope Analyser comprises laser analysis system, an internal computer, a liquid auto-sampler, a small membrane vacuum pump, and a room air intake line that passes air through a drierite column for moisture removal.

A 1–1.5 ml aliquot of a sample was pipetted into a 2 ml vial and closed with Polytetrafluoroethylene septum caps. About 1–1.5 ml aliquot of a sample (from the original sample bottle) was transferred into a 2 ml vial and closed with Polytetrafluoroethylene septum caps. A 0.75 µl was then infused through a PTFE septum within the auto-sampler using a Hamilton microliter syringe. Immediately upon injection, the injection port of the auto-sampler was heated to 46 °C to vaporise the test beneath vacuum. The vapour moves down via the transfer line into the void mirrored chamber for analysis. Five measures with known $\delta^{18}O$ and $\delta^{2}H$ values (5C: $\delta^{2}H$ −9.2±0.5‰, $\delta^{18}O$−2.69±0.15‰, 4C: $\delta^{2}H$−51.6±0.5‰, $\delta^{18}O$−7.94±0.15‰, 3C: $\delta^{2}H$ −97.3±0.5‰, $\delta^{18}O$ −13.39±0.15‰, 2C: $\delta^{2}H$ 123.7±0.5‰, $\delta^{18}O$ −16.24±0.15‰ and 1C: $\delta^{2}H$ −154±0.5‰, $\delta^{18}O$ −19.49±0.15‰) were utilized within the investigation technique and the laser analyzer thus calibrates itself and decides the stable isotope values respectively. Approximately 1‰ of accuracy for $\delta^{2}H$ and 0.2‰ for $\delta^{18}O$ in liquid water samples is provided (Abiye et al., 2018).

Tritium analyses

A total of nine samples (SD1-SD9 samples, excluding SD10 due to insufficient volume of water) were collected in 500ml polythene plastic bottles. Prior to sampling, the bottles were washed with

10% HCl acid and rinsed with distilled water. The sample bottles were filled to the brim and had minimal air contact. Furthermore, the samples were then stored in a cooler box, until submitted to iThemba LABS Environmental Isotope Laboratory in Johannesburg, Gauteng province in South Africa.

Tritium analysis was conducted as described by Butler, (2020). Nine samples (SD1 to SD9) were submitted to iThemba Laboratory, Johannesburg for tritium analysis. The Samples were distilled then enriched with electrolytes. The samples were distilled, then enriched by electrolysis. The electrolysis cells comprise two concentric metal tubes insulated from each other. The outer anode (the container) is made of stainless steel, while the inner cathode is of mild steel with a distinctive surface coating. About 500 ml of sample water, which was distilled and with some amount of sodium hydroxide was introduced into the cell. About 10-20 ampere direct current was then passed through the cell and later cooled. Several days later, the volume in the electrolyte was reduced to some 20 ml. The volume is reduced 25 times, producing a corresponding tritium enrichment factor of about 20. Known tritium concentration samples (spikes) were run in one cell of each batch to check on the attained enrichment.

For liquid scintillation, counting samples were prepared by directly distilling the enriched water sample from the now highly concentrated electrolyte. About 10 ml of the distilled water sample is mixed with 11 ml Ultima Gold and placed in a vial in the analyser and counted 2 to 3 cycles of 4 hours. Enriched samples have 0.2 TU detection limit (Butler, 2020).

4.2.2 Presentation of the results

4.2.2.1 Stable isotope approach

Bivariate analysis was used to interpret data in this study. Bivariate analysis is a simple statistical analysis method whereby two variables (e.g. isotopic values of $\delta^{2}H$ and $\delta^{18}O$ in this study) are compared. ESI (Environmental Stable Isotopes) data can be interpreted by reference to the meteoric line, a result of long-term collective records of stable isotope data for rainfall with comparable climate, geography, and location (Harris et al., 2010; Mengistu et al., 2015).

A plot of $\delta^{2}H$ versus $\delta^{18}O$ fitted with a local meteoric water line (LMWL) was used to understand and trace the source of collected seepage water at SDGM`s underground operation to see if it is related to the local groundwater. Pretoria Local Meteoritic Water Line (PMWL) was used in this study.

LMWL shows the relationship between rain ($\delta^{18}O$) and hydrogen ($\delta^{2}H$) isotopes and it serves as a basis for estimation of relative enrichment or depletion in isotopic content of sampled water (Maruyama and Kato 2017). Processes such as water/rock interactions (O only), H_2S exchange reactions (H only), evaporation, and/or condensation cause deviations from the LMWL, Figure 5-5.

4.2.2.2 ***Tritium dating and analysis***

The resident time of seepage is estimated from the current rainfall tritium concentration. This report assumes that tritium has a half-life of 12.43 years and the estimated current tritium concentration in precipitation in South Africa is approximately 5.6 TU (Abiye et al., 2015). With this assumption, it is, therefore, possible for one to estimate the resident times of SDGM`s seepage.

4.2.2.3 ***Water Chemistry***

Tri-linear diagrams are mostly used to show the hydrogeochemical characterisation of a chemical data set (Li et al., 2014). In this study, major ion chemistry is represented on hydrochemical pattern diagrams. Singhal and Gupta (2010) hold that the purpose of hydrochemical pattern diagrams is to represent the concentration (in mg/L or meq l^{-1}) of different cations and anions. In this study, the chemical data is represented on Piper, Durov, and Stiff diagrams which were plotted using AqQA and WISH software. According to Guan et al. (2019), the hydrogeochemical characteristics of water can be analysed by a Piper diagram which allows for the presentation of several water analyses. The Piper diagram classifies water types, and it indicates the possible mixing of waters.

Whereas the Durov diagram is a type of tri-linear diagram in which the concentration of major cations and anions in percentage meq l^{-1} are plotted in two separate triangles that are projected to a central square field that represents the overall chemical character of the samples (Singhal and Gupta, 2010). This diagram provides information about different water types and hydrochemical processes including the presence of ion exchange, simple dissolution, and mixing of waters of different qualities.

STIFF diagram graphically displays the ratios [equivalents per million (e.p.m). or meq/L] of the major ionic components in water (Sharp, 2003). Cations and anions distributions are well visualised and, one can identify the dominating ions in different samples, (Singhal and Gupta, 2010). STIFF diagrams allow one to work out the possible source of the ions which will lead to an explanation of the chemistry of the samples and the possible source of seepage underground.

In addition to tri-linear diagrams, bivariate analysis is used in this study to present data. Major ions are plotted on an excel spreadsheet and software (AqQA) to compare their relation/correlation. A strong correlation may suggest the same source of water, ions, mineral phases, and/or the same geochemical process of formation (Sello, 2019). Table 4.2 shows Guildford's rule of thumb for correlation coefficient classification. A correlation coefficient less than 0.20 shows a 'negligible' relationship; 0.20 to .040 implies a 'low' relationship; 0.41 to 0.70 shows a 'moderate' relationship; 0.70 to 0.90 indicated a 'high' relationship; while a coefficient greater than 0.90 propose a 'very high' relationship (Guildford, 1973).

Table 4.2: Guildford's rule of thumb correlation coefficients classification (Guildford, 1973)

Correlation coefficient (r-value)	Classification
0.0 – 0.29	Negligible correlation
0.3 – 0.49	Low correlation
0.50 – 0.69	Moderate correlation
0.70 – 0.89	Good correlation
0.90 – 1.00	Best correlation

CHAPTER 5

RESULTS AND DISCUSSION

Samples were collected from SDGM underground seepage points at 10 sampling sites (Table 5.1). Of these, two were from the exploration boreholes while the remaining eight samples were collected from the active mining zones. The results were compared with the existing monitoring data from the mine (APPENDIX A and APPENDIX B).

5.1 Hydrogeochemical Analysis

The measured pH values varied from 2.5 and 13.5. A pH between 2.5 and 13.5 indicates acidic to alkaline groundwater (Table 5.1). pH less than 5 and greater than 8.5 was considered as mine water while water with a pH between 5 and 8.5 was characterised as natural water (not impacted by mining activities) (Golder, 2020 and DWAF, 2018).

Sampling sites SD3, SD4, SD5 SD6, SD8, and SD9 have acidic pH ranging between 2.5 and 3.7 and can be characterised as mine water as it resembles mine impacted water (Table 5.1). The measured pH values at the exploration borehole void (sample station SD1) and sample station SD7 (nearby the mining zone-stope) correlates to the pH of natural waters (pH between 5 and 8). The measured pH values for groundwater monitoring boreholes as well as at the sampled water-bearing structures (i.e. faults, dykes, and joints) at SDGM varied between 7.3 and 8.3 with an average pH of 8 (APPENDIX A and APPENDIX C). The pH between 7.3 and 8.3 is indicative of natural groundwater (APPENDIX B and APPENDIX C). The pH of water collected from the backfilled long hole stope SD10 has a pH of 13.5 while the water quality from the underground exploration borehole SD2 had a pH of 10. The pH above 8 is considered alkaline waters and thus indicative of processed water.

The chemistry of the seepage water revealed two water types based on the pH, acidic seepage water found closer to the mined-out/ mining stopes, and the alkaline water from samples taken near a backfilling stope and the samples from exploration boreholes underground. Some samples had pH correlating to the pH of mine water . This may suggest different sources of seepage or the same source but different processes. The measured total dissolved solids (TDS) varied between 791 mg/L and 11300 mg/L. Borehole SD1 and SD7 had TDS below 1000 mg/L. TDS values below 1000 mg/L are understood as indicative of natural water (freshwater). The low TDS values seem to suggest that the source of seepage water at SD1 and SD7 is naturally occurring, from the deep

fractures. The measured TDS and pH values at SD1 and SD7 indicated that SD1 and SD7 can be characterised as freshwater.

In contrast, sampling sites SD2, SD3, SD4, SD5, SD6, SD8, SD9, and SD10 had TDS above1000 mg/L and these are indicative of brackish water. The cause of brackishness is understood to be attributed to the use and re-use of recycled water underground for mining purposes. Therefore, the source of seepage at SD2, SD3, SD4, SD5, SD6, SD8, SD9, and SD10 can be attributed to seepage from underground water facilities such as sumps, water-logged backfilled areas, and water that has accumulated over time in mined-out areas.

Table 5.1: Hydrochemical analyses of seepage samples at SDGM underground void

Sample ID		SD1	SD2	SD3	SD4	SD5	SD6	SD7	SD8	SD9	SD10
	Units										
pH		7.4	10.0	3.2	3.0	3.7	2.5	7.4	2.7	2.8	13.5
Electrical Conductivity	mS/m	135	361	661	674	290	858	73	712	854	775
Total Dissolved Solids	mg/L	791	2000	6580	6610	1830	10800	463	6960	11300	2910
Total Alkalinity	mg/L	47	31	3.5	3.5	3.5	3.5	97	3.5	3.5	131
Ammonia	mg/L	2.2	2.6	42	18	66	18	7	32	17	6
Calcium	mg/L	32	78	844	788	103	569	67	551	703	132
Chloride	mg/L	1530	2880	949	1700	1560	1530	1560	779	1700	677
Fluoride	mg/L	1.4	1.6	1.2	1	0.7	1.3	1.3	1.1	1.3	0.8
Magnesium	mg/L	7.2	9.1	121	213	33	445	24	273	647	7.9
Nitrate as N	mg/L	<0.5	2.5	3.6	44	1	37	<0.5	14	47.0	28
Potassium	mg/L	2.7	2.1	66	55	4.2	0.9	14	33	24	198
Sodium	mg/L	201	578	294	429	352	235	39	333	224	280
Sulphate	mg/L	123	193	4000	4070	592	7290	204	3510	5370	592.0
Aluminium	µg/l	<0.1	<0.1	<0.1	<0.1	<0.1	<0.1	<0.1	<0.1	<0.1	<0.1
Iron	µg/l	<0.1	<0.1	1076	135	0	80	2	57	140.0	3.3
Manganese	µg/l	<0.1	<0.1	84	8.3	1	20	1	13	21.0	0.2

5.2 Seepage Characterisation

The Stiff diagrams (Figure 5-1) are used to characterise the concentration of the major cations (Ca^{2+}, Mg^{2+}, Na+K) and anions (SO_4^{2-}, Cl^- and HCO_3^-) at the seepage points.

The Piper diagram (Figure 5-2) is convenient in classifying distinct clusters of the underground seepage. Based on Piper's interpretation, the cation trilinear plot shows enrichment in Ca^{2+}, Na^+ and K^+ waters, while anion trilinear shows enrichment in Cl^- and SO_4^{2-} waters. The dominating cations and anions, Ca^{2+}, Cl^- and SO_4^{2-} are further indicated by Stiff diagrams (Figure 5-1). Based on the visual observation on the Piper Diagram the Bicarbonate concentration is zero as this plot on the line on the anion trilianer plot and this is due to the excessive Cl and SO_4 concentration (approximately >1000 mg/L) compared to relative low bicarbonate concentration (Table 5.1). This is also observed on the STIFF diagram (Figure 5-1).

Based on the Stiff and Expanded Durov diagram (Figure 5-3), the water can be classified into 4 groups. The first group is characterised as *Mg-SO_4* water type (i.e. SD6 and SD9). This group is characterised by the increased SO_4^{2-} signature. SO_4^{2-} is the dominant anion while Mg^{2+} is the dominant cation. This water type suggests SO_4^{2-} contamination from the mine and/ or a mix of different water types due to the re-use of recycled water for mining activities. The occurrence of sulphate is associated with sulphide minerals and/ or sulphide bearing rocks. In this study, the sulphate contamination is associated with the dissolution of the host rock. The occurrence of magnesium is naturally due to the dissolution of the host rock.

The second group is characterised as *Na-Cl water type* (SD1, SD2, SD5, SD7 and SD10). Na^+ and K^+ are the dominant cations while Cl^- is the dominant anion with SO_4^{2-} to a lesser extent at SD5 and SD10. This group suggests three possible hydrogeochemical characteristics and/or sources (i) end of the hydrogeological cycle, (ii) old/stagnant water, and (iii) NaCl source affected.

The first hydrochemical water type characterised with *NaCl* is SD1. The hydrochemical facies for SD1 suggests that the source of seepage water at the sampled site is a regional groundwater source and this is supported by the pH and TDS analysis which suggested that the source of seepage is natural water/freshwater (Section 5.1). This water type can be characterised as the end of hydrogeological cycle type water where old groundwater has resided within the groundwater system. This is also confirmed by the apparent groundwater age based on the

tritium analysis which suggests that SD1 sample water was recharged prior 1952 (under Section 5.2.2).

SD1 samples were collected from an exploration borehole drilled from the lowest mining level at SDGM Level-F and it is drilling towards South-East direction at 161º bearing (Figure 5-4 and Figure 5-11) from the footwall (EB quartzite) to the hanging wall (Lava) ahead of the current mining position. Further, is located approximately 3 km below ground level, and the area is characterised by low permeability host rocks compounded by low recharge values/aquifer renewability (Section 3.4).

The second hydrochemical type of water characterised with NaCl is SD2 . The hydrochemical analysis indicated that the water quality at SD2 is brackish and characterised by alkaline pH. The hydrochemical facies at SD2 suggests that the water type represents old/stagnant groundwater. This is confirmed by tritium dating which suggests that SD2 water can be characterised as sub-modern water probably recharged before the 1950s. Therefore, the possible source of seepage at SD2 is the mined out areas as the boreholes are drilled through the mined-out waterlogged backfilled areas.

SD7 also showed characters of NaCl water type. SD7 is dominated by Cl^- with no dominant cation. This water type can be characterised and/ or suggest Cl- contamination or the water results from a mixture of different types due to the use and re-use of recycled water.

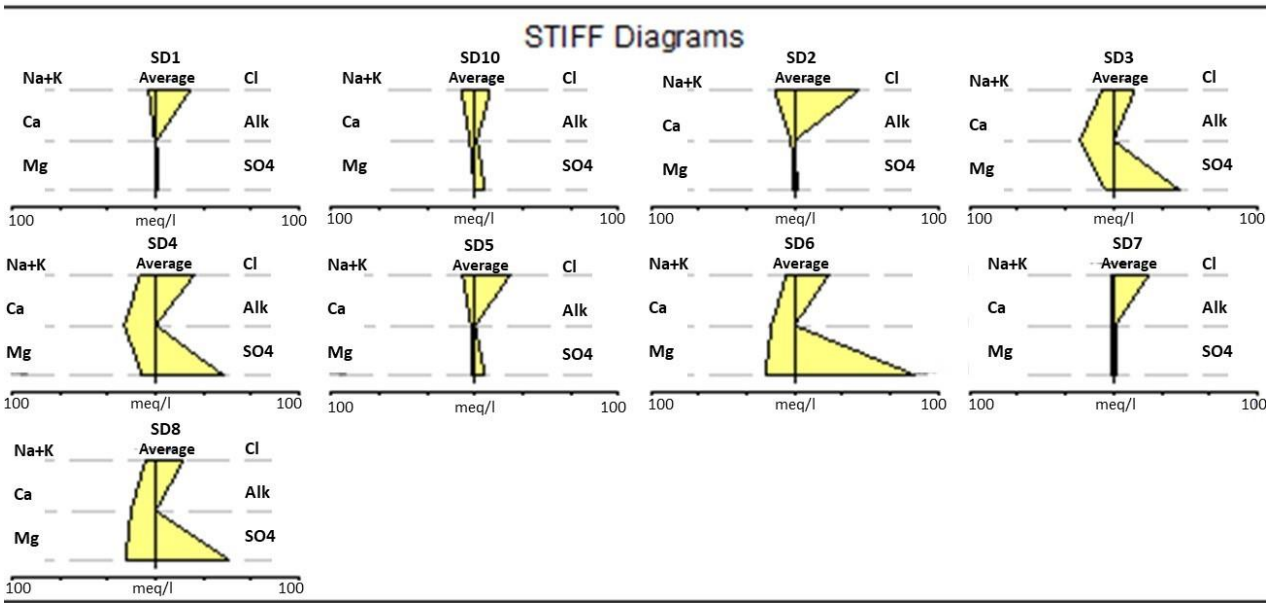

Figure 5-1: Stiff diagram graphically displays the ratios [equivalents per million (e.p.m). or meq/L] of the major ionic components in water

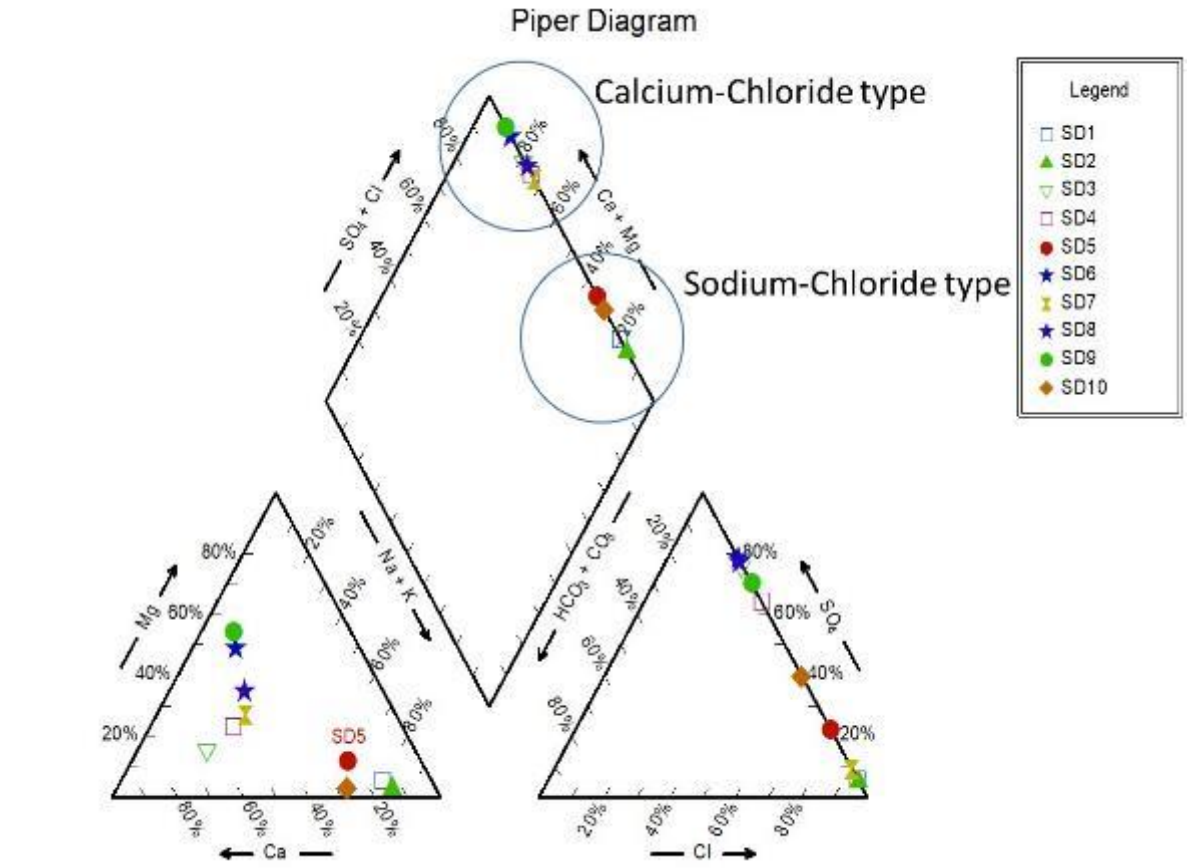

Figure 5-2: Piper diagram presenting SDGM`s underground seepage hydrochemical characteristics and water types.

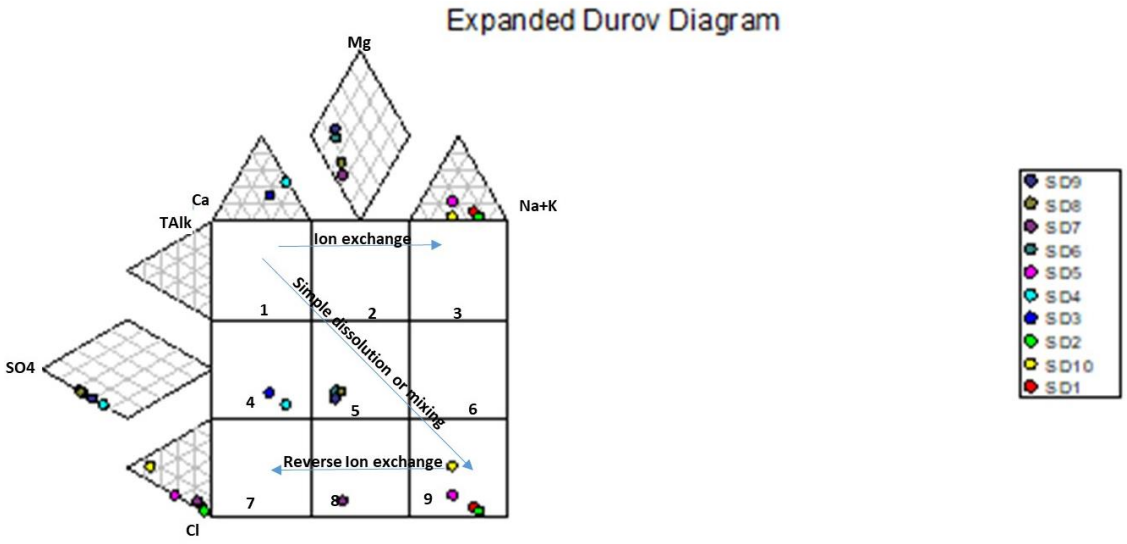

Figure 5-3: Expanded Durov diagram displaying water types and hydrochemical processes in the samples.

Furthermore, the hydrochemical facies at SD10 also suggested that the water type is NaCl source affected. The results suggested that the source of seepage at SD10 is from the water-logged backfilled stopes above the current mining cut.

The third group is characterised as *Ca-SO_4 water type* (i.e. SD3 and SD4). This group is characterised by an increased SO_4^{2-} concentration, with Ca^{2+} as the dominant cation. Sulphides (sulphides bearing rocks) are known to exist on-site and hence, the most likely source of the elevated sulphate is the oxidation of sulphide (pyrite) bearing rocks (Equation 3).

$$\text{Sulfidic mineral} + H_2O + O_2 \xrightarrow{\text{Bacteria}} \text{acid} + \text{metals}$$

Equation 3 (Warren, 2011)

On the other hand, the occurrence of calcium is understood to be natural due to the dissolution of the host rock. These results suggest that the source of seepage at SD3 and SD4 is mine water and this is observed in (Section 5.1) which is characterised by SD3 and SD4 sampling sites as mine impacted water.

The fourth group is characterised as *Ca-Mg-SO_4 water type* (i.e. SD6 and SD8). This group is characterised by an increased SO_4^{2-} content and Ca^{2+} and Mg^{2+} as the dominant cation. This water type signifies SO_4^{2-} contaminated water as a result of historical and/ or current mining activities. The dominant process in this facies is mixing and reverse ion exchange.

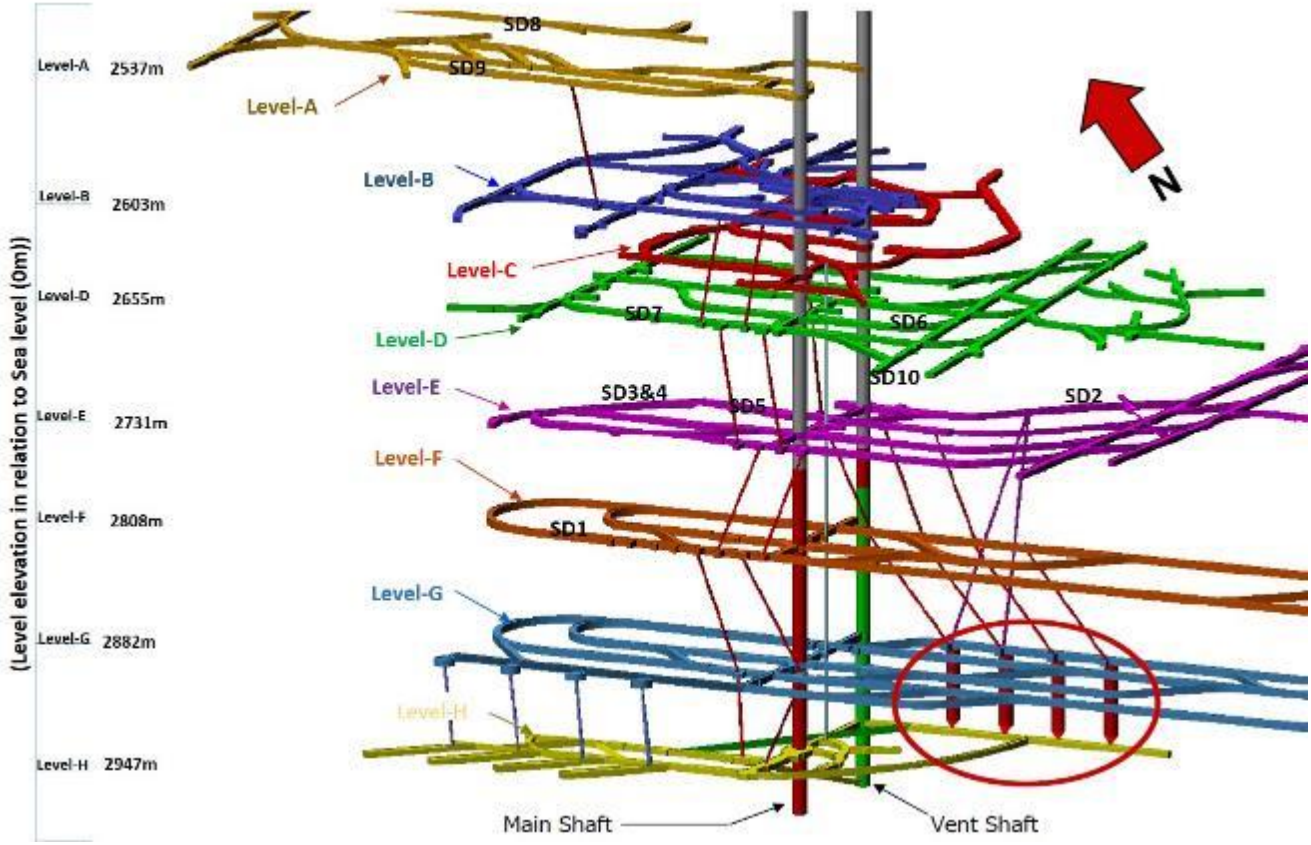

Figure 5-4:3D schematic figure of SDGM showing Main Shaft (twin shaft) and location of sampling points.

5.2.1 Stable Isotope Signatures

Seepage water from the study area (Table 5.2 and Figure 5-5) showed slightly distinct isotopic composition which made it possible to characterise the source of seepage, evaluate the degree of mixing if any, characterise the processes governing recharge mechanism, characterise groundwater flow pathways as well as the evolution of groundwater chemistry.

A total of 10 underground seepage samples (SD1-SD10) were collected and analysed for stable isotopes $\delta^{18}O$ and $\delta^{2}H$. The stable isotope of $\delta^{18}O$ and $\delta^{2}H$ results are shown in Table 5.2. Stable isotope results of $\delta^{18}O$ and $\delta^{2}H$ are presented in Figure 5-5.

Local Meteoric Water Line

The Global Meteoric Water Line (GMWL) and the Local (Pretoria) Meteoric Water Line (LMWL) are used, with an assumption that the local rainfall has a similar isotopic composition

as the Pretoria rainfall isotopic composition. The LMWL and GMWL based on $\delta^{18}O$ and $\delta^{2}H$ data are given by the following equations:

δD = 6.7 x δ18O + 7.2 ‰ **Equation 4 (Abiye, 2013)**

δD = 8 x δ18O + 10 ‰ **Equation 5 (Craig, 1961)**

D-excess is calculated using the following formula:

$$d = \delta 2H - 6.7\ \delta 18O$$ **Equation 6 (Abiye, 2013)**

LMWL characterises precipitation with slope S=6.7 and d-excess of 7.2. The slope and the d-excess of the LMWL are lower than that of the GMWL (S=8 and d-excess=10), thus, suggestive of secondary evaporation enrichment or humidity variation in precipitation. According to Wu (2005) as in Baqa (2017), a slope less than that of the GMWL is known to have resulted from secondary evaporation during precipitation in South Africa. This phenomenon tends to cause enrichment in $\delta^{18}O$ and δD (the heavy isotope) in the residual liquid water (rainfall) and as a result, causes a decrease in deuterium excess (d-excess value).

Stable Isotope Seepage Characterisation

The stable isotope results of $\delta^{18}O$ and δD varied from -31.6 ±0.2 ‰ and -8.58 ±0.0 ‰ at SD2 to -0.5 ±0.5 ‰ and -0.78 ±0.1 ‰ at SD10, respectively. The sampled seepage water were all highly depleted concerning $\delta^{18}O$ and δD (Figure 5-5). Seepage samples SD1, SD2, SD5, SD7, SD9, and SD6 plotted above the GMWL and LMWL while SD6 and SD9 plotted slightly above the GMWL/LMWL. These samples showed no sign of evaporation where most of the data plotting on and above the GMWL/LMWL. Generally, samples plotting above the LMWL relate to low rainfall during dry air conditions (Clark and Frits, 1997). Such rainfalls are characterised by low air humidity where the first rain is generally depleted and the precipitation plot well above the meteoric water line.

As previously mentioned, seepage samples SD1, SD2, SD5, SD6, SD7, and SD9, plotted above the GMWL and LPMWL. These samples suggest that the local rainfall could have been subjected to the condensation effect or mixing of air masses before recharge, which is controlled by regional air circulation (Abiye, 2013). The cause of depleted isotopic composition at these sampling sites can be attributed to the condensation effect which is controlled by regional air circulation from the South Atlantic and Indian Ocean air masses.

On the other hand, seepage sample SD8 plotted both on the GMWL as well as on the LMWL. A plot on either the GMWL and/ or the LWML indicates that the seepage sample at SD8 has a similar isotopic composition with rainfall and this could be as a result of direct rainfall infiltration through fractures, faults, weathered dykes, joints, and mining-induced hydrogeological structures that outcrop on the surface resulting in groundwater isotopic signature similar to rainfall isotopic signature (Figure 3-15).

Seepage samples SD3, SD4, and SD10, plotted below and slightly deviating from both the LMWL and GMWL. A deviation from the LMWL signifies secondary evaporation before and/ or during infiltration. In this instance, a possible deviation from the LMWL could be a result of diffused or sluggish water movement within the subsurface zone permitting isotope fractionation.

SDGM isotopic composition showed that the seepage samples plot above and below the meteoric water lines, suggesting that different processes control the recharge mechanism in the study area. Correlation between δ^2H and $\delta^{18}O$ mainly showed three distinct groups, which are all clustered within the fourth quadrant (depleted in δ^2H and $\delta^{18}O$ values). These groups were distinguished based on showing evaporation signs or not. However, both evaporated and un-evaporated samples cluster around both GMWL and LMWL suggest that these waters are of atmospheric origin. The first group is depleted with respect to δ^2H and $\delta^{18}O$. This group is indicative of condensation effect/water mass mixing, which is controlled by regional air circulation from the South Atlantic and Indian Ocean air masses. The second group plots on top of the GMWL and LMWL resembling local rain events thus suggesting recharge occurs through direct rainfall recharge from high and short intense rainfall events during summer months. The third group plotted below and deviating from both the LMWL and GMWL. These samples are indicative of secondary evaporation during and/ or before rainfall recharge.

Table 5.2: Stable isotope of δ ^{18}O and δD.

Sample Name	δ^2H (‰)	± 2H StDev (‰)	$\delta^{18}O$ (‰)	± 18O StDev (‰)
SD1	-29.5	0.6	-6.36	0.1
SD2	-31.6	0.2	-8.58	0.0
SD3	-4.2	1.0	-1.48	0.1
SD4	-3.6	0.3	-1.40	0.0
SD5	-26.1	0.7	-6.79	0.1
SD6	-6.8	0.9	-2.55	0.1
SD7	-28.6	0.8	-5.87	0.1

SD8	-5.1	0.8	-1.84	0.1
SD9	-12.9	0.3	-3.36	0.0
SD10	-0.5	0.5	-0.78	0.1

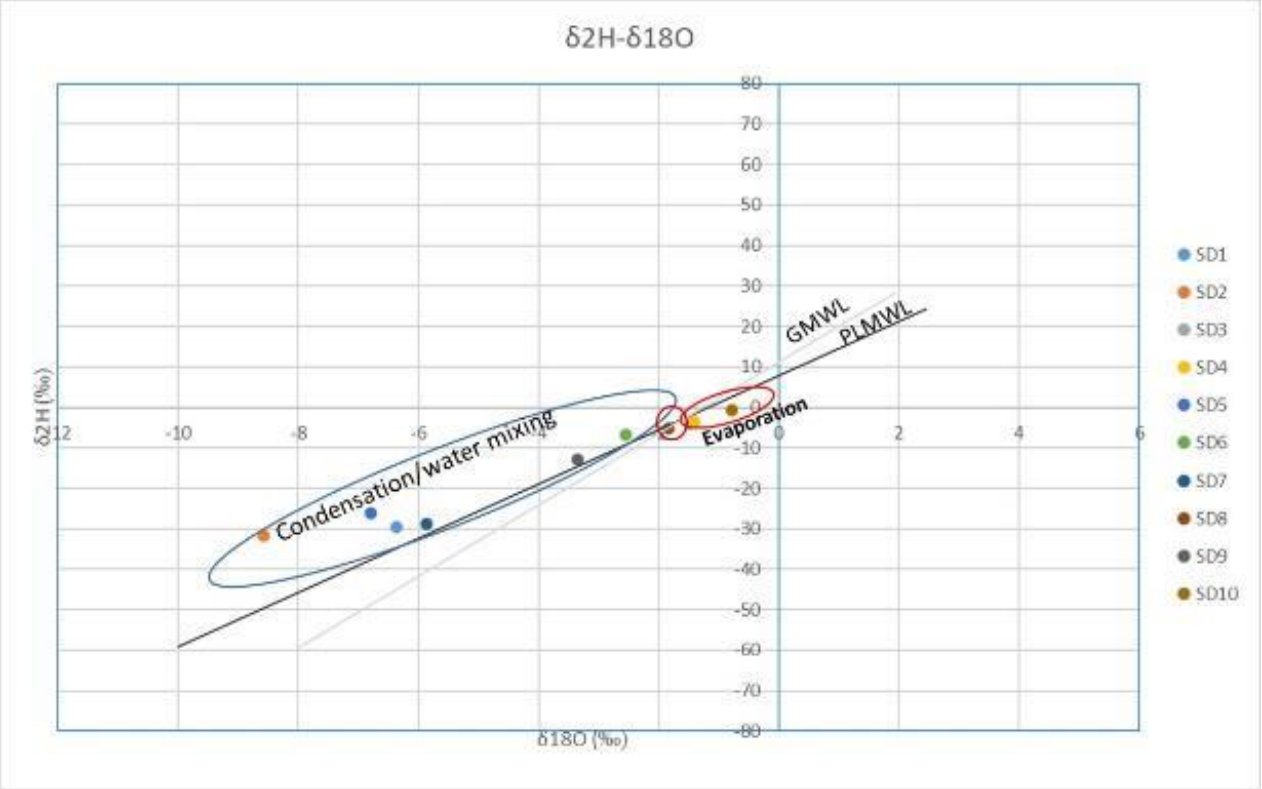

Figure 5-5: Correlation of $\delta^{18}O$ vs δ D ($\delta^{2}H$) diagram of seepage samples collected at SDGMs underground workings. GMWL and PLMWL are fitted for comparison.

5.2.2 ^{3}H-Tritium Dating

Nine seepage stations (SD1-SD9) were sampled in October 2020 for Tritium (^{3}H) analysis, however, SD10 did not have enough volume for analysis. The tritium results are shown in Table 5.3. The tritium values in seepage water range from 0.0-1.8 T.U. The seepage water samples SD2, SD7, and SD8 contained low tritium content below 0.4 TU compared to seepage water samples SD1, SD3, SD6, and SD9 which had a varying Tritium content between 0.6-1.8 TU.

SD1, SD2, SD5, SD7, and SD8 have ^{3}H content <0.8 TU which was interpreted as sub-modern water, probably recharged before the 1950s (see Section 4.2.2). Low to zero tritium content in a seepage water sample (SD2 and SD7) suggests no active recharge (Abiye, 2013). SD3, SD4, SD6, and SD9 have tritium concentrations ranging between 0.8-1.8 TU and this was interpreted as a mixture of sub-modern and hence, indicative of recently recharged waters. Low

measurable tritium suggests longer residence times for groundwater because of the delay in the unsaturated zone or low recharge/storage ratio in the unsaturated zone (Abiye, 2013).

In South Africa, rainwater has natural tritium at concentrations of approximately 5.6 TU (Abiye et al., 2015) and therefore, seepage tritium values similar to that in current-day rainfall tritium would indicate active recharge. Currently, at SDGM, none of the sampled seepage water matches the current concentration of tritium in precipitation and thus the sampled seepage samples indicate that no recharge has taken place over the past 12.43 years except at SD6 and SD9.

Table 5.3: Tritium results of underground seepage water.

Sample	**Tritium**			**Apparent Residence Time**
Identification	**(T.U.)**			**Years**
SD-1	0.7	±	0.2	37
SD-2	0.0	±	0.2	old
SD-3	1.1	±	0.3	29
SD-4	1.3	±	0.3	26
SD-5	0.6	±	0.2	40
SD-6	1.8	±	0.3	20
SD-7	0.0	±	0.3	old
SD-8	0.4	±	0.2	47
SD-9	1.4	±	0.3	25

Based on the above tritium values, SDGM`s underground seepage water can be characterised into two groups, namely, the sub-modern (recharged before the 1950s) and the mixture of sub-modern and recent recharge.

Based on the assumption made in chapter 4, the residence time (apparent age) for the water seepage samples is calculated about the 5.6 TU concentration of the recent rainfall. With the knowledge that, tritium has a half-life of 12.43 years, the samples with concentrations greater than ±2.8 TU will suggest the presence of water recharged in the past 12.43 years. Sample SD6 has the highest tritium concentration (1.8 TU) and can be approximated to have been recharged 20 years ago. Low tritium values exist (<0.8 TU, approximately recharged prior to 1952) suggesting very old water or deep circulating groundwater, this may indicate the presence of a hydraulic connection between the aquifer and the mine void (up to 3 km deep). The deep groundwater may reach the mine void through geological structures.

From the isotopic analysis above, two types of water are defined:

- a mixture of sub-modern and recent recharge, with tritium concentration between the 0.8-1.8 TU and where recharge within the age range +20 to 35 years ago; and
- the low tritium waters, <0.8 TU, categorised as sub-modern (recharged before 1952), age range between +35 to +47 years, indicating the presence of deep circulating groundwater.

5.3 Possible Water Pathways

Seepage stations were mapped and are plotted on mine plans (Figure 5-10 to Figure 5-17). Several seepage points are characterised by geological structures (faults, bedding planes, and joints), and the presence of drilled rock support holes. During the survey, it was observed that most of the seepage water occurs along with geological structures such as faults, joints, fractures (Figure 5-6), geological contacts, bedding planes as well as mining-induced fractures, exploration boreholes, and drilled rock support holes.

Figure 5-6: BH_Y core illustrating diced core, faults, and joints that can allow the flow of water and is associated with sample SD2

The chemistry of seepage water at SD1 is collected from a Long-Inclined Borehole (LIB_X) suggested natural waters. The water chemistry of SD1 has pH, TDS, and EC relating to natural waters (pH=7.4, EC=135 mS/m and TDS=791 mg/L).

Figure 5-9 and Figure 5-11 show a cross-section of LIB_X (500 m long) and a picture of LIB_X core. The boreholes are highly fractured and diced, illustrating the presence of weak zones that can allow groundwater flow. SD1 water sample can be interpreted as groundwater. LIB_X was

drilled up to 500 m, which is 30 m from the lava position. The cross-section illustrates the faulting of the orebody. SD1 may be groundwater that travelled through faulted orebody and then found a way into the drilled borehole void through bedding planes, faults, and fractures. If there are any geological structures (faults, fractures, or bedding planes) connecting the aquifer and the void, it is then possible for the groundwater to flow through the borehole void into the underground workings.

High seepage flows were observed along the bedding plane as well as the exploration boreholes. Seepage water along the bedding planes (Figure 5-7) such as at SD3 and SD4 (both located at level-E, Figure 5-4, approximately 2.7 km), showed an increased SO_4^{2-} concentration, with Ca^{+} as the dominant cation. These sampling stations suggest that the source of seepage is mine impacted water and this was observed in Section 5.1. Stable isotope analysis signified that these samples (SD3 and SD4) had undergone secondary evaporation through a diffused or sluggish water movement within the subsurface zone permitting for isotope fractionation. However, tritium analysis indicated that water along these structures (bedding planes) is indicative of recently recharged water, where recharge occurred between the age range +26 to 29 years ago.

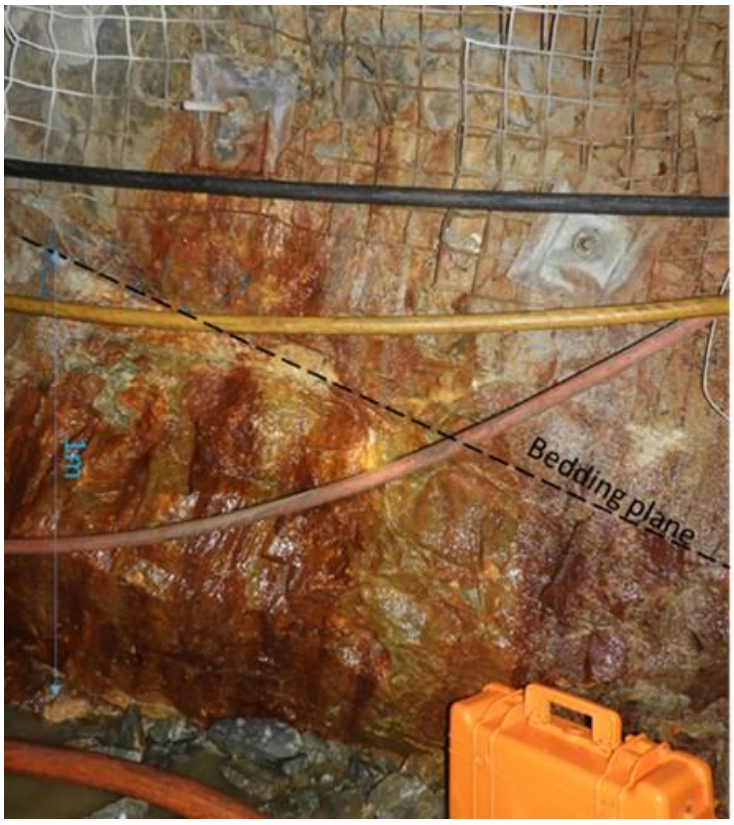

Figure 5-7: Seepage water collected from bedding plane/reef contact at SD 4 and SD5 at SDGM.

Furthermore, major seepage flows were observed on the hanging wall, Figure 5-8. Hydrochemical analysis suggests that seepage samples (SD5-SD10) along with these structures (faults, joints, and drilled support holes as indicated from mine plans Figure 5-13 to Figure 5-17) have undergone various hydrochemical evolution. Stable isotope analysis suggested that these samples were recharged under different recharge mechanisms as well as a unique isotope fractionation process. Seepage samples SD5, SD6, SD7, and SD9, plotted above the GMWL and LMWL, suggesting that the local rainfall could have been subjected to the condensation effect prior to recharge or water mass mixing. These samples contained varying tritium content from 0 to 1.8 TU. Seepage samples (SD5 and SD7) with tritium content <0.8 TU indicated that the seepage water from these structures was recharge prior to the 1950s and thus signifying that no active recharge is taking place along these structures. Conversely, SD6 and SD9 had tritium content >0.8 TU and this indicated that the seepage water from these structures was recharged approximately +20 years ago signifying recently recharged waters.

Seepage sample SD10, sampled from the hanging wall along the mining-induced structures (such as joints) plotted below the LMWL, thus, indicative of secondary evaporation prior to recharge. Further hydrochemical facies indicated that the source of the sample is a NaCl water type. A NaCl type water is/was understood to be associated with the water-logged backfilled stopes above the current mining cut.

Seepage SD8 located along the fault line and at the shallow mining zone at Level-A (Figure 5-4, Figure 5-14, and Figure 5-15) showed no signs of evaporation and/ or condensation effect and hence plotting on both the LMWL as well as the GMWL. This indicated recharge as the source of the seepage sample which occurred through direct rainfall recharge along the fault line/fault outcropping at the surface resulting in groundwater isotopic signature similar to rainfall isotopic signature. However, the sample contained low tritium content of about 0.4 TU and thus indicative of deep circulating water approximately recharged about+47 years ago.

Figure 5-8: Seepage water collection from hanging wall at SDGM associated with mapped faults and joints.

Apart from the sample sites, seepage water was also observed in the active mining zones. The seepage flow through active mining zones is understood to be associated with mining induced fractures (i.e. blasting of long hole stopes)which can create and/ or enhance the fracture networks resulting on the seepage generation on the underlying mining zones. Furthermore, earth-shaking due to blasting and/ or seismicity can also enhance the existing water-bearing structure (fracture, joint, etc) openings and drilled holes (support holes or exploration holes).

The reefs at SDGM dip towards the South. In the past, SDGM used to mine using the conventional stope method, which means, mining following reef bands along dip. Most of the old stopes are backfilled. The current SDGM`s mining method mines below the old stopes in the current mine. This however constitutes approximately 30% of the total mining footprint and will be diminishing in the next few years as mining will be concentrated in the ground to the North of the Wrench Fault.. Backfilling requires a lot of water and proper water management. Experience shows that backfill material takes ±30 days to dry. Water seeps out from the backfill material and flows until it is accumulated where mining stops. If the water is not adequately managed (i.e., pumped), it remains at the same position until it gets pathways

to flow. Moreover, water during backfilling needs to be pumped, but if the water is not well managed, backfill material and water can flow to the walkway and cause muddy surfaces.

Further, inadequate management of service water including damaged/broken pipes and blocked water dams contribute to the accumulated water in both active and old mining levels. As soon as the water finds pathways, it flows to the next level, this could be the reason for the observed hanging wall seepages and mixing waters chemistry.

Seepage water/fissure water from underground geology exploration boreholes (SD1 and SD2) indicated deep circulating groundwater and/ or old mined-out voids with accumulated water. This is further supported by the hydrochemical facies which suggested (i) the end of the geohydrological cycle or (ii) old/stagnant water. Some boreholes are drilled within mining vicinities (for example, SD2) and such boreholes may deflect and hole into current mining areas. An exploration-drilling borehole may deflect and hole into an old or active mining stope. In cases where the stope contains/has old accumulated water, it is likely that the water will flow through the drilled borehole void to the level where the drilling machine is located at a lower level.

At SDGM, some exploration boreholes are drilled from inactive mining levels and are mostly drilled ahead of mining to the lava position or drilled up or down to confirm certain structures or reefs. Some boreholes are drilled between active mining levels. For example, SD2, (sample collected from Borehole BH_Y) water chemistry indicated the chemistry is similar to mine water from backfilled levels, high salinity, and alkaline (pH=10). This water may be from levels where there are sumps and old mined-out areas with accumulated backfill water.

Correlation between $\delta^{2}H$ and $\delta^{18}O$ provided more useful ideas on the sources of seepage as well as the dominant processes/mechanism governing recharge. Based on the stable isotope analysis the seepage samples were conceptually characterised into three groups: the first group plotted above and on the local meteoric water line, signifying un-evaporated isotopic composition. This group was understood to be indicative of condensation effect/water mass mixing, which is controlled by regional air circulation from the South Atlantic and Indian Ocean air masses. The second group plotted on top of the GMWL and LMWL resembling local rain events thus suggesting recharge occurs through direct rainfall recharge from high and short intense rainfall events during summer months. The third group plotted below and deviating

from both the LMWL and GMWL. These samples were indicative of secondary evaporation during and/ or before rainfall recharge.

All seepage samples contained detectable amounts of tritium and hence indicative of recharge/aquifer renewability. Tritium signature varied from 0.0 TU to 1.8 TU. Seepage water was characterised as a mixture of sub-modern and recent recharge, with the tritium concentration ranging between 0.8 and1.8 TU. These samples were understood to be recently recharged in the past +20 to 35 years. Seepage samples with low tritium content <0.8 TU, and were categorised as sub-modern, recharged before the 1950s. These samples indicated that recharge along those structures mainly occurred approximately +35 to +70 years ago, indicating the presence of deep circulating groundwater that emerges as condensation/water mass mixing.

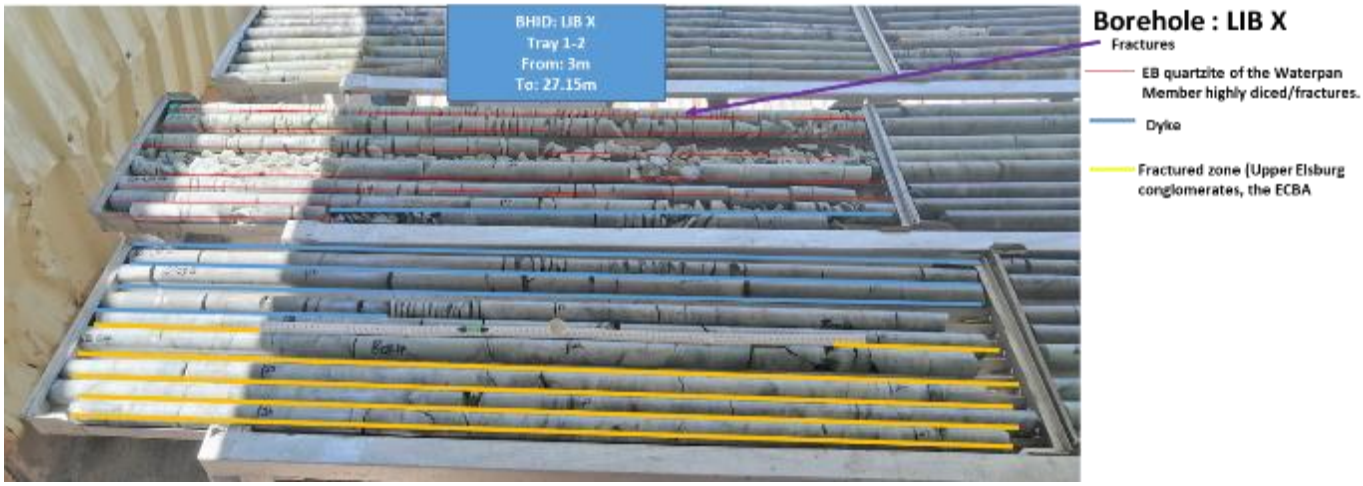

Figure 5-9: LIB _X drilled core associated with SD1

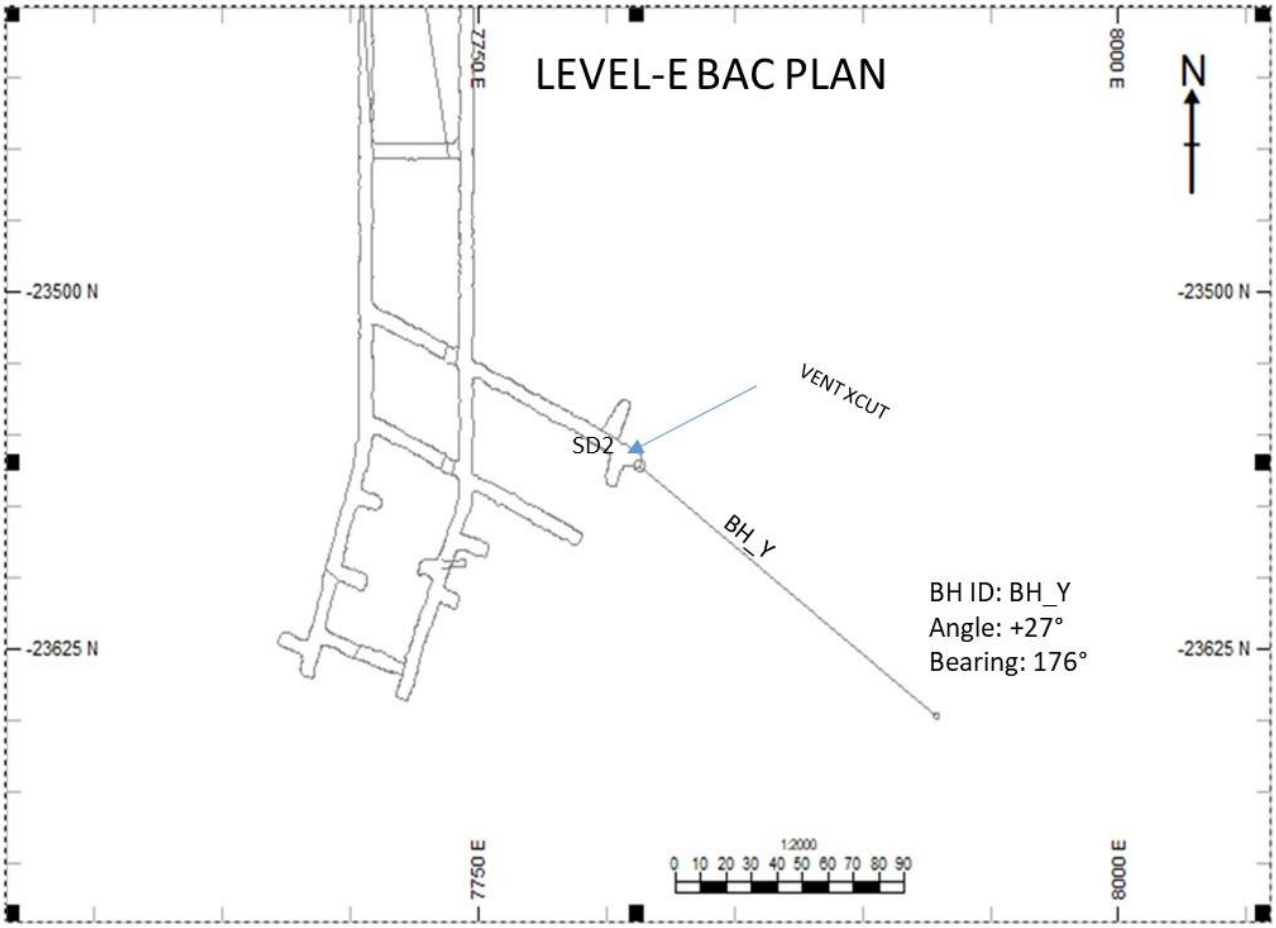

Figure 5-10: Level-E plan showing SD2 sampling station

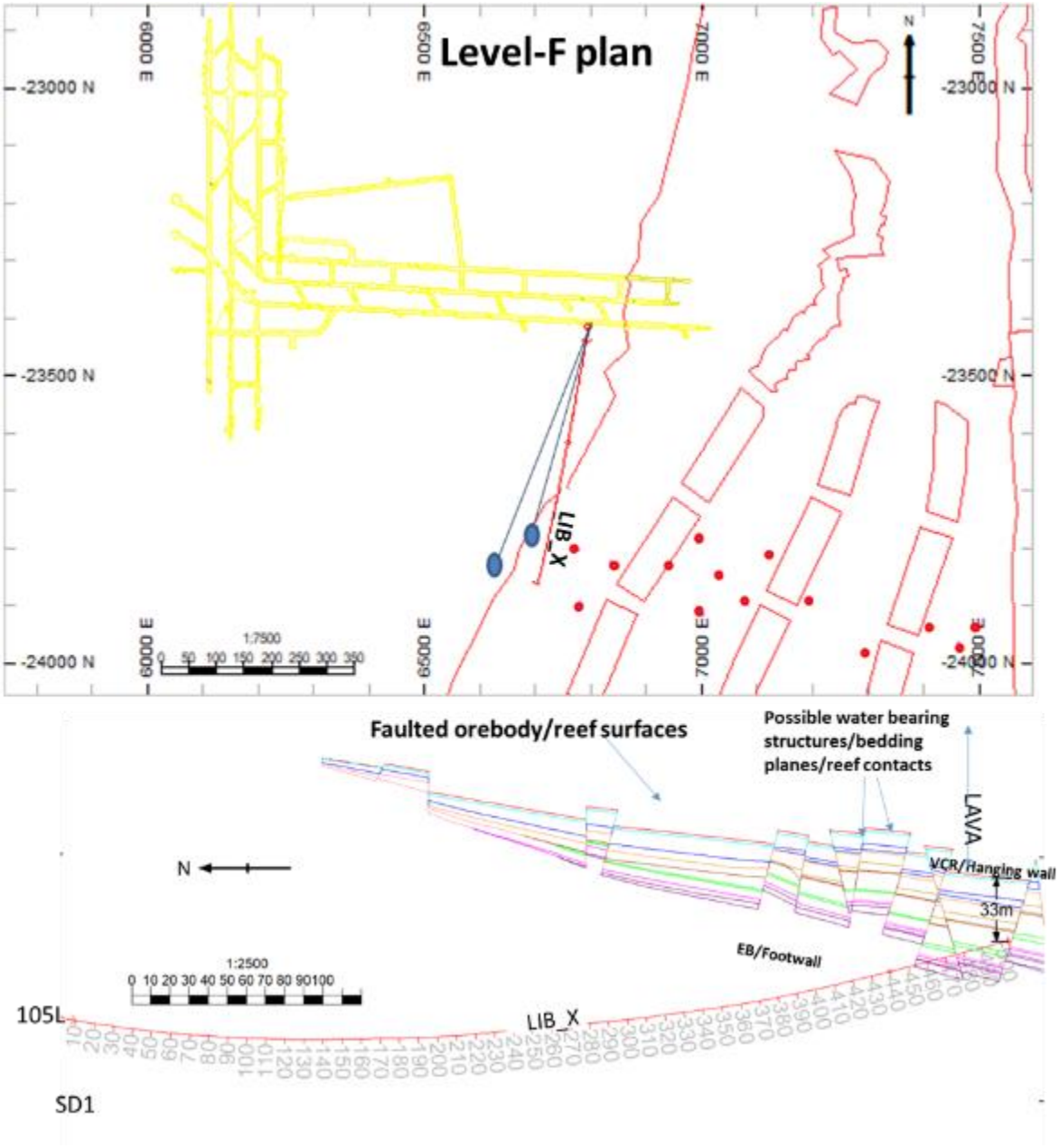

Figure 5-11: Level-F plan showing SD1 sampling station and a North to South cross-section of BH LIB_X

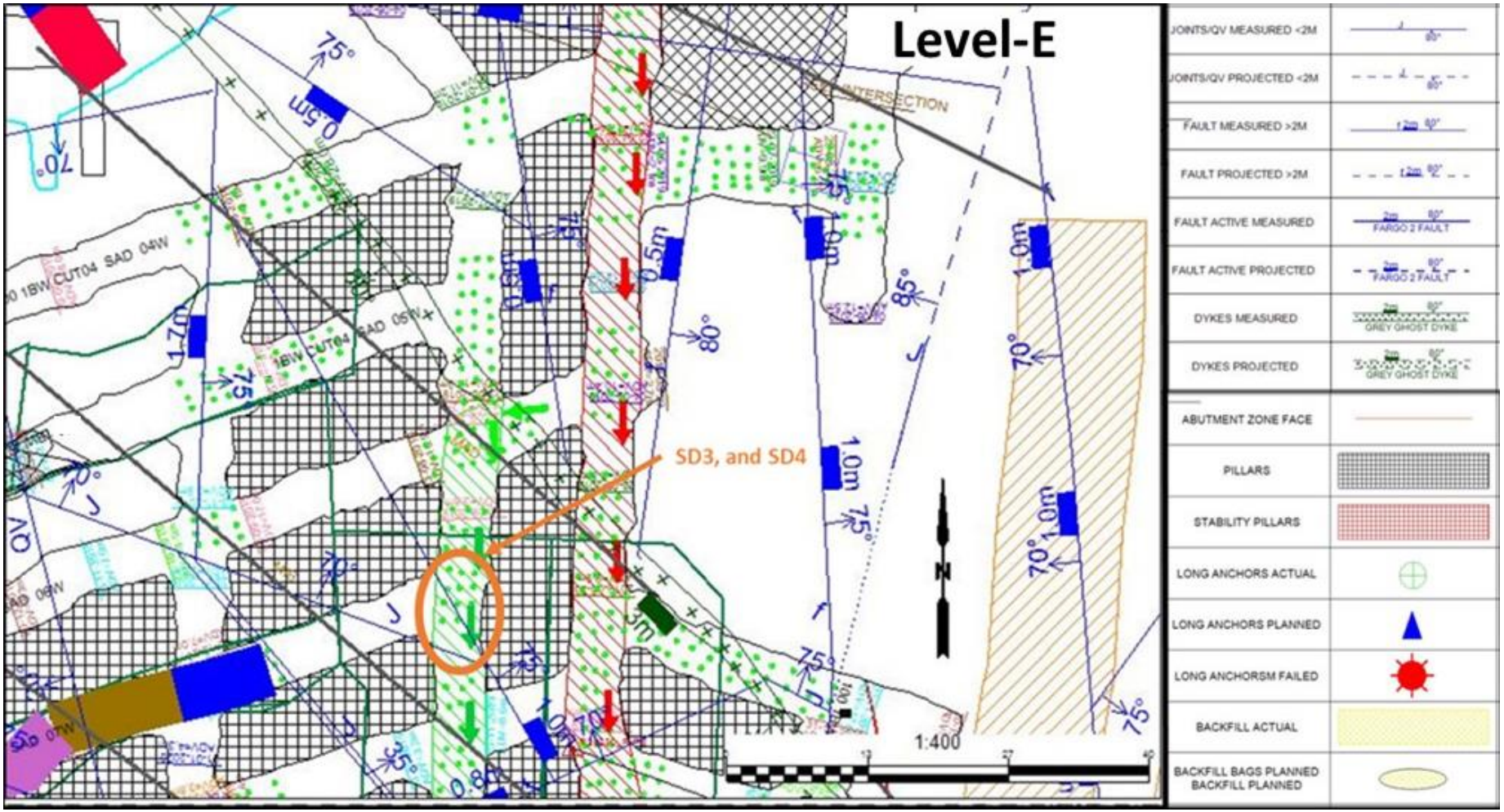

Figure 5-12:Level-E CUT04 plan showing SD3 and SD4 sampling stations.

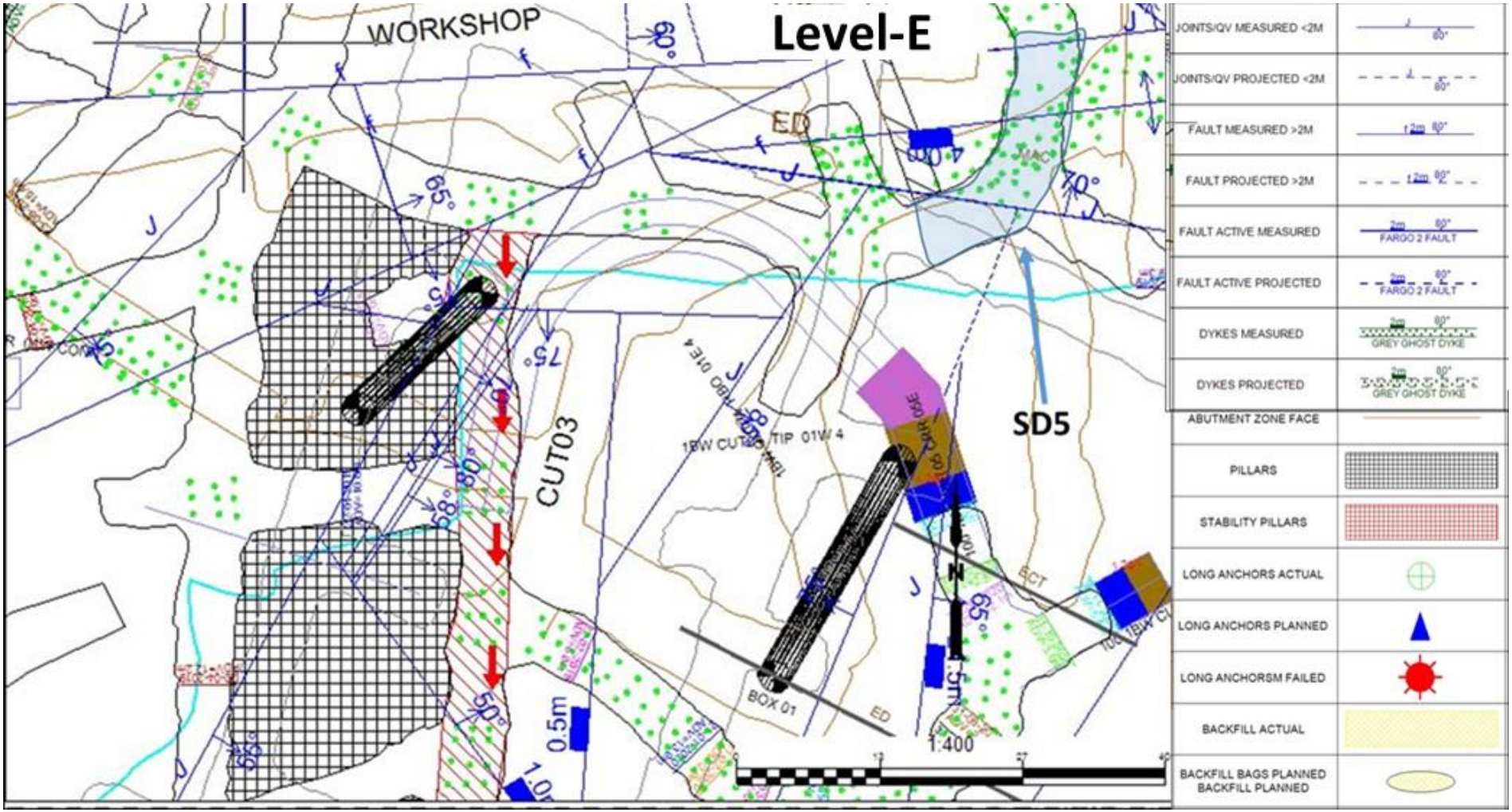

Figure 5-13: Level-E 1BW CUT04 plan showing SD5 sampling station.

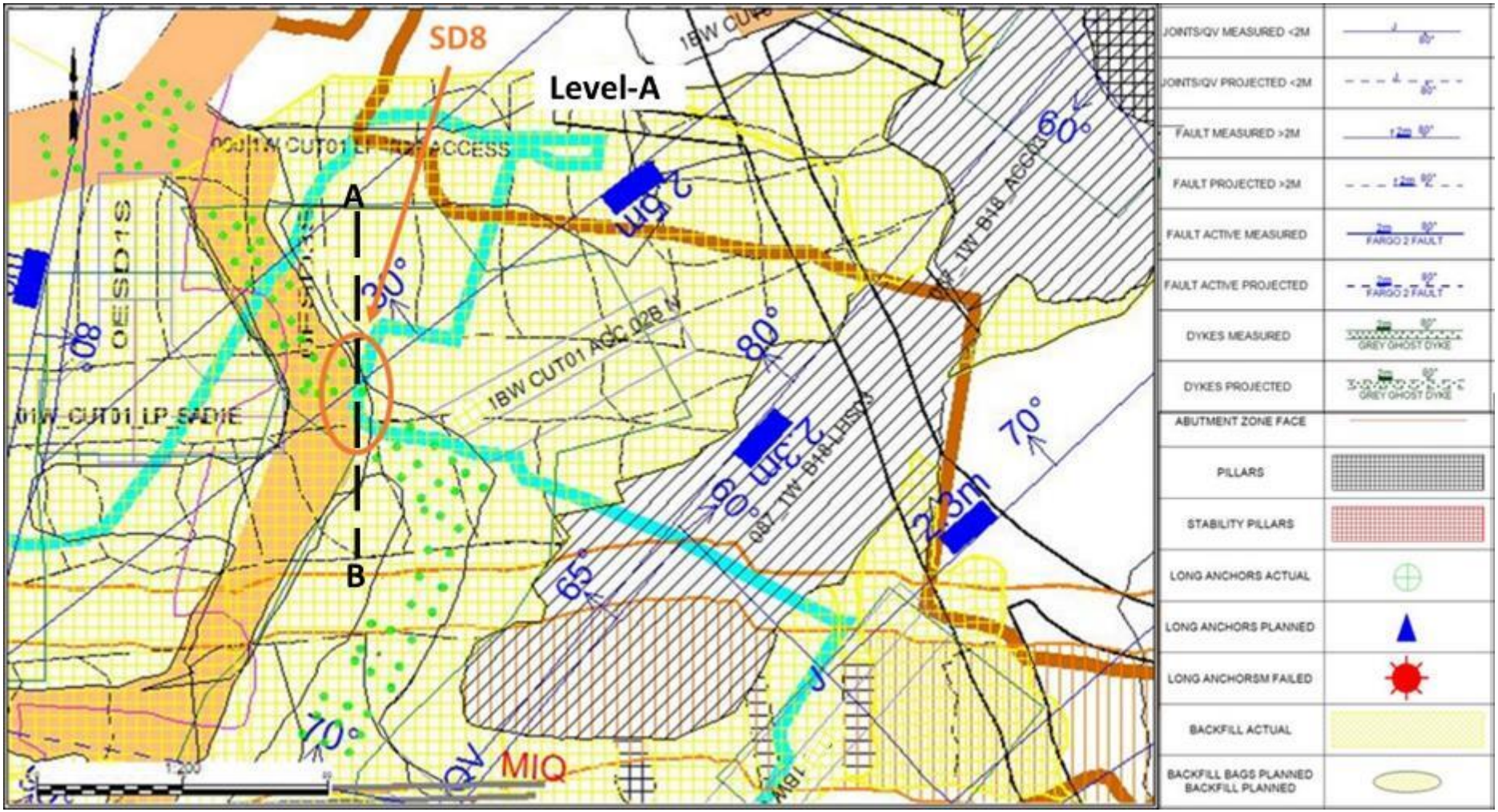

Figure 5-14: Level-A 1BW CUT01 plan showing SD8 sampling station.

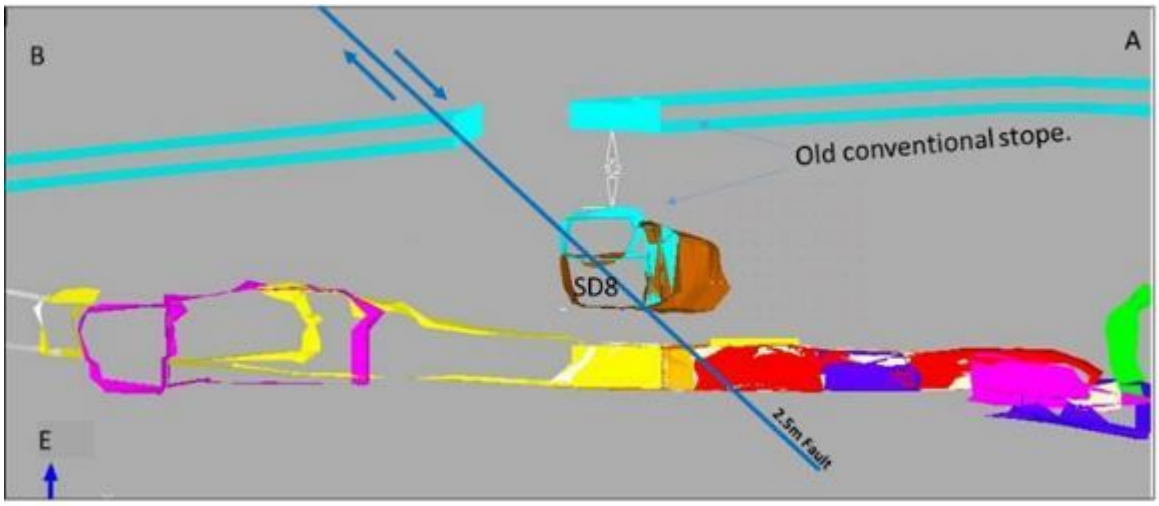

Figure 5-15: A South to North cross-section through SD8 sampling point.

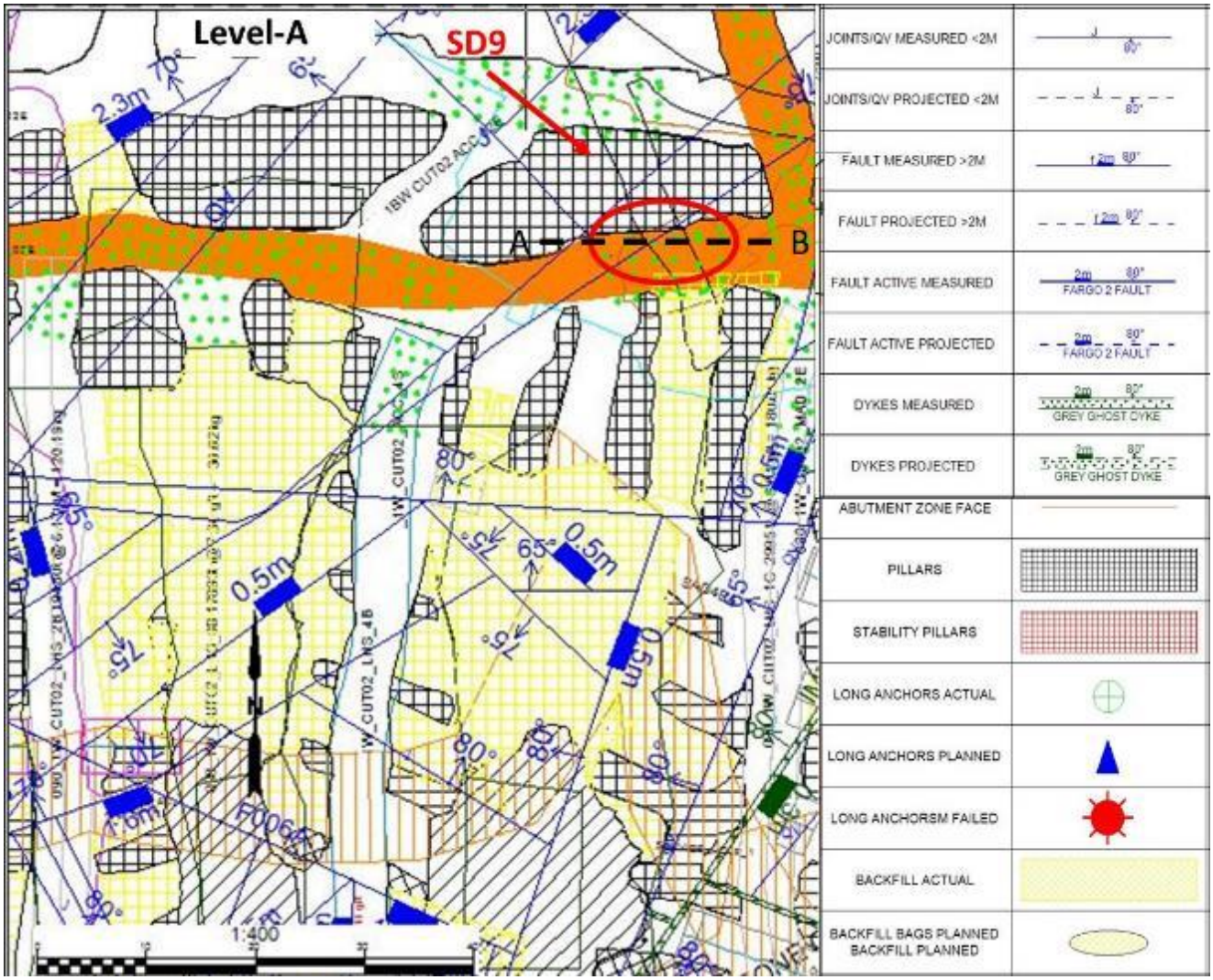

Figure 5-16: Level-A 1W CUT02 plan showing SD9 sampling point.

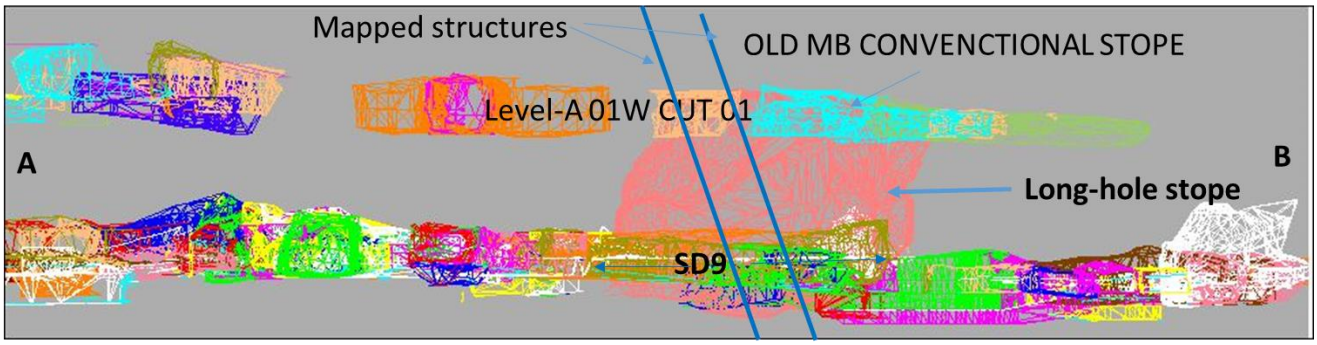

Figure 5-17: A West to East cross-section through SD9 sampling point illustrating mapped geological structures, old convectional stopes, and long hole stope.

CHAPTER 6

CONCLUSION AND RECOMMENDATIONS

6.1 Conclusion

Evaluation of the characteristics of the seepage at SDGM`s underground void was made through reviewing the local hydrology, geology, physiography, climate, and the review of previous hydrogeology work done at the mine. Based on the hydrochemical facies, the seepage water is characterised into four groups.

The first group is *Mg-SO_4* water type (i.e. SD6 and SD9). This group is characterised by the increased SO_4^{2-} signature. This water type suggests SO_4^{2-} contamination from the mine and/ or a mix of different water types due to the re-use of recycled water for mining activities.

The second group is *NaCl water type* (SD1) indicative of a regional groundwater source. This water type can be characterised as the end of hydrogeological cycle type water where old groundwater has resided within the groundwater system.

The second hydrochemical type of water characterised with NaCl is SD2. The hydrochemical analysis indicated that the water quality at SD2 is brackish and characterised with alkaline pH. The hydrochemical facies at SD2 suggests that the water type represents old/stagnant groundwater. This is confirmed by the Tritium dating which suggests that SD2 water can be characterised as sub-modern water probably recharged before 1952. Therefore, the possible source of seepage at SD2 are the minedout areas as the boreholes are drilled throughout the mined-out waterlogged areas.

SD7 also indicated characters of NaCl water type. The sample had no dominant cation. This water type can be characterised and/ or suggest NaCl contamination or the water results from a mixture of different types due to the use and re-use of recycled water

The third group is characterised as *Ca-SO_4 water type* (i.e. SD3 and SD4). This group is characterised by an increased SO_4^{2-} concentration, with Ca^{+} as the dominant cation. Sulphides (sulphides bearing rocks) are known to exist on-site and hence, the most likely source of the elevated sulphate is the oxidation of sulphide bearing rocks. On the contrary, the occurrence of calcium is understood to be natural due to the dissolution of the host rock. These results suggest that the source of seepage at SD3 and SD4 is mine water.

The fourth group is characterised as *Ca-Mg-SO_4 water type* (i.e. SD6 and SD8). This group is characterised by an increased SO_4^{2-} content and Ca^{2+} and Mg^{2+} as the dominant cation. This water type signifies SO_4 contaminated water as a result of historical and/ or current mining activities. The dominating process in this facies is mixing processes and reverse ion exchange.

Based on the stable isotope analysis the seepage samples were conceptually characterised into three groups: the first group plotted above and on the local meteoric water line, signifying un-evaporated isotopic composition. This group was understood to be indicative of condensation effect/water mass mixing, which is controlled by regional air circulation from the South Atlantic and Indian Ocean air masses. The second group plotted on top of the GMWL and LMWL resembling local rain events thus suggesting recharge occurs through direct rainfall from high and short intense rainfall events during summer months. The third group plotted below and deviating from both the LMWL and GMWL. These samples were indicative of secondary evaporation during and/ or before rainfall recharge.

All seepage water contained detectable amounts of tritium and hence indicative of recharge/aquifer renewability. Tritium signature varied from 0.0 TU to 1.8 TU. Seepage water with tritium content between 0.8 and1.8 TU was characterised as a mixture of sub-modern and recently recharged water. These samples were understood to be recently recharged in the past +20 to <35 years. Seepage samples with low tritium content <0.8 TU, were categorised as sub modern, recharged prior to 1950s. These results indicated that recharge mainly occurred approximately +25 to +75 years ago thus, indicating the presence of deep circulating groundwater that emerges as condensation/water mass mixing.

Based on the hydrogeological characterisation/conceptualisation of the main source of seepage within the study or from the study, it was observed that seepage is associated with the backfilled areas on the level above, places closer to active mining (i.e. long hole blasting), along the abutment zones, the geological structures such as faults and mining-induced fractures, worsened/compounded by inadequate mine-water management. Seepage water was also observed on drilled boreholes, which holed to active or old abandoned mining levels with accumulated water. Possibly groundwater may flow into the mine void through borehole voids that drilled up to the lava position or intersected structures with the potential of connecting the aquifer and the mine void, hence the observed natural water in SD1.

A way forward to ensure the safety of the mine`s employees, and damage of mine property for a successful safe, and productive South Deep Gold Mine, strict and long-term excess water and service water management underground is recommended.

6.2 Recommendations

A quantifiable and qualitative research methodology was taken to investigate the source of seepage and its governing processes within SDGM`s underground void. However, additional investigations and improvements are advisable to expand the reliability of these research discoveries:

- Collection and mapping of more underground seepage samples to analyse the chemistry and isotopic signatures which will assist in improving the seepage and fissure water data at the study area. This can be done over time by monitoring the defined wet places underground.

- Collection of groundwater and surface water samples in the study area to analyse for isotopes. This will define the isotopic signature of the study area.

- Improved underground mine water management such as at backfilling areas and active stopes is recommended to minimise the source of seepage. Further, proper management and maintenance of damaged water pipes and overflowing/blocked dams is also recomended.

REFERENCES

Abiye, T. (Editor). 2013. The use of isotope hydrology to characterize and assess water resources in South (ern) Africa. WRS Report No TT 570/13 Pretoria. 211pp.

Abiye, T.A., Mengistu, H., Masindi, K. and Demlie, M. 2015. Surface water and groundwater interaction in the upper Crocodile River Basin, Johannesburg, South Africa: Environmental isotope approach. *South African Journal of Geology*, **118**(2):109-118.

Abiye, T.A., Bybee, G. and Leshomo, J. 2018. Fluoride concentrations in the arid Namaqualand and the Waterberg groundwater, South Africa: Understanding the controls of mobilization through hydrogeochemical and environmental isotopic approaches, Groundwater for Sustainable Development, **6**:112 – 120.Adams, R. and Younger, P.L. 2001. A strategy for modeling ground water rebound in abandoned deep mine systems. Groundwater, **39**(2):.249-261.

Anna, L.O. 1986. Geologic framework of the ground-water system in Jurassic and Cretaceous rocks in the Northern Great Plains, in parts of Montana, North Dakota, South Dakota, and Wyoming. US Government Printing Office.

ArcMap (version 10.6). Software. Redlands, CA: Esri Inc, 2018.

Ashton, P.J., Love, D., Mahachi, H. and Dirks, P.H.G.M. 2001. An overview of the impact of mining and mineral processing operations on water resources and water quality in the Zambezi, Limpopo and Olifants Catchments in Southern Africa. Contract Report to the Mining, Minerals and Sustainable Development (Southern Africa) Project, by CSIR-Environmental, Pretoria and Geology Department, University of Zimbabwe-Harare. Report No. ENV-PC, 42, pp.1-362.

Aston, T.R.C. and Singh, R.N. 1983. A reappraisal of investigations into strata permeability changes associated with longwall mining. *International journal of mine water*, **2**(1):1-14.

Bai, Q. and Tu, S., 2019. A general review on longwall mining-induced fractures in near-face regions. Geofluids, 2019.

Barnard, H.C. 1999. Hydrogeological map series of the Republic of South Africa, Johannesburg.

Baqa, S.S. 2017. Groundwater recharge assessment in the upper Limpopo River basin: a case study in Ramotswa dolomitic aquifer (Doctoral dissertation).

Bridgwood, E.W., Singh, R.N. and Atkins, A.S. 1983. Selection and optimization of mine pumping systems. *International journal of mine water*, **2**(2):1-19.

Butler, M.J, 2020. Environmental isotope analysis on nine (9) water samples, Johannesburg: iThemba LABS. Environmental Isotope Laboratory

Clark, I. and Fritz, P. 1997. Environmental Isotopes in Hydrogeology. Lewis Publishers. Boca Raton. New York

Cook, P. 2020. Introduction to Isotopes and Environmental Tracers as Indicators of Groundwater. Guelph, Ontario: Groundwater Project.

Cook, P.G. 2003. A guide to regional groundwater flow in fractured rock aquifers (p. 151). Henley Beach, South Australia: Seaview Press

Cozma, A.I., Baciu, C., Moldovan, M. and Pop, I.C. 2016. Using natural tracers to track the groundwater flow in a mining area. *Procedia Environmental Sciences*, **32**:211-220.

Craig, H. 1961. Isotopic Variations in Meteoric Waters. Science. 133:1702-1703.

Dalasile, P.K., 2018. Hydrogeological study of geological features in the groundwater system of Tweefontein 360KT farm, Limpopo Province (Doctoral dissertation).

Dankert, B.T. and Hein, K.A. 2010. Evaluating the structural character and tectonic history of the Witwatersrand Basin. Precambrian Research, **177**(1-2):1-22.

Department of Water Affairs and Forestry (DWAF). 2008. Best Practice Guideline A6: Water Management for Underground Mines. Department of Water Affairs and Forestry, Pretoria.

De Roer, K. 2004. The hydrological impact of the rewatering of the Gemsbokfontein dolomitic compartment on the Wonderfonteinspruit (dissertation, North-West University) Doctoral

Dill, S., Boer, R.H., Boshoff, H.J.J., James, A.R. and Stobart, B.I. 2007. An Assessment of the Impacts of Groundwater Quality Associated with the Backfilling of Dolomitic Cavities with Gold Mine Tailings. Pretoria: Water Research Commission.

Etikan, I., Musa, S.A. and Alkassim, R.S. 2016. Comparison of convenience sampling and purposive sampling. *American journal of theoretical and applied statistics*, **5**(1):1-4.

Fernandez Rubio, R., Carvalho, P., Real, F. 1988. Mining-hydrological characteristics of the underground cooper mine of Water problems in Spanish coal mining. *International Journal of mine water*, (5):13-28, Madrid. Spain.

Frimmel, H.E. and Minter, W.E.L. 2002. Recent developments concerning the geological history and genesis of the Witwatersrand gold deposits, South Africa. Special Publication-society of Economic Geologists, **9**:17-46.

Funke, J.W. 1990. The Water Requirements and Pollution Potential of South African Gold and Uranium Mines. WRC report KV 9/90.

Golder. 2016, Development of a Post Closure Water Management Plan- Conceptual Model Report-Goldfields South Deep Mine. Golder Associates report 1531509-303709-1.

Golder. 2018. Development of a post closure Water Management Plan -Phase 2 Decant Study Report, Goldfields, South Deep Mine. Golder Associates report 18102152-323463-1.

Golder. 2020. Development of a post closure Water Management Plan -Phase 2 Decant Study Report, Goldfields, South Deep Mine. Golder Associates report 18102152-325627-2

Goldfields. 2012. South Deep Gold Mine Technical Short Form Report.

Goldfields. 2012. South Deep Mine Geological Handbook. Nonpublished report.

Goldfields LTD. 2011.South Deep Gold Mine. Competent persons Report. Johannesburg. South Africa. Pp. 22-52.

Guan, Z., Jia, Z., Zhao, Z. and You, Q. 2019. Identification of inrush water recharge sources using hydrochemistry and stable isotopes: A case study of Mindong No. 1 coal mine in north-east Inner Mongolia, China. *Journal of Earth System Science*, **128**(7):200.

Guilford, J. P. (1973). Fundamental statistics in psychology and education. New York, NY: McGraw-Hill.

Hanhu, L. and Yunquan, C. 2011. Technologies of preventing coal mine water hazards for sustainable development in North China. Geotechnical and Geological Engineering, **29**(1):1-5.

Harris, C., Burgers, C., Miller, J. and Rawoot, F., 2010. O-and H-isotope record of Cape Town rainfall from 1996 to 2008, and its application to recharge studies of Table Mountain groundwater, South Africa. South African Journal of Geology, 113(1), pp.33-56.

Hem, J.D. 1985. Study and interpretation of the chemical characteristics of natural water (Vol. 2254). Department of the Interior, US Geological Survey.

Hiscock, K.M. 2009. Hydrogeology: principles and practice. John Wiley & Sons.

Horstmann, U.E. and Coetzee, H. 2004a. A strategic water management plan for prevention of water ingress into underground workings of the Witwatersrand mining 110 basins – Western Basin Stable Isotope Study – report on project period up to 15 December 2004: Council for Geoscience, Pretoria, Stable Isotope Laboratory Report 2004-06, pp. 16.

Horstmann, U.E., Coetzee, H., Ntsume, G. and Croukamp, L. 2004b Isotopic fingerprinting of water entering abandoned and working mines on the Witwatersrand. In Geoscience Africa. Johannesburg: Geological Society of South Africa.

Jackson, R.L., Drummond, D.K. and Camara, S., 2007. What is qualitative research?. Qualitative research reports in communication, 8(1), pp.21-28.

Jhariya, D., Khan, R. and Thakur, G.S. 2016. Impact of mining activity on water resource: an overview study. Proceedings of the Recent Practices and Innovations in Mining Industry, Raipur, India, pp.19-20.

Kipko, E.J., Polozov, Y.A., Lushinkova, O.Y., Lagunov, V.A. and Svirskiy, Y.I. 1984. Integrated grouting and hydrogeology of fractured rocks in the USSR. In Spetstamponazhgeologia Enterprises, Antratsit, Ukraine. Nedra Moscow.

Kipko, E.J. 1988, October. Application of grouting techniques for the solution of environmental problems during mining. In Third International Mine Water Congress (Vol. 23, p. 28). Australasian Institute of Mining and Metallurgy Melbourne, Vic.

Krige, W.G. 1999. An investigation into groundwater recharge derived from the upper Klip River tributaries where these cross the Main, Bird and Kimberley reef outcrops and associated shallow mine workings: African Environmental Development, 14 pp.

Kusumayudha, S.B., Pratiknyo, P., Purwanto, Riswandi, H., Ciptahening, A.N. and Hermawanti, N. 2018. Fissure structure analysis to unravel groundwater inflow problem in gold mining site of Pongkor area, West Java, Indonesia. *International Journal of Hydrology Science and Technology*, **8**(2):148-162.

Leibundgut, C. and Seibert, J. 2011. Tracer Hydrology. In: Peter Wilderer (ed.) Treatise on Water Science, vol. 2, pp. 215–236 Oxford: Academic Press

Li, P., Qian, H. and Wu, J. 2014. Hydrogeochemistry and quality assessment of shallow groundwater in the southern part of the Yellow River alluvial plain (Zhongwei section), Northwest China. *Earth Sciences Research Journal*, **18**(1):27-38.

Ma, D., Duan, H., Cai, X., Li, Z., Li, Q. and Zhang, Q., 2018. A global optimization-based method for the prediction of water inrush hazard from mining floor. Water, 10(11):1618.

Majumder, R.K. and Shimada, J. 2016. Hydrochemistry and environmental isotopes to identify the origin of barapukuria coal mine inflow water, Northwestern Bangladesh. Austin *Journal of Hydrology*, **3**(1):1019.

Manzi, M.S., Hein, K.A., King, N. and Durrheim, R.J. 2013. Neoarchaean tectonic history of the Witwatersrand Basin and Ventersdorp Supergroup: New constraints from high-resolution 3D seismic reflection data. *Tectonophysics*, 590:94-105.

Maruyama, S. and Kato, H. 2017. Identification of waters incorporated in Laguna Lake, republic of the philippines, based on oxygen and hydrogen isotopic ratios. *Water*, **9**(5)328.

Mazor, E. 2004. Chemical and Isotopic Groundwater Hydrology. Third Edition. ISBN: 0-

8247-4704-6

Mengistu, H., Tessema, A., Abiye, T., Demlie, M. and Lin, H. 2015. Numerical modeling and environmental isotope methods in integrated mine-water management: a case study from the Witwatersrand basin, South Africa. *Hydrogeology Journal*, **23**(3):533-550.

Menschik, F., 2015. Analysis of Performance and Wear of Electrical Rock Hammer Drills (Doctoral dissertation, Technische Universität München).

Mook, W.G. 2000. Environmental isotopes in the hydrological cycle. Principles and Applications, IHP-V, Technical Documents in Hydrology, 1.

Mook, W.G. and De Vries, J.J. 2000. Environmental Isotopes in the Hydrological Cycle: Principles and Applications, vol. 4, Introduction: Theory, Methods, Review. International Atomic Energy Agency.

Mook, W. and Rozanski, K. 2000. Environmental isotopes in the hydrological cycle. IAEA Publish, 39.

Mulenga, S.C. Fernandez Rubio. R, Leon, A. and Baquero, J.C. 1992). Estimation of quantitative water inflow from different sources in Konkola mine. *Mine water and Environment*, **11**(4):1-22.

Mulenga, S.C. 1993. Solution to Konkola Mine water inflow problem. In International Mine Water Association, Symposium, Kitwe, Zambia (pp. 60-97).

Osburn, K., H. Pretorius, D. Kock, N. King, R. Pillaye, and M. Hlangwane. "Enhanced geological modelling of the Upper Elsburg reefs and VCR to optimize mechanized mine planning at South Deep Gold Mine." Journal of the Southern African Institute of Mining and Metallurgy 114, no. 3 (2014): 265-273.

Prinsloo, M. 2020. Groundwater quality monitoring: South Deep Gold Mine, Pretoria: Rison Groundwater Consulting.

Prinsloo, M. 2019. Groundwater quality monitoring: South Deep Gold Mine, Pretoria: Rison Groundwater Consulting.

Robb, L.J. and Meyer, F.M. 1995. The Witwatersrand Basin, South Africa: geological framework and mineralization processes. Ore Geology Reviews, **10**(2):67-94

Rubio, R.F., Fabregas, A.L., Ubeda, J.C.B., Lorca, D., Alenza, I., Engineers, F.C. and Madrid, S.P. 1998. Underground Mining Drainage. State of the Art. In International Mine Water Association Symposium (pp. 87-112).

SACS, 1980. Stratigraphy of South Africa, Part 1: “Randian Erathem”. Pretoria: Geol. Surv. S. Afr.

Sami, K. 1992. Recharge mechanisms and geochemical processes in a semi-arid sedimentary basin, Eastern Cape, South Africa. *Journal of Hydrology*, **139**(1-4):27-48.

Sami, K., 2009. Groundwater exploration and development. The Basement Aquifers of Southern Africa, p.19.

Scott, R., 1995. Flooding of the Central and East Rand gold mines. Report to the Water Research Commission WRC report, (481/1), p.95.

Sello, J. J. 2019. Geochemical controls and characteristics of natural seepage of carbon dioxide along the Bongwana Fault, KwaZulu-Natal and Eastern Cape Provinces.2019. Masters Research Report University of the Witwatersrand

Sharp, J.M. 2003. A glossary of hydrogeological terms. Department of Geological Sciences, The University of Texas.

Sieber, A. and Uhlenbrook, S. 2005. Sensitivity analyses of a distributed catchment model to verify the model structure. *Journal of Hydrology*, **310**(1-4):216-235.

Singh, R.N. 1986. Mine Inundation, *International Journal of mine water*, **5** (2):28.

Singh.R.N. 1986. The Establishment of a mine water research division at the central mining research institute, Dhanbad, India, UNDP Report, January 1986, pp 163.

Singhal, B.B.S. and Gupta, R.P. 2010. Applied hydrogeology of fractured rocks. Springer Science & Business Media.

South Deep Gold Mine (SDGM). 2010. Technical Short Form Report. Gold Fields Limited, Sandton.

South Deep Gold Mine. 2011. Technical Short Form Report. Gold Fields Limited in compliance with the SAMREC Code (2007 edition).

SRK. 1985. Evaluation of the Impact of Mine Dewatering on the Water Table Elevations. James Park Info Center. Unpub.Report M1. 4685.Unpublished.

Talma, A. and Van Wyk, E. 2013. Rainfall and groundwater isotope atlas. Report. South Africa: Water Research Commission.

Titus, R., Beekman, H., Adams, S. and Strachan, L., 2009. The basement aquifers of Southern Africa. Water Research Commission report no. TT, pp.428-09.

Titus, R., Witthüser, K. and Walters, B. 2009. Groundwater and mining in the Bushveld Igneous Complex. Proceedings of the International Mine Water Conference, Pretoria, South Africa, 19-23 October 2009. Water Institute of Southern Africa and International Mine Water Association.

Toens, P.D. and Griffith, G.H. 1964. The geology of the West Rand. In: Haughton, S.H. (Ed.), The Geology of Some Ore Deposits in Southern Africa. Geological Society of South Africa, Johannesburg, pp. 283–322.

Tucker, R.F., Viljoen, R.P. and Viljoen, M.J. 2016. A Review of the Witwatersrand Basin-The World's greatest goldfield. Episodes, **39**(2):105-133.

Van Biljon, M., Swart, A.H. and Brawner, C.O., 2006. Geology, hydrogeology and structural competency of the boundary pillar at South Deep Gold Mine. *Journal of the Southern African Institute of Mining and Metallurgy*, *106*(5), pp.317-329.

Van Biljon, M. 2000. Geohydrological investigation for the establishment of a groundwater monitoring program. Report prepared by Rison Consulting for Placer Dome Western Areas Joint Venture, August 2000.

Warren L.A. (2011) Acid Rock Drainage. In: Reitner J., Thiel V. (eds) Encyclopedia of Geobiology. Encyclopedia of Earth Sciences Series. Springer, Dordrecht. https://doi.org/10.1007/978-1-4020-9212-1_3

Wang, W.X., Sui, W.H., Faybishenko, B. and Stringfellow, W.T., 2016. Permeability variations within mining-induced fractured rock mass and its influence on groundwater inrush. Environmental Earth Sciences, 75(4), p.326.

West Rand District Municipality (WRDM). 2017. Local Action for Biodiversity (Lab): Westlands South Africa, s.l.: West Rand District Municipality.

Wu, J., Cui, F.P., Zhao, S.Q., Liu, S.J., Ceng, Y.F. and Gu, Y.W. 2013. Type classification and main characteristics of mine water disasters. *Journal of China Coal Society*, **38**(4):561-565.

Xi-bing, L.J.T.L., Xi-ran, G.F.Q.W. and Jiao, L.I.U. 2012. Recognizing of Mine Water Inrush Sources Based on Principal Components Analysis and Fisher Discrimination Analysis Method [J]. *China Safety Science Journal*, 7.

Zabidi, H., Rahim, A. and Trisugiwo, M. 2019. Structural controls on groundwater inflow analysis of hardrock TBM. Cogent Geoscience, **5**(1):1637556.

Zhang, J., Yao, D. and Su, Y. 2018. February. Multivariate matrix model for source identification of inrush water: A case study from Renlou and Tongting coal mine in northern Anhui province, China. In IOP conference series: Earth and environmental science (Vol. 113, No. 1, p. 012212). IOP Publishing

*APPENDIX A*SDGM`S 2020 MONITORING BOREHOLES WATER QUALITY RESULTS (Source: Prinsloo (2020)

BH ID	Date	pH	Cond	TDS	Cl	SO4	NO3	o-PO4	CN - Total	CN - WAD	Ca	Fe	K	Na	Mg	T Hard	T Alk	F	Al	NH4	Mn	As	Hg	Zn	Total U	SOG
			mS/m	mg/l	mg/l	mg/l	mg/l	mg/l	mg/l	mg/l	mg/l	ug/l	mg/l	mg/l	mg/l	mg/l	mg/l	mg/l	ug/l	mg/l	ug/l	ug/l	ug/l	ug/l	ug/l	mg/l
		5 – 9.7	≤ 170	≤ 1 200	≤ 300	≤ 500	≤ 11	NS	≤ 0.2	NS	NS	≤ 2000	NS	≤ 200	NS	NS	NS	≤ 1.6	≤ 300	NS	≤ 400	≤ 10	≤ 6	≤ 5 000	≤ 30	NS
SD 1	23/01/2020	7.41	204	105	2.3	3.3	0.3	<0.06	<0.01	<0.01	25	<20	1.3	2.4	4.2	80.1	103	<0.3	<20	0.35	513	2.6	<1	10	<5	<50
SD 2	23/01/2020	7.18	105	70	2	25.7	5.5	<0.06	<0.01	<0.01	7.7	<20	0.3	3.5	5.2	41.1	18	<0.3	<20	<0.03	<2	<2.5	<1	10	<5	<50
SD 3	23/01/2020	7.26	50	<35	4.9	0.9	2.5	<0.06	<0.01	<0.01	4.8	<20	0.4	2.8	1.1	16.6	11	<0.3	<20	<0.03	16	<2.5	<1	16	<5	<50
SD 5	23/01/2020	7.79	2410	2069	112.1	1577.4	<0.2	<0.06	<0.01	<0.01	351.6	<20	1.4	34.1	72.2	1182.2	127	<0.3	<20	0.17	567	5.4	<1	107	<5	<50
SD 6	23/01/2020	7.44	114	78	7.3	6.3	2.3	0.07	<0.01	<0.01	9.2	<20	0.5	4.3	3.8	39	32	<0.3	<20	<0.03	<2	<2.5	<1	9	<5	<50
SD 7	23/01/2020	7.64	2780	2458	157.6	1737.6	<0.2	<0.06	0.12	0.02	292.7	24	3.5	105	153.1	1374.8	63	<0.3	<20	1.27	1632	<2.5	<1	5	<5	<50
SD 8	23/01/2020	7.67	2530	2231	188.2	1358.2	<0.2	<0.06	0.15	0.05	348.5	<20	1.6	69.1	89.9	1248.8	60	<0.3	<20	<0.03	12	<2.5	<1	5	<5	<50
SD 9	23/01/2020	7.91	2370	2111	119.5	1393.6	<0.2	<0.06	<0.01	<0.01	338.1	<20	2.3	43	96.4	1250.1	103	<0.3	<20	0.43	893	5.7	<1	6	<5	<50
SD 10	23/01/2020	8.08	2860	2650	157.5	1607.7	<0.2	0.12	0.13	0.04	420.6	436	3.3	70.5	118.9	1550.9	202	<0.3	<20	4.34	896	3.5	<1	5	<5	<50
SD 12	23/01/2020	8.19	410	218	27.2	11.5	4.9	<0.06	<0.01	<0.01	20.8	<20	10.8	28	16.7	122.1	140	<0.3	<20	2.93	208	<2.5	<1	4	<5	<50
SD 13	23/01/2020	8.14	393	270	95.7	2.7	<0.2	<0.06	<0.01	<0.01	23.4	44	1	33.1	7.4	89.6	18	<0.3	<20	0.21	396	<2.5	<1	4	<5	<50
SD 14	23/01/2020	7.88	267	177	5.2	84.3	2.1	<0.06	<0.01	<0.01	19	<20	2.5	8.7	12	97.9	29	<0.3	<20	<0.03	15	<2.5	<1	7	<5	<50
SD 15	23/01/2020	8.16	107	68	2.3	3.7	0.3	<0.06	<0.01	<0.01	11.3	35	0.9	7.4	3.2	41.7	44	<0.3	33	<0.03	<2	<2.5	<1	12	<5	<50
SD 16	23/01/2020	8	426	267	34.7	24.4	3.6	<0.06	<0.01	<0.01	24.4	<20	2.8	20.3	21.3	150.5	125	<0.3	<20	<0.03	3	<2.5	<1	8	<5	<50
SD 17	23/01/2020	8.18	1828	728	73.9	245.5	<0.2	23.28	0.03	<0.01	89.7	51	24.7	42.4	40.9	396	601	<0.3	<20	131.92	179	<2.5	<1	<3	<5	<50
SD 18	23/01/2020	8.05	1451	1202	93.5	542.5	<0.2	1.04	0.02	0.01	151.1	<20	3.2	37.1	67	659.2	140	<0.3	<20	2.94	82	<2.5	<1	37	<5	<50
SD 19	23/01/2020	7.41	93	54	1.4	16.3	2.7	<0.06	<0.01	<0.01	7.7	<20	0.3	6.5	1.5	25.6	20	<0.3	<20	<0.03	3	<2.5	<1	6	<5	<50
SD 23 D	23/01/2020	7.61	1611	1056	119.2	490.9	6.8	<0.06	0.04	0.03	79.1	<20	1.4	165.2	51.7	414.9	243	0.7	<20	<0.03	<2	<2.5	<1	7	<5	<50
SD 23 S	23/01/2020	8.16	1793	1176	129.6	519.3	3.3	<0.06	0.02	<0.01	54.3	<20	1	244.3	56.2	371.8	278	1.1	<20	<0.03	<2	<2.5	<1	8	<5	<50
SD 24 D	23/01/2020	7.52	278	134	1.6	2	<0.2	<0.06	<0.01	<0.01	8.1	<20	1.1	31.1	5.6	43.8	139	<0.3	<20	0.6	151	<2.5	<1	12	<5	<50
SD 24 S	23/01/2020	7.44	211	109	0.9	1.4	0.7	<0.06	<0.01	<0.01	7.9	<20	0.9	22	5.4	42.4	92	<0.3	<20	<0.03	<2	<2.5	<1	7	<5	<50
SD 25	23/01/2020	7.96	1829	1614	83.8	934.3	<0.2	0.37	<0.01	<0.01	274.6	<20	2.9	29.9	50.7	899.4	120	<0.3	<20	0.44	214	5.6	<1	11	<5	<50
SD 27	23/01/2020	7.95	510	280	3.8	1.2	23.4	<0.06	<0.01	<0.01	31.9	116	1.9	17.5	23.3	177.6	232	<0.3	<20	0.05	<2	<2.5	<1	9	<5	<50
SD 28D	23/01/2020	8.04	977	573	119.5	230.1	2	<0.06	<0.01	<0.01	52.7	<20	0.7	33.6	67.1	413.6	120	<0.3	<20	<0.03	<2	<2.5	<1	7	<5	<50
SD 28S	23/01/2020	8.28	1012	641	90	218	0.3	<0.06	0.04	<0.01	67.8	42	<0.1	45.1	57.1	409.3	216	<0.3	36	<0.03	22	<2.5	<1	13	<5	<50
SD 29	23/01/2020	8.01	521	338	19.9	89.2	39.2	<0.06	0.05	0.02	37.2	<20	2.4	17.8	24.3	195.1	107	<0.3	<20	<0.03	<2	<2.5	<1	6	<5	<50
SD 30D	23/01/2020	7.92	1737	1285	150	898.6	31.5	<0.06	0.07	<0.01	164.4	<20	1.9	37.1	112.4	883.1	161	<0.3	<20	<0.03	<2	<2.5	<1	10	<5	<50
SD 31	23/01/2020	8.02	473	291	39.8	98	0.2	<0.06	<0.01	<0.01	21.1	<20	1.8	33.7	20.2	137.6	71	<0.3	<20	0.17	64	<2.5	<1	<3	<5	<50
SD 32	23/01/2020	7.96	735	471	60.4	247.9	<0.2	<0.06	<0.01	<0.01	27	<20	5.7	23.2	50.8	280.9	49	<0.3	<20	3.75	96	3	<1	<3	<5	<50
SD 35	23/01/2020	8.08	634	303	3.8	5.6	<0.2	<0.06	<0.01	<0.01	27.2	<20	1.9	23.7	27.3	182.7	312	<0.3	<20	0.38	133	<2.5	<1	5	<5	<50
SD 36	23/01/2020	7.87	1590	1215	117.9	699	3.6	<0.06	0.04	<0.01	133.2	<20	2	42.7	90.5	713.1	214	<0.3	<20	0.03	<2	<2.5	<1	7	<5	<50
SD 38	23/01/2020	7.8	1407	989	138.3	586.8	12.3	<0.06	0.1	0.03	106.6	<20	1.8	60.1	74.9	581.1	88	<0.3	<20	<0.03	4	<2.5	<1	7	<5	<50
SD 39	23/01/2020	7.89	2620	2266	190.6	1281.8	20.9	<0.06	0.08	<0.01	282.1	<20	3.3	48.7	173.2	1432.7	138	<0.3	<20	<0.03	<2	<2.5	<1	10	<5	<50
SD 40	23/01/2020	8.04	2032	1602	176.4	892.3	11.3	<0.06	0.04	<0.01	174.3	<20	1	54.4	125.2	961.6	170	<0.3	<20	<0.03	<2	<2.5	<1	6	<5	<50
SD 41	23/01/2020	7.66	1649	1374	149	972	23	<0.06	0.09	<0.01	161.2	<20	1.7	28.6	106	856.6	92	<0.3	<20	<0.03	15	<2.5	<1	7	<5	<50
SD 42	23/01/2020	7.81	2500	2123	197.4	1332.1	17.9	<0.06	0.11	0.02	295.7	<20	2.8	38.9	171.2	1458.3	136	<0.3	<20	<0.03	<2	<2.5	<1	4	<5	<50
SD 43	23/01/2020	7.6	3000	2693	192.4	1721.8	12.5	<0.06	0.12	<0.01	346.5	<20	3.6	49.3	220	1790.3	136	<0.3	<20	<0.03	3	<2.5	<1	10	<5	<50
SD 44	23/01/2020	7.79	1964	1539	189	834.7	11.4	<0.06	0.11	<0.01	166.5	<20	2.3	43	129.9	961.8	119	<0.3	<20	<0.03	<2	<2.5	<1	5	<5	<50
SD 45	23/01/2020	8.01	45	<35	1.5	3.4	0.4	<0.06	<0.01	<0.01	5.7	<20	1.4	4.4	1.3	19.7	12	<0.3	<20	0.53	20	<2.5	<1	13	<5	<50
SD 46	23/01/2020	8.13	499	358	4.1	4.4	0.3	<0.06	<0.01	<0.01	27.8	<20	1	30.5	10.7	114.4	242	<0.3	<20	<0.03	<2	<2.5	<1	7	<5	<50
SDS 5	23/01/2020	7.79	1997	1556	150.6	991.6	<0.2	<0.06	0.05	<0.01	245.9	1005	3.1	72	68.2	901.2	15	<0.3	<20	0.39	210	<2.5	<1	5	<5	<50
BH1	23/01/2020	7.82	2750	2521	195.7	1631.6	30.4	<0.06	0.08	<0.01	300.4	<20	3.3	42.8	183.5	1521.7	151	<0.3	<20	<0.03	22	<2.5	<1	56	<5	<50
DP	23/01/2020	8.06	744	445	37.9	9.4	75	<0.06	<0.01	<0.01	53	<20	1.6	25.6	38.4	293.8	244	<0.3	<20	<0.03	<2	<2.5	<1	765	<5	<50
New FBH 11	23/01/2020	8.22	1873	1590	87.7	1110.8	<0.2	<0.06	<0.01	<0.01	175.5	<20	1.1	50	103	871.4	209	<0.3	<20	<0.03	<2	<2.5	<1	11	<5	<50
FBH14	23/01/2020	7.94	943	533	101.9	26.3	112	<0.06	<0.01	<0.01	43.7	<20	1.3	90.4	27.6	225.2	181	0.6	<20	<0.03	38	<2.5	<1	8	<5	<50
FBH 15	23/01/2020	7.78	1452	1055	91.6	645.8	31.9	<0.06	<0.01	<0.01	122.5	<20	1.6	36.7	89.7	683	204	<0.3	<20	0.98	<2	<2.5	<1	3	<5	<50
FBH16	23/01/2020	8.13	1697	1352	80.2	913.2	2.1	<0.06	0.01	0.01	167.8	<20	2.1	39.9	92.1	806.3	189	<0.3	<20	<0.03	3	<2.5	<1	11	<5	<50
FBH18	23/01/2020	8.21	289	180	11	17.1	1.2	<0.06	0.06	<0.01	30.9	<20	0.5	8.7	9.4	116.7	112	<0.3	<20	<0.03	40	42.4	<1	97	<5	<50
FBH19	23/01/2020	7.82	762	412	42.5	26.4	79.8	<0.06	<0.01	<0.01	52.9	<20	1.7	20.3	42.9	312.4	209	<0.3	<20	<0.03	<2	<2.5	<1	15	<5	<50
FERREIRA	23/01/2020	8.27	495	302	17.6	106.7	1.2	<0.06	<0.01	<0.01	50.4	<20	0.6	16.5	17.7	200.3	129	<0.3	<20	0.04	<2	18.6	<1	26	<5	<50
SC38	23/01/2020	7.72	2168	1752	195.4	1058.1	12.7	<0.06	0.17	0.02	228.9	23	3.8	36	140.5	1162.4	104	<0.3	<20	<0.03	<2	<2.5	<1	6	<5	<50
SC43	23/01/2020	7.69	3060	2874	188.3	1778.4	9.3	<0.06	0.14	0.01	357.1	22	3.3	54.1	229.1	1855	140	<0.3	<20	<0.03	<2	<2.5	<1	4	<5	<50
SC45	23/01/2020	7.75	2870	2614	188.7	1509.8	4.4	<0.06	0.14	<0.01	307.4	<20	3.8	44.3	193.9	1582.9	153	<0.3	<20	<0.03	<2	3.1	<1	7	<5	<50
SC46	23/01/2020	8.02	1999	1801	174.4	862.1	13.6	<0.06	0.13	<0.01	198.4	<20	3	39.1	117.8	990.8	136	<0.3	<20	<0.03	<2	<2.5	<1	6	<5	<50
SC49	23/01/2020	7.87	2220	1826	189.8	1078.6	9.8	<0.06	0.16	0.02	229	<20	3.4	40.4	140.9	1164.3	123	<0.3	<20	<0.03	<2	<2.5	<1	3	<5	<50
SC50	23/01/2020	7.6	1971	1544	177.2	805.2	16.7	<0.06	0.12	0.02	184.3	<20	3.6	43.1	118.3	957.6	131	<0.3	<20	<0.03	<2	<2.5	<1	6	<5	<50
SC51	23/01/2020	7.91	3030	2722	240	2264.6	6.1	<0.06	0.14	0.02	321.7	<20	2.8	52.7	184.4	1578.7	129	<0.3	<20	<0.03	<2	<2.5	<1	5	<5	<50
SC54	23/01/2020	7.84	3020	2710	219.1	1894.5	9.1	<0.06	0.13	<0.01	352.5	<20	3	51.3	234.5	1866.2	119	<0.3	<20	<0.03	<2	<2.5	<1	3	<5	<50

APPENDIX B

PIPER DIAGRAM REPRESENTING SDGM`S GROUNDWATER TYPES (Source: Prinsloo, 2020)

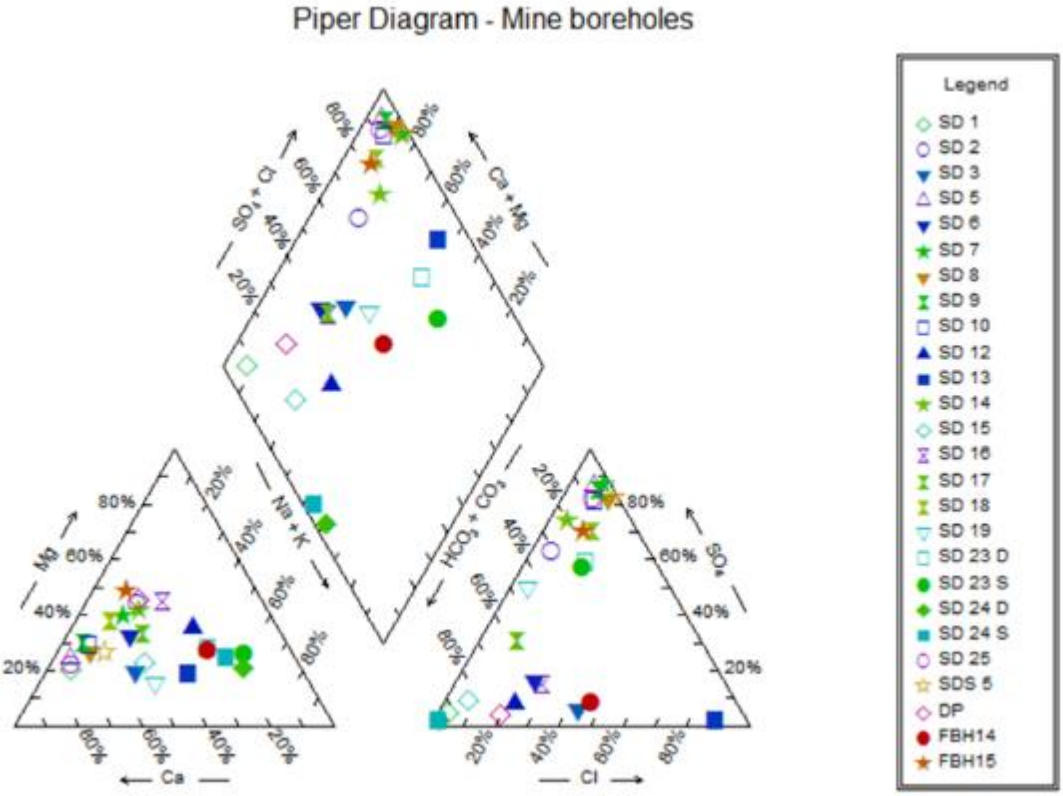

APPENDIX C

A SCHEMATIC DIAGRAM OF SDGM`S UNDERGROUND BLOCK CONCEPTUAL MODEL OF SDGM (Golder, 2018)

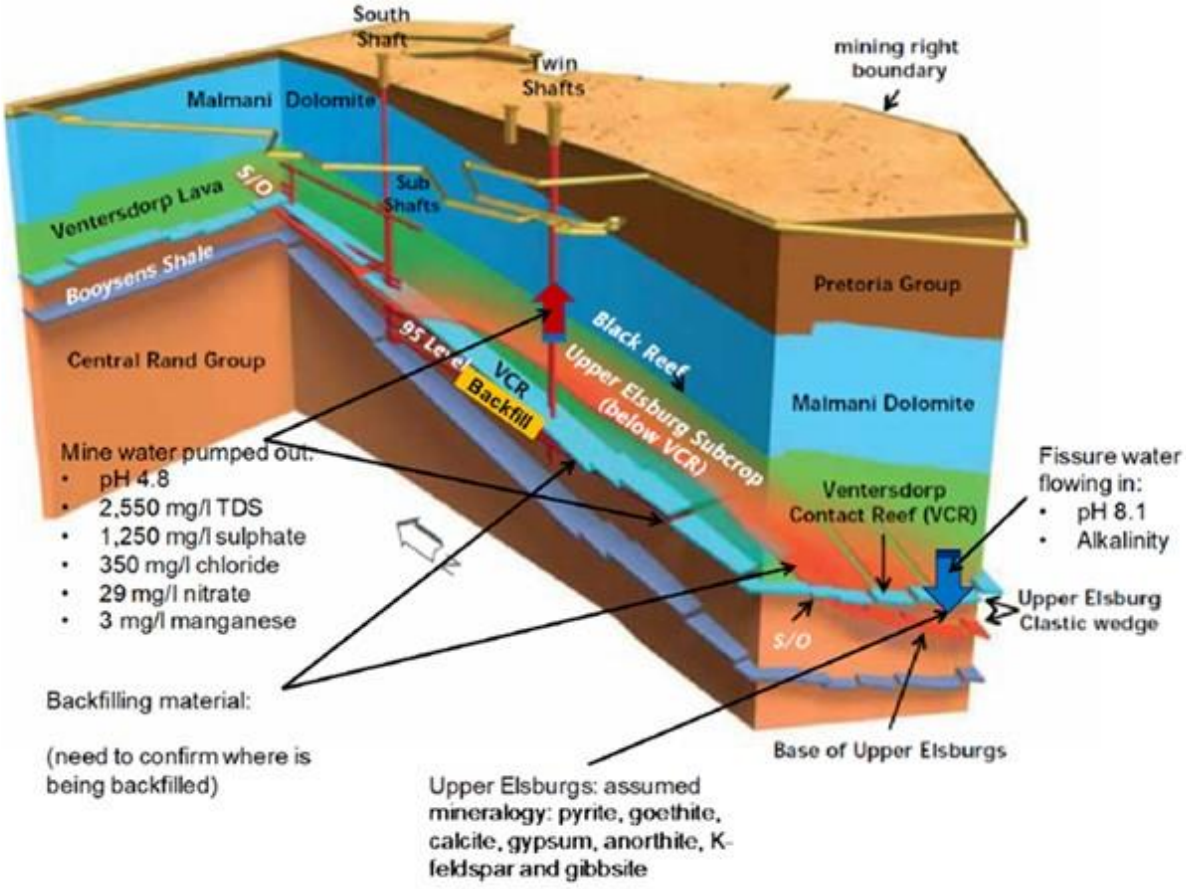

Blue arrows = fissure water; red arrows = mine affected water.